

A Framework for the Statistical Shape Analysis using SPHARM-PDM
combined with ITK Conformal Flattening Filter

By

Zhengyang Fang

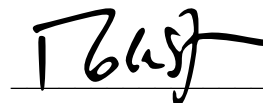
Senior Honors Thesis

Department of Computer Science

University of North Carolina at Chapel Hill

04/27/2018

Approved:

A handwritten signature in black ink, appearing to read 'M. Styner', is written over a horizontal line.

Martin Styner

ABSTRACT

Shape analysis is an important and powerful method used in neuroimaging research community due to its potential to precisely locate morphological changes between healthy and pathological structures. A popular shape analysis in the neuroimaging community is based on encoding surface locations in terms of spherical harmonics for a representation called SPHARM-PDM [1]. The SPHARM-PDM pipeline takes a set of brain segmentation of a single brain structure (for example, the hippocampus or the caudate nucleus) as input and converts them into a corresponding spherical harmonic description (SPHARM), which is then sampled into a triangulated surface (SPHARM-PDM).

At present, the SPHARM-PDM pipeline utilizes heat-equation mapping initialization parametrization of the surface mesh to the unit sphere and optimization for uniformity of area ratio between the surface mesh and the parametrized unit sphere. In the case of objects with complex shape, this initial mapping will suffer from a high degree of mapping distortion that cannot always be corrected by the following optimization procedure. Here we propose the use of an alternative initialization parametrization based on the ITK Conformal Flattening filter, which is an implementation of a paper by Sigurd Angenent, et al., “On the Laplace-Beltrami Operator and Brain Surface Flattening” [2] done by Yi Gao, et al. [3]. This method adopts a bijective angle preserving conformal flattening scheme to replace the heat equation mapping scheme as initialization parametrization for use in the SPHARM-PDM pipeline. The major scientific contribution of this work is made through the experiments I have done. When comparing the

resulting SPHARM surfaces calculated from various structures such as the femur and the mandible between the original and the newly proposed pipeline, I conclude that in most cases, the new pipeline produces dramatically better results than the old pipeline based on quantitative measures of shape. Yet, for some other cases, the conformal flattening based scheme produced marginally worse results than the heat equation based scheme. The main system contribution of this work is a command line tool that merges the ITK Conformal Flattening filter into the SPHARM-PDM pipeline for use in the SALT shape analysis toolbox.

1. INTRODUCTION

For a long time, researchers in the neuro-image area has been using volumetric analysis to assess the morphology of different brain structures. Even though volume change can be an intuitive feature to detect dilation and atrophy due to illness, it can be of inadequate help in assessing illness that cause little to no volume change. To address this issue, neuroimaging community has started setting its eyes on shape analysis methodology to catch morphological changes between healthy and pathological structures [1].

In 2006 a framework for the statistical shape analysis of brain structures called SPHARM-PDM was proposed. Its objective is to bring populations of an anatomic object into optimal correspondence and thus to allow statistical shape analysis. As we can see from the SPHARM-PDM shape analysis scheme in figure 1, we start with a segmentation of the brain structures. Next, using the output binary 3D image, we ensure its spherical topology via the command line tool called SegPostProcess. In the next step, we first extract the surface of input label segmentation by

following the ‘cracks’ between the foreground (label) and the background. the derived surface mesh is then mapped to sphere using a method proposed by Brechbühler, et al., “Parametrization of closed surfaces for 3-D shape description” [4]. The proposed method parametrizes the surface by defining a continuous, one-to-one mapping from the surface of the original object to the surface of a unit sphere. It formulates the parametrization as a constraint optimization problem and gets the practicable starting values by an initial mapping based on a heat equation model. Brechbühler performs the initialization parametrization considering two criteria:

1. Area preservation: Every object region must map to a region of proportional area in parameter space, with the constant of proportionality uniform across the surface
2. Minimal distortion: Every quadrilateral of the object should map to a spherical quadrilateral that has side length equals to the corresponding center angle (in radian) as the sphere has unit radius in parameter space

Brechbühler then calculates out system of nonlinear equations after establishing constraints for area preservation with half of the sum of the perimeters of all quadrilaterals being the objective function. Finally, Brechbühler solves the system of nonlinear equations by linearizing them and taking Newton steps.

In the fourth step, the framework computes the SPHARM-PDM representation and resolves correspondence and alignment issues. It takes the surface mesh and its spherical correspondence as input and produces a series of SPHARM coefficients and SPHARM-PDM meshes, one set in the original coordinate system, one in the first order ellipsoid aligned coordinate system and one in the Procrustes aligned coordinate system. However, for complex or skinny objects, the current heat equation model based initialization will reconstruct the SPHARM surface mesh with a high

degree of distortion that cannot always be corrected by the following optimization procedure.

The final step of the SPHARM-PDM shape analysis framework serves mainly to assess the group differences of the local surface point distributions by using the StatNonParamTestPDM command line tool. It can derive two main types of results. a) descriptive group statistics which includes mean and covariance information; b) group mean difference hypothesis testing.

In 2006, a conformal flattening ITK filter [3] was developed based on the paper by Sigurd Angenent, et al., “On the Laplace-Beltrami Operator and Brain Surface Flattening” [2]. The proposed filter performs an angle preserving map of any genus zero (i.e., no handles) surface to the sphere or to the plane.

In this paper, I propose the use of the above mentioned conformal flattening ITK filter to serve as the initial parametrization method in the SPHARM-PDM framework by replacing the current heat equation model based initialization. Specifically, it modified the command line tool called GenParaMesh used in the third step of the SPHARM-PDM shape analysis framework to improve the quality of the reconstructed 3D surface mesh (See Figure 2). To test the advantage of the proposed framework, I employed three datasets of the femur structure, four datasets of the mandible structure, eight datasets of the mandible condyle structure, sixteen of the molar structure and four of the cerebral ventricle structure to test both the old and the new SPHARM-PDM pipeline. Among them, I used two of the three datasets of the femur structure, one of the four datasets of the mandible structure, one of the eight datasets of the Condyle structure, three of the sixteen datasets of the molar structure to perform the evaluation between the surface mesh and the SPHARM surface mesh or between the surface mesh and the SPHARM surface mesh with conformal

mapping initialization parametrization.

I analyzed the datasets results by measuring the mean absolute distance (MAD), average cell area, the standard deviation of the cell area and by calculating the coefficient of variation of the cell area between the surface mesh of segmentation and the SPHARM surface mesh in the original coordinate using two software called MeshValMet [5] and MeshQuality (a tool to analyze cell area and cell edge ratio developed in UNC Neuro Image Research and Analysis Laboratories(NIRAL)). As it turns out, the SPHARM surface meshes derived with conformal mapping initialization parametrization is significantly better in quality than that derived with heat equation mapping initialization parametrization on complex structures such as the femur and the mandible. The quality of SPHARM surface meshes with conformal mapping initialization parametrization converges faster on all datasets than those with heat equation mapping initialization parametrization notwithstanding with enough iterations, the former is slightly worse than the latter on the molar and the condyle structures.

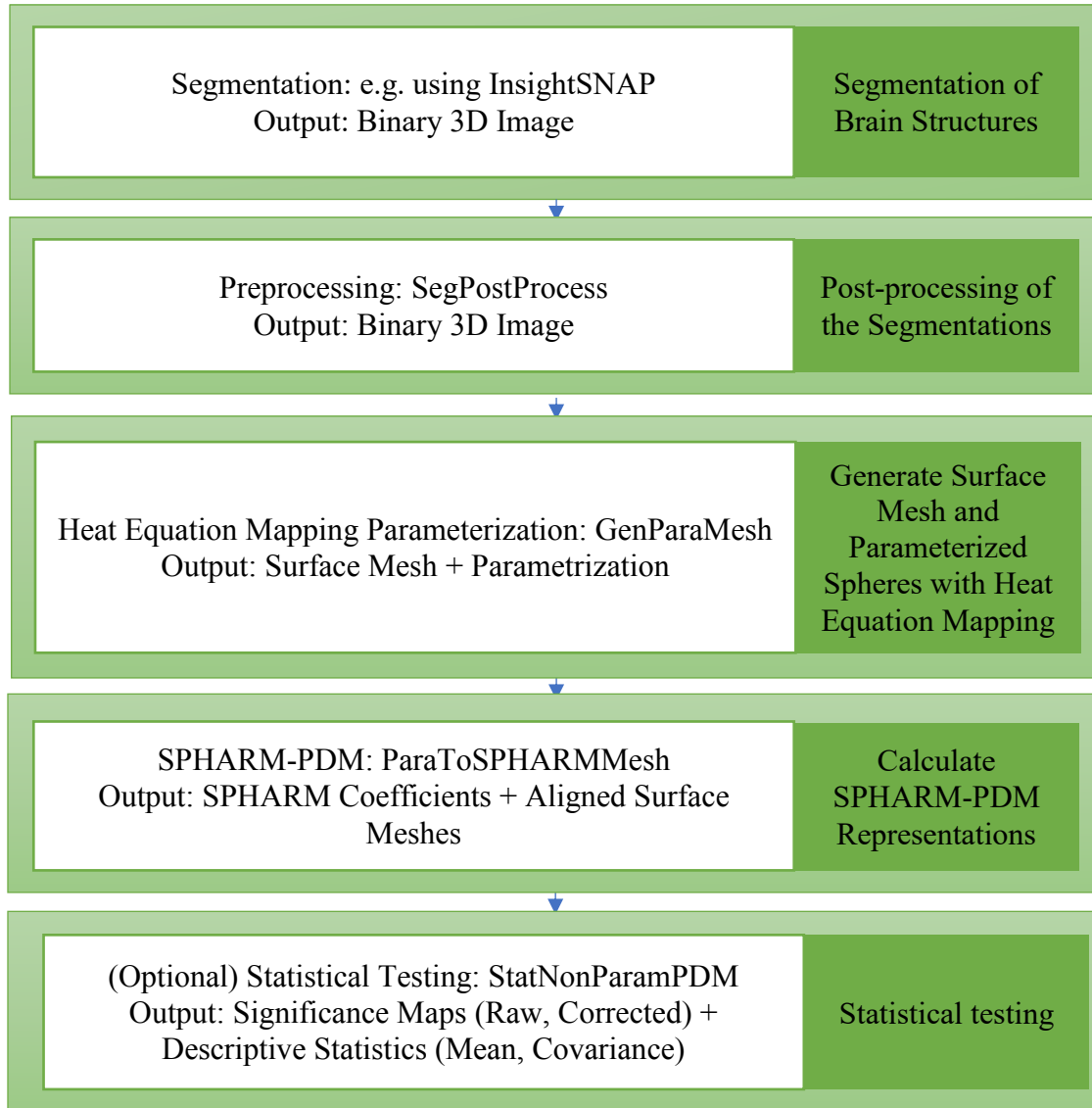


Figure 1: The original SPHARM-PDM shape analysis pipeline

2. METHODS AND MATERIALS

Our framework for SPHARM-PDM combined with conformal ITK filter consists of five steps:

- (1) Segmentation of target organ structures
- (2) Post-processing of the segmentations

(3) Generation of surface mesh and parametrized spheres with conformal mapping based initialization parametrization

(4) Calculation of SPHARM-PDM representations

(5) Statistical testing

The newly proposed pipeline is visualized in figure 2. The detailed description of each step lies on the left of the figure. As you can see, each step utilizes a command line interface tool that takes the output generated from previous steps as input (except in the first step where we acquire data from outside sources) and generate respective outputs.

In the third step of our newly proposed framework, I made the contribution by replacing the complicated sub-steps which uses both GenParaMesh and itkConformalMappingFilter command line tools into one step, where the user can use only the GenParaMesh command line tool with “—conf” flag on to choose to use conformal initialization parametrization.

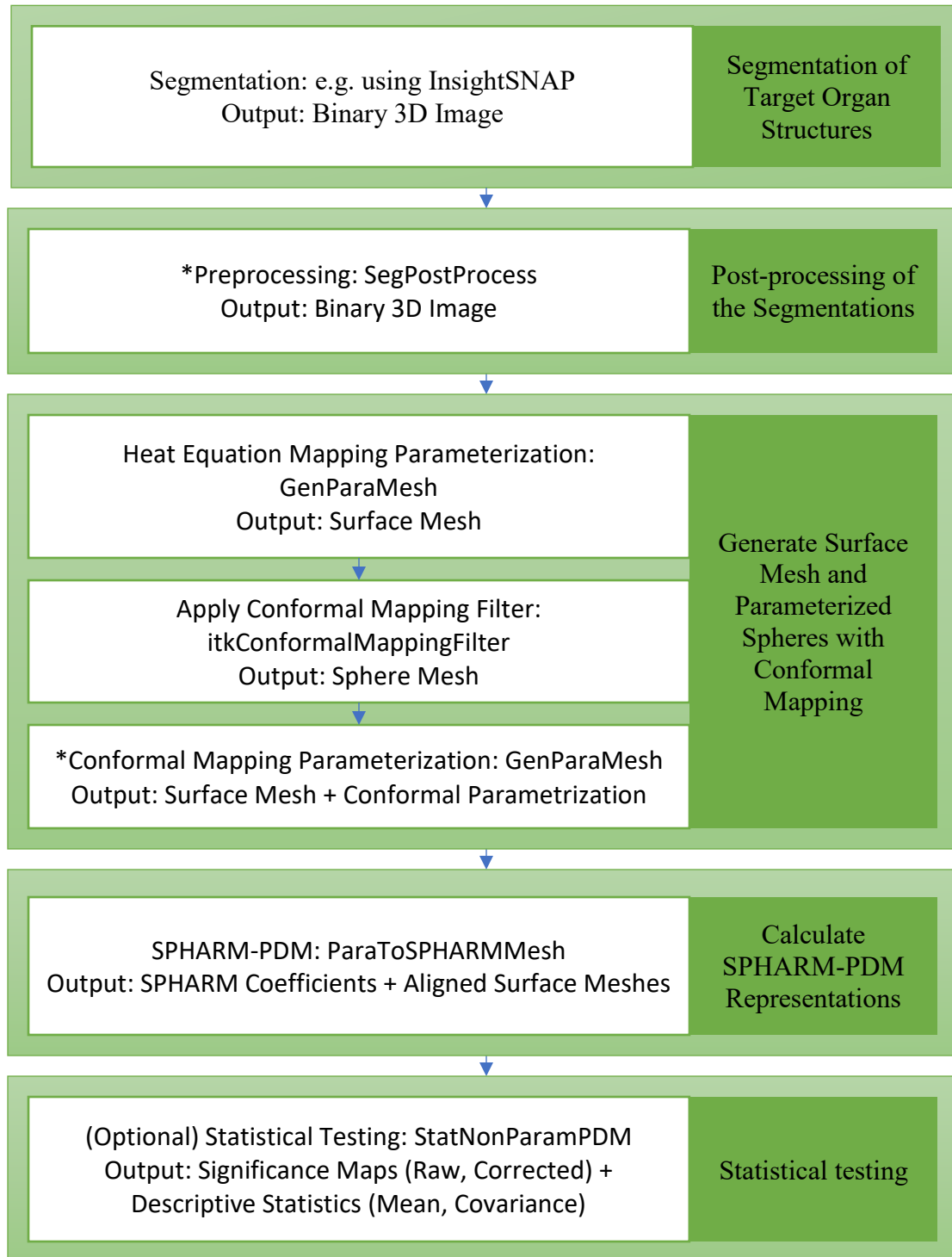


Figure 2: I proposed the modified SPHARM-PDM shape analysis framework utilizing conformal flattening filter as the initial parametrization method

*: The output of the Preprocessing step is used as input in Conformal Mapping Parametrization step

2.1 Subjects and Acquisition

I applied both the newly proposed SPHARM-PDM shape analysis framework with conformal mapping initialization parametrization and the original SPHARM-PDM shape analysis framework with heat equation initialization parametrization to five datasets (the femur, the mandible, the molar, the condyle and the ventricle) acquired from different sources.

From these data, I used the following outputs generated in the pipeline to measure and compare the quality of the reconstructed SPHARM surface meshes using either the old or the new SPHARM-PDM framework:

- (1) Surface mesh of the segmentation obtained in the GenParaMesh step
- (2) SPHARM surface mesh in the original coordination system obtained in the ParaToSPHARMMesh Step

2.1.1 The Femur Data Reference

The femur data were obtained from a collaboration with the University of Bern in 2004. The exact origin of the data is unfortunately unknown.



Figure 3: One of the three Femur volumes visualized in 3D Slicer [11] Volume Module

2.1.2 The Mandible & The Condyle Data Reference

The mandible and Condyle data was a subset of the data used in the study “3D superimposition and understanding temporomandibular joint arthritis” [6]. In the original study, the Department of Orthodontics and Pediatric Dentistry at the University of Michigan acquired Cone beam CT scans from 69 subjects with long-term temporomandibular joint (TMJ) osteoarthritis (OA, mean age 39.1 ± 15.7 years), 15 subjects at initial consult diagnosis of OA (mean age 44.9 ± 14.8 years), and seven healthy controls (mean age 43 ± 12.4 years).

The original data format of the condyle data was vtk, but the GenParaMesh command line tool does not accept vtk file format as input file format. Therefore, UNC graduate student Mahmoud Mostapha used an open source command line tool called PolyDataToImageData to convert the original vtk poly data files into nrrd file format [12].

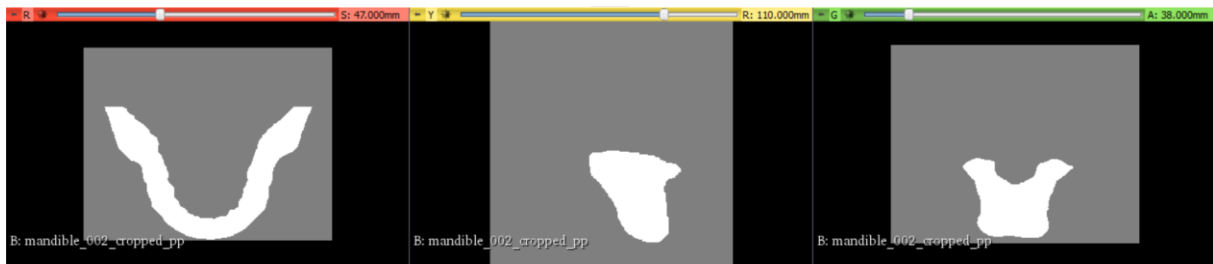


Figure 4: One of the four Mandible volumes visualized in 3D Slicer [11] Volume Module

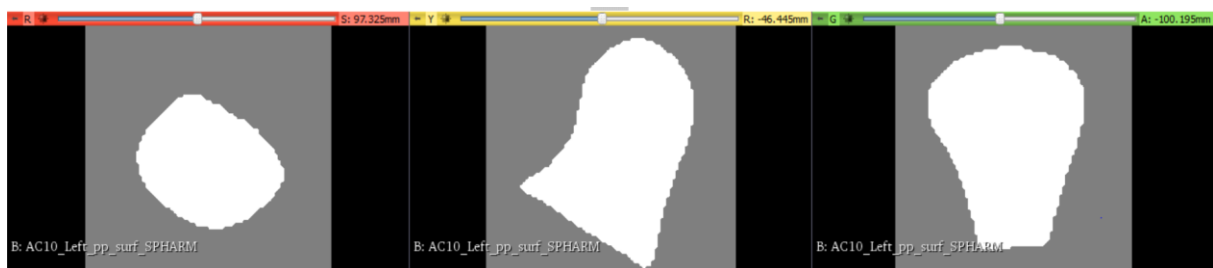


Figure 5: One of the three Condyle volumes visualized in 3D Slicer [11] Volume Module

2.1.3 The Molar Data Reference

The molar data used in my study is a subset of the data used in the study of [7] and “Group-wise shape correspondence of variable and complex objects” [8], and a detailed explanation of sample preparation can be found in [9]. In short, molds of actual tooth-rows were molded using a polyvinylsiloxane material (PresidentJet Plus) and cast in epoxy EpoTek 301. The second mandibular molar was trimmed from the tooth row and scanned with the Scanco μ CT-40 machine at Stony Brook University's Center for Biotechnology. Three-dimensional surfaces of each tooth were segmented from the resulting DICOM or TIFF stacks using Amira 5.1 or Avizo 6.0.



Figure 6: One of the sixteen Molar volumes visualized in 3D Slicer [11] Volume Module

2.1.4 The Ventricle Data Reference

High-resolution MRI scans were acquired from three different subject groups [10 monozygotic (MZ) twin pairs discordant for schizophrenia (DS), 9 healthy MZ twin pairs, and 10 healthy dizygotic (DZ) twin pairs imaged on the same scanner]. All three groups were matched for age,

gender, and handedness. A fourth group consisting of 10 healthy nonrelated (NR) subject pairs also matched for age, gender, and handedness was selected from the two healthy groups.

Volumetric differences as well as 3D maps representing magnitude and significance of shape differences between the twin pairs and between subject groups were computed and visualized. These dataset was then processed by using a rater-independent, automatic tissue-segmentation method. For detail of the image processing, see the Image Processing section in “Morphometric analysis of lateral ventricles in schizophrenia and healthy controls regarding genetic and disease-specific factors” [10].



Figure 7: One of the four Ventricle volumes visualized in 3D Slicer [11] Volume Module

2.2 Original Surface Mesh

I first use the SegPostProcess command line tool to extract a single binary label and apply heuristic methods to ensure the spherical topology of the segmentation. After this, I apply GenParaMesh command line tool to compute the surface mesh corresponding to the segmentation. I obtain the surface meshes of the segmentations and compare them with the SPHARM surface with either heat equation mapping initialization parametrization or conformal mapping initialization parametrization.

2.3 SPHARM Surface Mesh

I apply the GenParaMesh command line tool with different iterations and with either heat equation mapping initialization parametrization or conformal mapping initialization parametrization. Specifically, using the original heat equation mapping initialization parametrization, I pick 0, 50, 100, 150 ... 500 iterations and save the surface meshes and their parametrized spheres. With conformal mapping initialization parametrization, I pick the same number of iterations as with heat equation mapping initialization parametrization. Before I develop the command line tool to perform GenParaMesh with conformal mapping initialization parametrization, in order to test the newly proposed pipeline, I first apply GenParaMesh with 0 iterations (to save computing time) to get the surface mesh, then use the conformal mapping command line tool to convert the surface mesh to conformal mapping based parametrized sphere, next set the conformal mapping parametrized sphere as the initialization parametrization through the “--initPara” option of the GenParaMesh command line tool and lastly set the number of iteration to be 0, 50, 100, 150 ... 500 for comparison with the original pipeline. I then apply the ParaToSPHARMMesh command line tool using the surface mesh and the parametrized sphere with different iterations and with either heat equation mapping initialization parametrization or conformal mapping initialization parametrization as inputs and obtain the output SPHARM surface mesh in the original coordinate system for comparison with the surface mesh of the segmentation.

2.4 Command Line Tool

It is important to let researchers in neuro-imaging community use SPHARM-PDM with conformal mapping initialization parametrization conveniently. Thus, I developed a command line tool based on the Slicer Execution Model that will be used in the Slicer SALT Shape Analysis Toolbox in the future. Before the command line tool was developed, researchers has to do the following in order to apply GenParaMesh command line tool with conformal mapping initialization parametrization:

- (1) Apply GenParaMesh command line tool on the target dataset with 0 iteration (to save computing time) to obtain the surface mesh of the segmentation
- (2) Apply the ITK conformal flattening filter command line tool on the surface mesh to obtain the conformal parametrized sphere
- (3) Apply the GenParaMesh command line tool with the conformal parametrized sphere as the initialization parametrization by setting the “--initPara” option in the GenParaMesh command line tool

With the new tool, researchers only need to set the “--conf” flag on in the GenParaMesh command line tool in order to use conformal mapping initialization parametrization.

During each usage of GenParaMesh with “--conf” flag, three intermediate files will be written to the output directory. Specifically they are

- (1) \$ppcase-iter[iteration number]-surf0.vtk
- (2) \$ppcase-iter[iteration number]-confPara0.vtk

(3) \$ppcase-iter[iteration number]-confPara0.meta

The first file is the surface mesh of segmentation. The second file is the parametrized sphere of the surface mesh with conformal mapping initialization parametrization. The third file is the “meta” format version of the second file which has to be created due to code implementation reason. To enable the user to apply the GenParaMesh command line tool with conformal mapping initialization parametrization in parallel to the datasets, I assign each intermediate file a unique name associated with its label name (\$ppcase) and iteration number.

3. RESULTS

To test the proposed framework, I used the condyle, the femur, the mandible, the molar and the ventricle datasets as discussed in Subjects and Acquisition section. The surface mesh of the segmentation and the SPHARM surface mesh were computed with either heat equation mapping initialization parametrization or conformal mapping initialization parametrization. There are two kinds of statistics that can help us to evaluate the quality of the reconstructed SPHARM surface:

- (1) Measurement of the distance from the original surface mesh to the reconstructed SPHARM surface mesh between two triangle meshes using uniform sampling
- (2) Measurement of the average cell (it is not to be confused with the word “cell” used in the field of biology; in this context, the word “cell” means a triangle of the surface mesh) area of the SPHARM surface, standard deviation of cell area of the SPHARM surface and the coefficient of variation of cell area of the SPHARM surface by dividing the standard deviation of cell area of the SPHARM surface by the average cell area of the SPHARM surface

It is clear that the quality of the reconstructed SPHARM surface can be determined by its distance to the original surface; therefore, the first measurement is a perfectly valid measurement of the goodness of the reconstructed SPHARM surface. Because of the uniform cell correspondence across the SPHARM surface between the parametrized sphere and the SPHARM surface, the coefficient of variation of the cell area of the SPHARM surface is equal to the coefficient of variation of the cell area of the parametrized sphere. Since the variation of cell area of the parametrized sphere is a determining factor of the quality of the approximation of the original surface mesh, the coefficient of variation of the cell area of the SPHARM surface mesh is also a valid measure of the quality of SPHARM reconstruction, i.e., the second measurement is also valid. It is clear that the first measurement is the best when its value becomes zero, when the original surface mesh and the reconstructed SPHARM surface mesh are completely overlapping, i.e., identical. Because the optimization procedure of the GenParaMesh step converges when the triangles of the parametrized sphere have equal area, the standard deviation of the cell area of the SPHARM surface approaches zero when the quality of the surface is the best. Therefore, the second measurement also becomes better as its value gets closer to zero.

Therefore, to measure the quality of these SPHARM surface meshes, my advisor, Dr. Martin Styner, and I carefully chose two software tools for statistical shape analysis: MeshValMet [5] and MeshQuality (a command line tool developed by UNC PhD student Mahmoud Mostapha at the Neuro Image Research and Analysis Laboratories (NIRAL) of the University of North Carolina at Chapel Hill) with each one of them produces one of the two kinds of shape statistics as described above. Specifically, MeshValMet software can produce the Mean Absolute

Distance (MAD) between the original surface mesh and the reconstructed SPHARM surface mesh by averaging the sum of absolute distance between each vertex of the original surface and the SPHARM surface. When utilizing the MeshValMet software, I import the original surface mesh as model A (abbreviated A) and the reconstructed SPHARM surface mesh as model B (abbreviated B), then I set the “sampling step” to be “0.5%”, the “minimum sampling frequency” to be “2”, compute settings to be “A->B, B->A”, “number of bins” to be “256” and let “compute” be “signed distance”. With 0.5% sampling step and 2 minimum sampling frequency, MeshValMet can compute the distance between model A and model B in the error space with a fine sampling level; due to assymetric property of the Hausdorff distance, I choose “A->B, B->A” as the compute setting; since we do not need the histogram information in the MeshValMet software, I leave the “number of bins” to be its default value – “256”; since I only need the absolute distance between model A and model B, I choose “absolute distance” in the “compute” option. With the reconstructed SPHARM surface as input, MeshQuality command line tool can produce Average Cell Area of the SPHARM surface, Standard Deviation of Cell Area of the SPHARM surface and the Coefficient of Variance of Cell Area of the SPHARM surface by dividing the Standard Deviation of Cell Area of the SPHARM surface by the Average Cell Area of the SPHARM surface. Ideally, we only need the MAD to measure the quality of SPHARM surface mesh, but since MeshValMet tool will crash while analyzing some of the datasets, we have to adopt the MeshQuality command line tool to calculate the Coefficient of Variance of Cell Area of the SPHARM surface to measure the quality of SPHARM surface mesh. I collected all the data and used line charts to quantitatively show the quality of the SPHARM surface meshes with either one of the two different initialization parametrizations. As a rule of thumb, the MAD (Mean Absolute Distance) is the decisive measure of goodness that

suggests better reconstruction quality as its value approaches 0. The coefficient of variation of cell area is an intermediate measure of goodness that also indicates better reconstruction quality as its value approaches 0.

The femur datasets:

All three of the femur volume datasets can be successfully reconstructed with both heat equation mapping initialization parametrization and conformal mapping initialization parametrization. I measured two of the three datasets of the femur using MeshValMet [5] and MeshQuality and record and visualize the result in line charts to show the quality of SPHARM surface meshes with either heat equation mapping initialization parametrization or conformal mapping initialization parametrization.

(1) The femur dataset labeled 001:

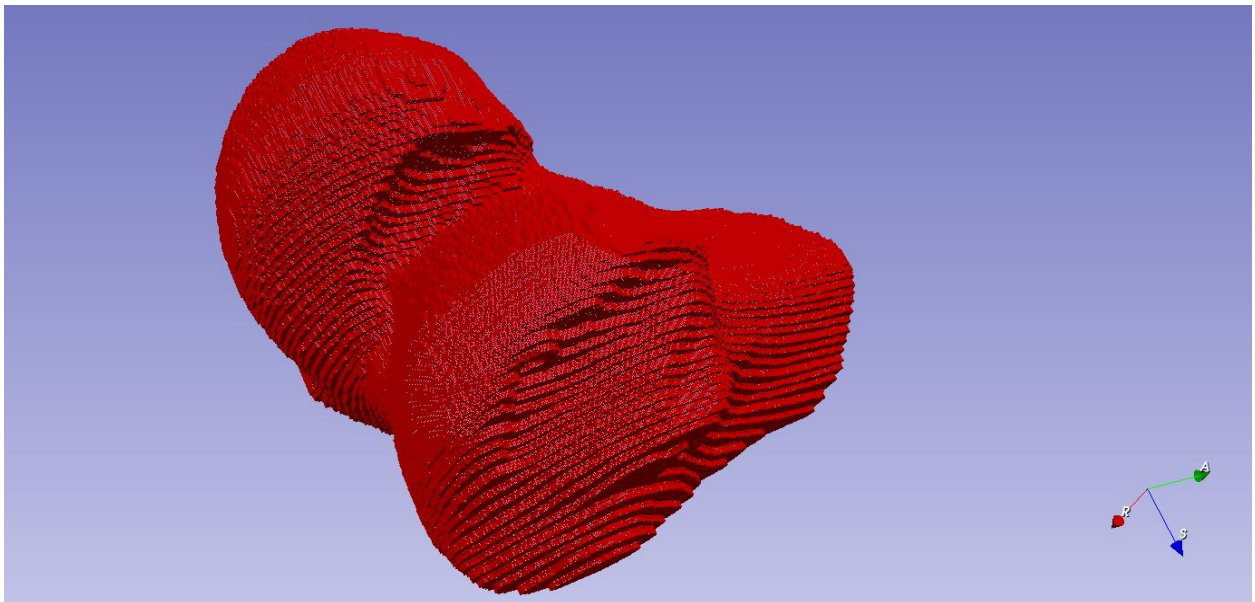


Figure 8: The surface mesh of the femur dataset labeled 001, which is the output of GenParaMesh and will then be mapped onto parametrized spheres with different iterations. Visualized in 3D Slicer [11] Model Module.

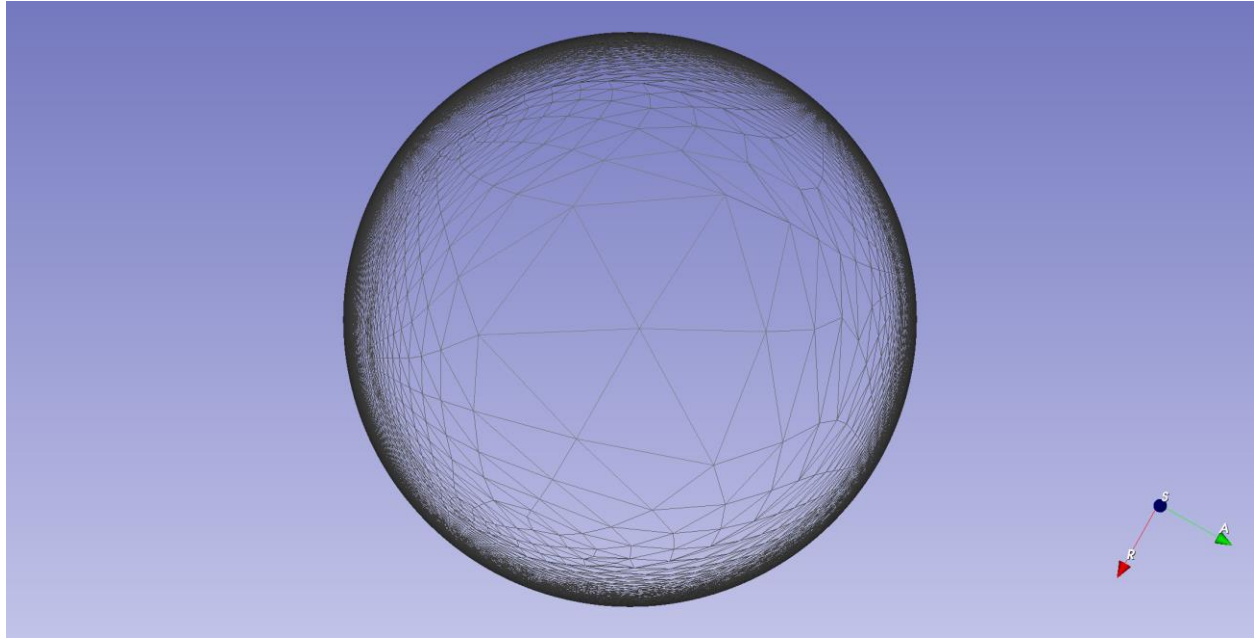


Figure 9: Heat equation mapping as initialization parametrization parametrized sphere of the femur dataset labeled 001 with iteration 0. It has bad quality because of the great variation in size of all triangles across the surface. Visualized in 3D Slicer [11] Model Module.

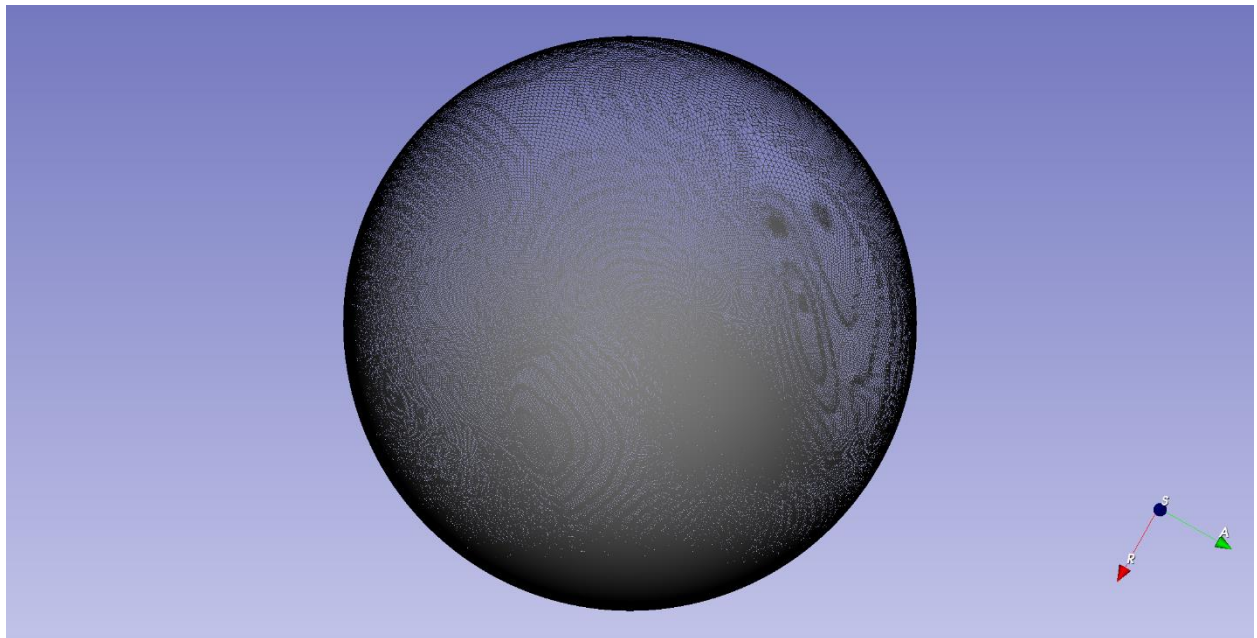


Figure 10: Conformal mapping as initialization parametrization parametrized sphere of the femur dataset labeled 001 with iteration 0. Even though it has very densely populated area (the dark regions), It is still a great initialization parametrization given the complexity of the femur structure. Visualized in 3D Slicer [11] Model Module.

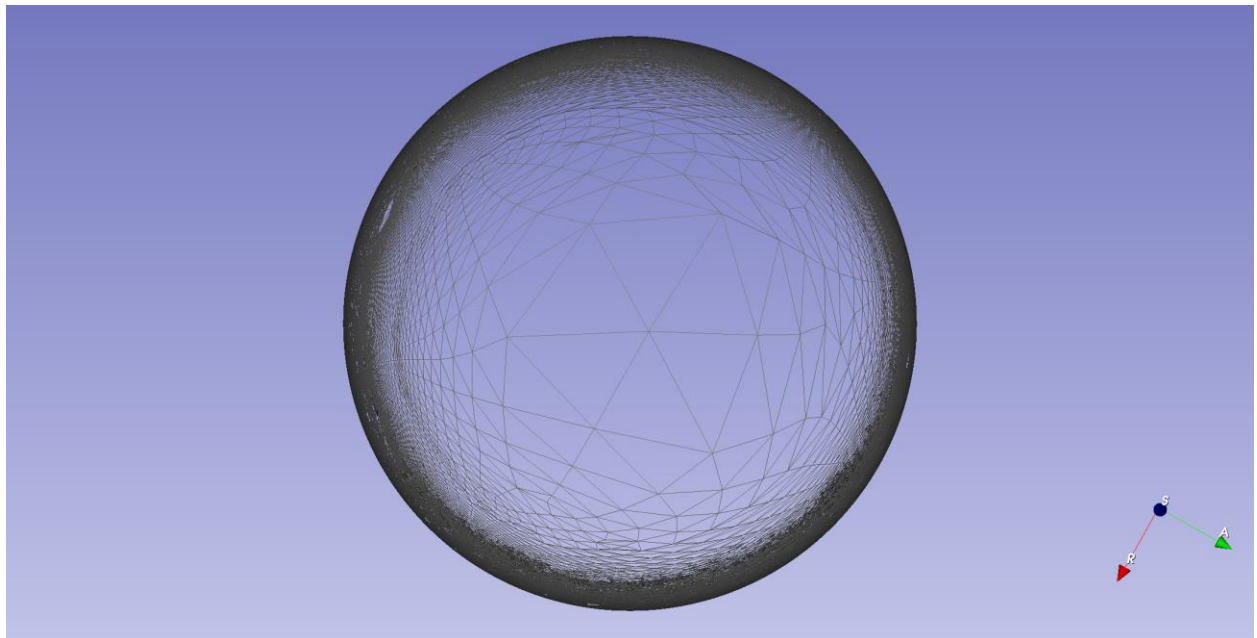


Figure 11: Heat equation mapping as initialization parametrization parametrized sphere of the femur dataset labeled 001 with iteration 50, which still have a bad quality given the large variation in the size of triangles across the sphere. It is similar in quality compared to the heat equation mapping as initialization parametrization parametrized sphere with iteration 0. Visualized in 3D Slicer [11] Model Module.

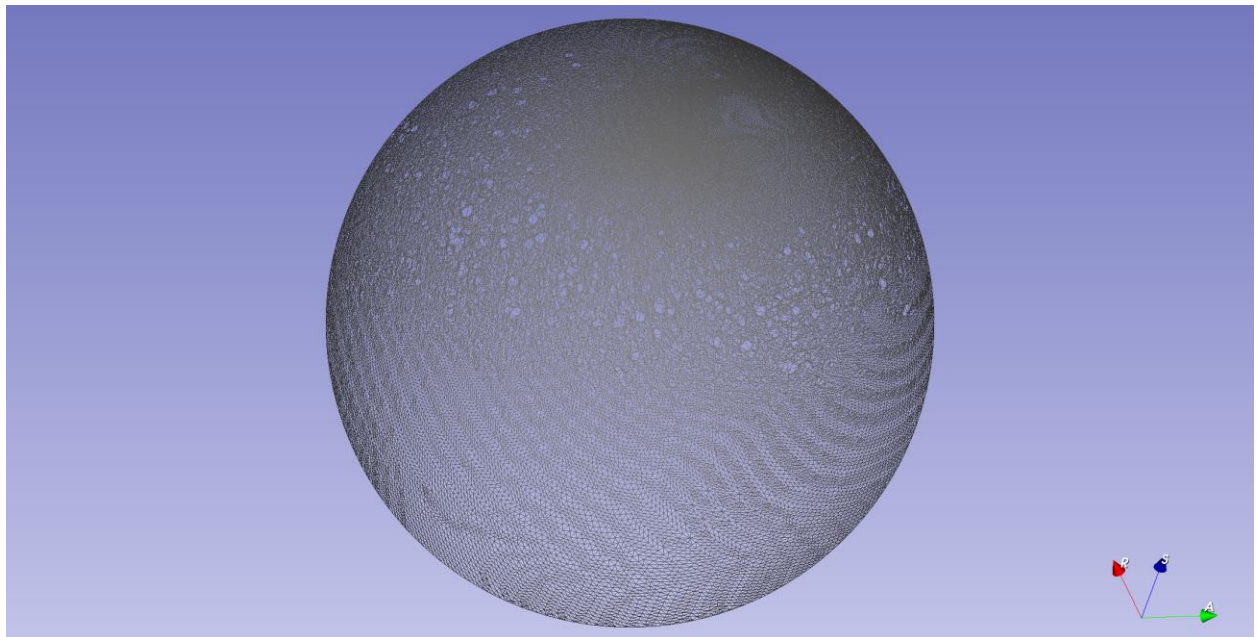


Figure 12: Conformal mapping as initialization parametrization parametrized sphere of the femur dataset labeled 001 with iteration 50. The quality has been improved as the triangles become more uniformly distributed and there are no more densely populated regions. Visualized in 3D Slicer [11] Model Module.

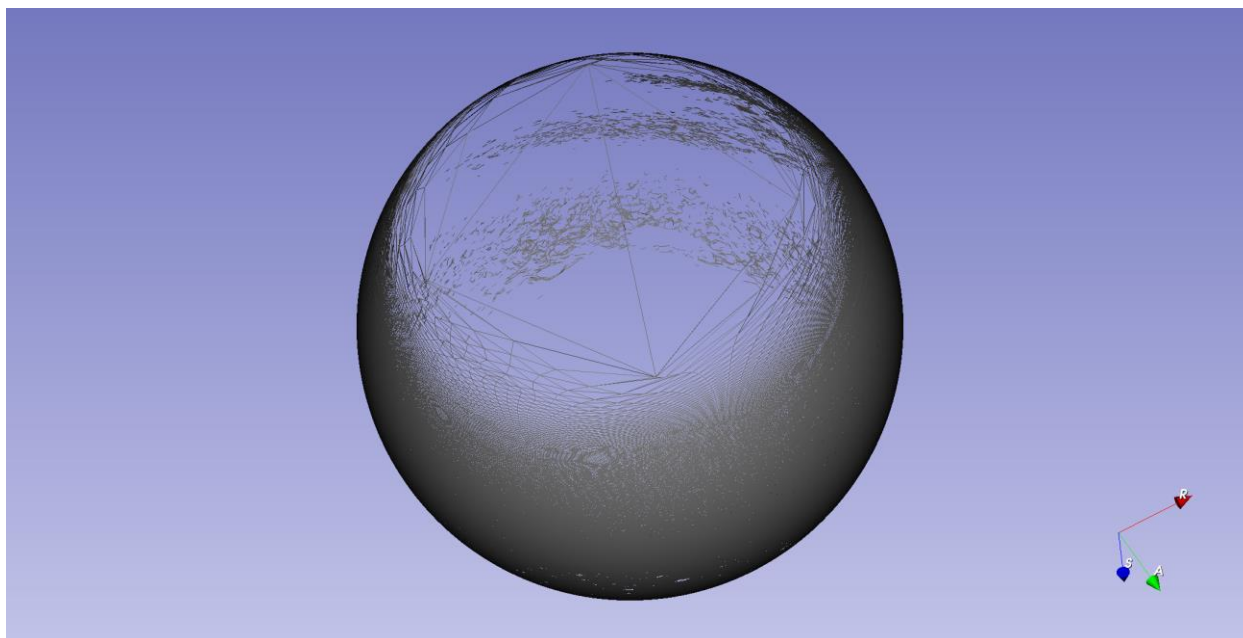


Figure 13: Heat equation mapping as initialization parametrization parametrized sphere of the femur dataset labeled 001 with iteration 100. It still has poor quality overall. Visualized in 3D Slicer [11] Model Module.

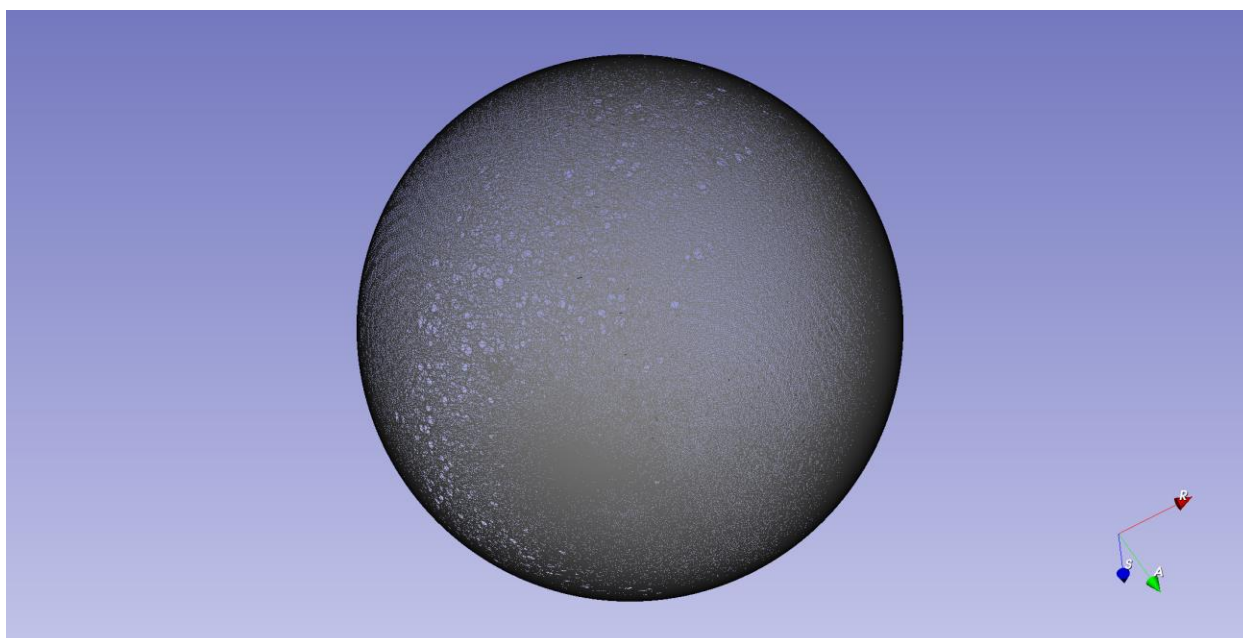


Figure 14: Conformal mapping as initialization parametrization parametrized sphere of the femur dataset labeled 001 with iteration 100. It has better quality than the conformal mapping as initialization parametrization parametrized sphere with iteration 0 and 50 because the ripples on the surface become less obvious. Visualized in 3D Slicer [11] Model Module.

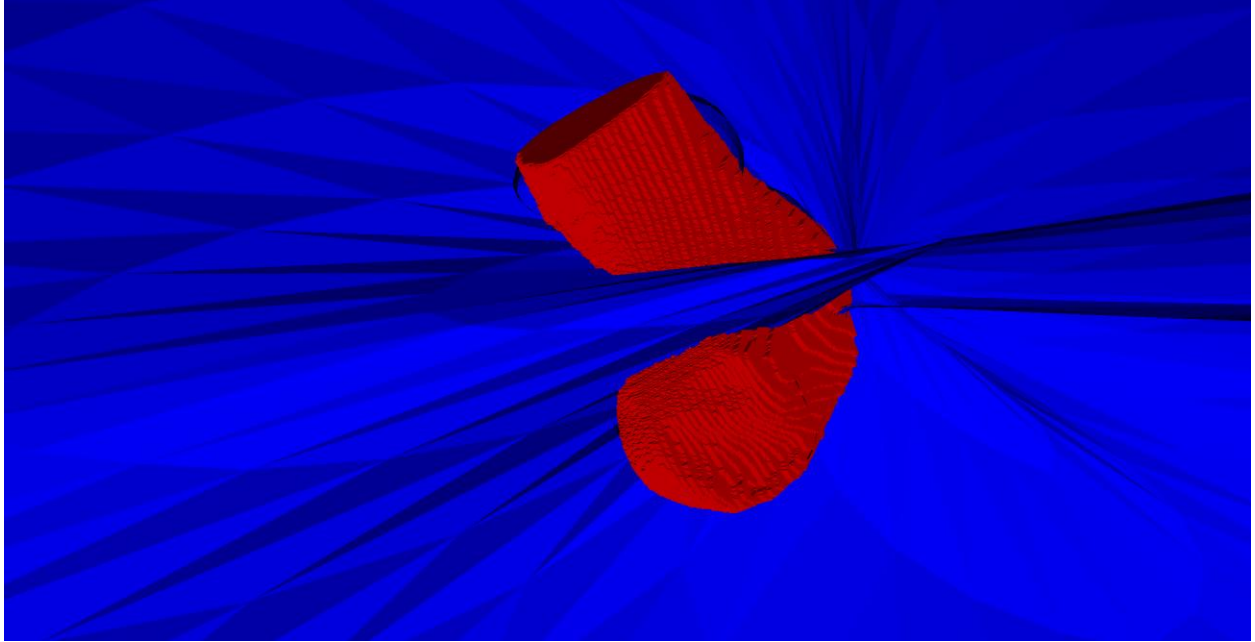


Figure 15: The overlay of the original surface mesh (red) of the femur dataset labeled 001 and the SPHARM surface mesh of it with heat equation mapping initialization parametrization with iteration 500 (blue). Since the SPHARM surface (blue) does not even look like the femur structure, it is clear that the SPHARM surface with heat equation mapping initialization parametrization failed to provide a good representation of the original surface mesh. Visualized in 3D Slicer [11] Model Module.

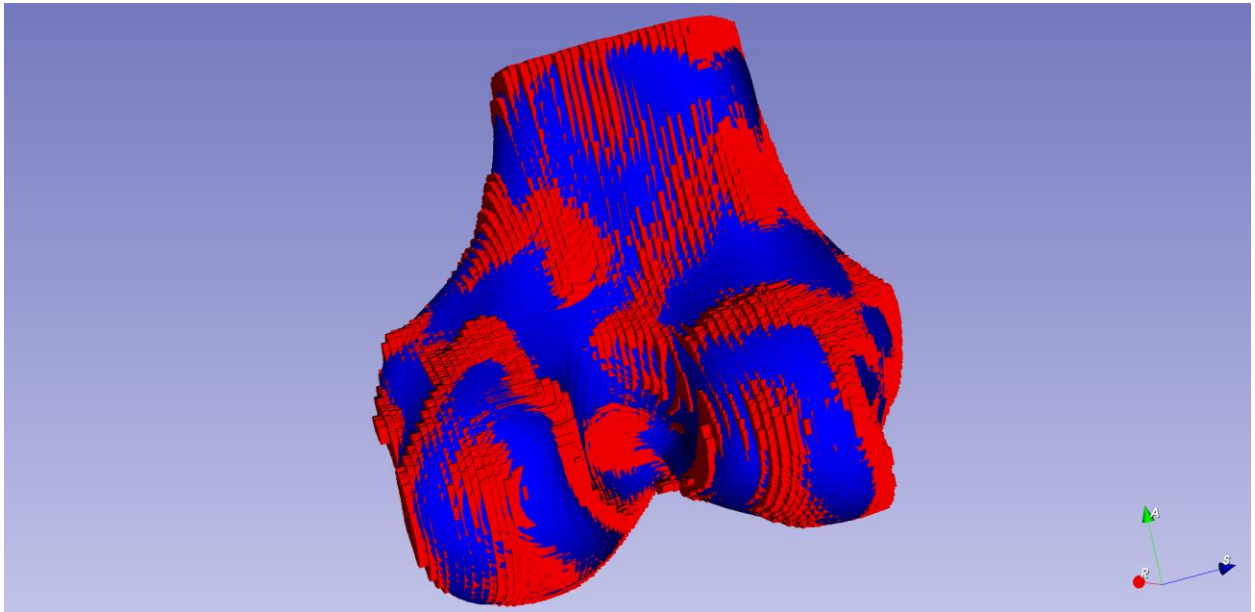


Figure 16: The overlay of the original surface mesh (red) of the femur dataset labeled 001 and the SPHARM surface mesh of it with conformal mapping initialization parametrization with iteration 500 (blue). Since the SPHARM surface with conformal mapping initialization parametrization looks like the femur structure and has a lot of overlapping regions, the SPHARM surface mesh with conformal mapping initialization parametrization is a clear winner over that with heat equation mapping initialization parametrization with 500 iterations. Visualized in 3D Slicer [11] Model Module.

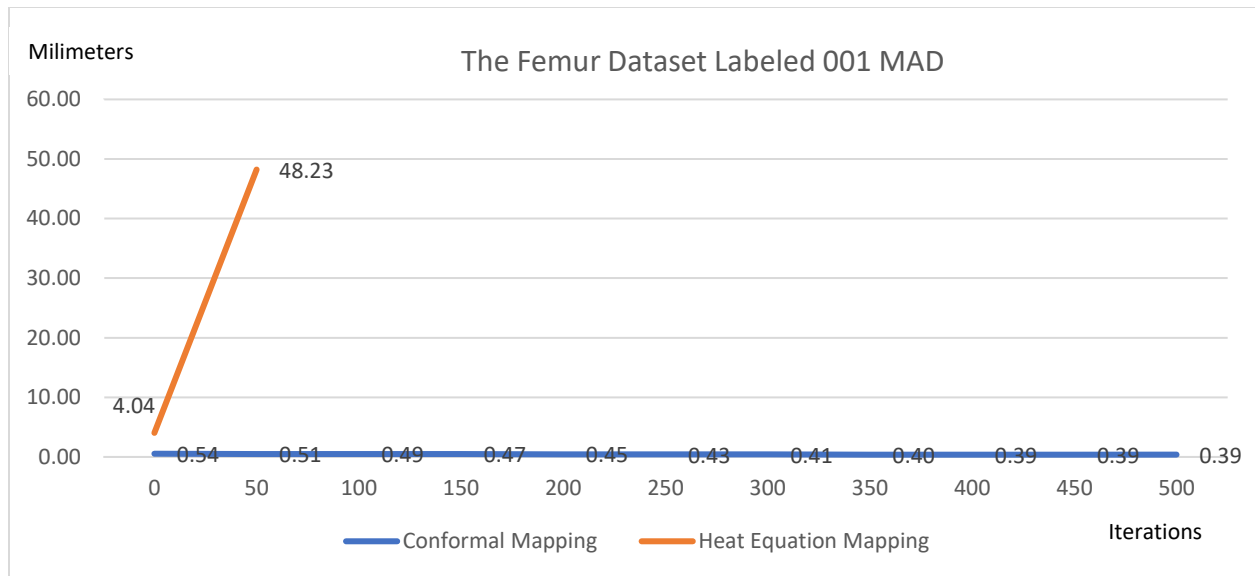


Figure 17: The femur dataset labeled 001 Mean Absolute Distance (MAD). MeshValMet Software failed to make measurement after 50 iterations between the SPHARM surface mesh with heat equation mapping initialization parametrization and the original surface, so the orange line has blanks after 50 iterations. With this much information, it is still clear that conformal mapping initialization parametrization performs very well and consistent in quality on the femur data, yet the SPHARM surface with heat equation mapping initialization parametrization has poor quality overall.

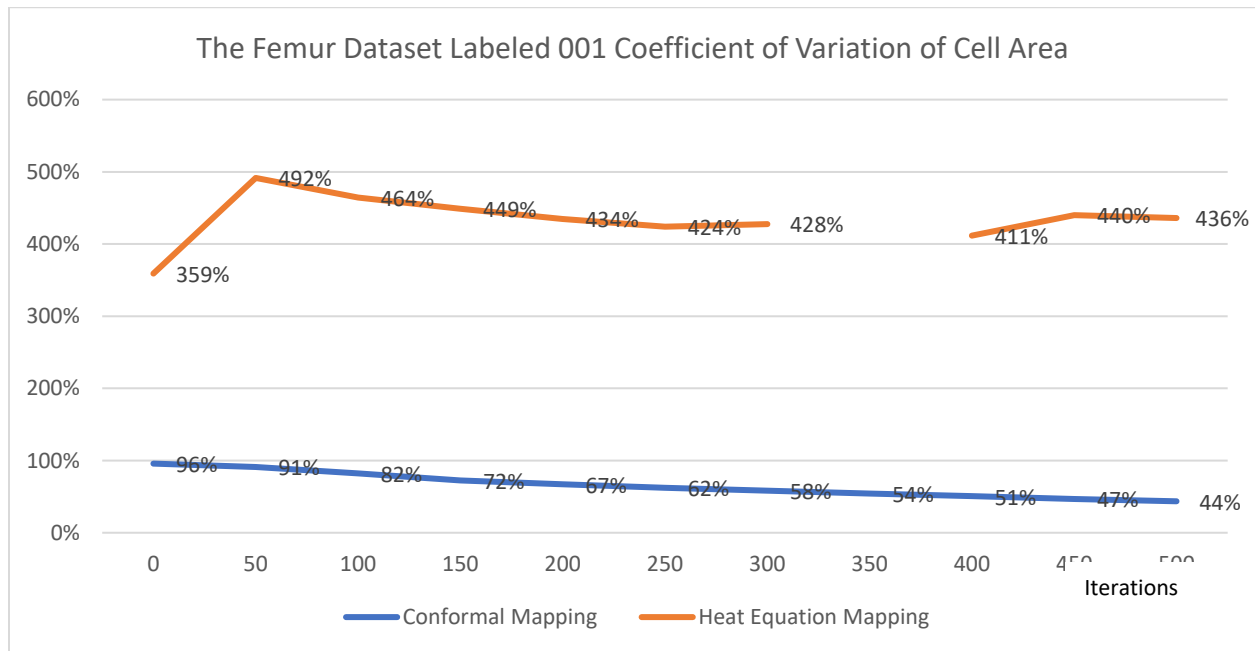


Figure 18: the femur dataset labeled 001 Coefficient of Variation of Cell Area. MeshQuality command line tool crashed when measure the SPHARM surface mesh with heat equation mapping initialization parametrization, so there is a blank on the orange line. However, it is obvious that the SPHARM surfaces with heat equation mapping initialization parametrization has poor and consistent quality overall. And it agrees with the result as suggested in the MAD chart that conformal mapping initialization parametrization provides SPHARM surface meshes with good and consistent quality

The blank spaces were caused by failure of the software to analyze data. Still, with the information acquired, we can see that the quality of SPHARM surface with conformal mapping initialization parametrization is significantly better than that with heat equation mapping initialization parametrization.

(2) The femur dataset labeled 002:

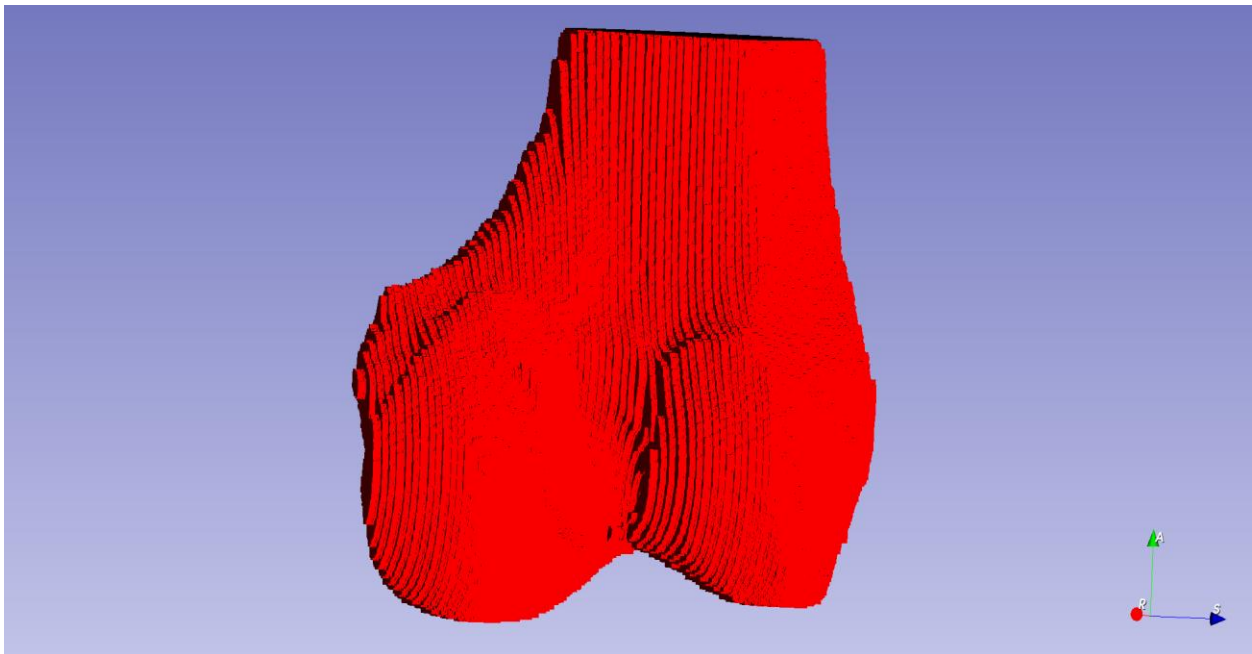


Figure 19: Surface mesh of the femur dataset labeled 002, which is the output of GenParaMesh and will then be mapped onto parametrized spheres with different iterations. Visualized in 3D Slicer [11] Model Module.

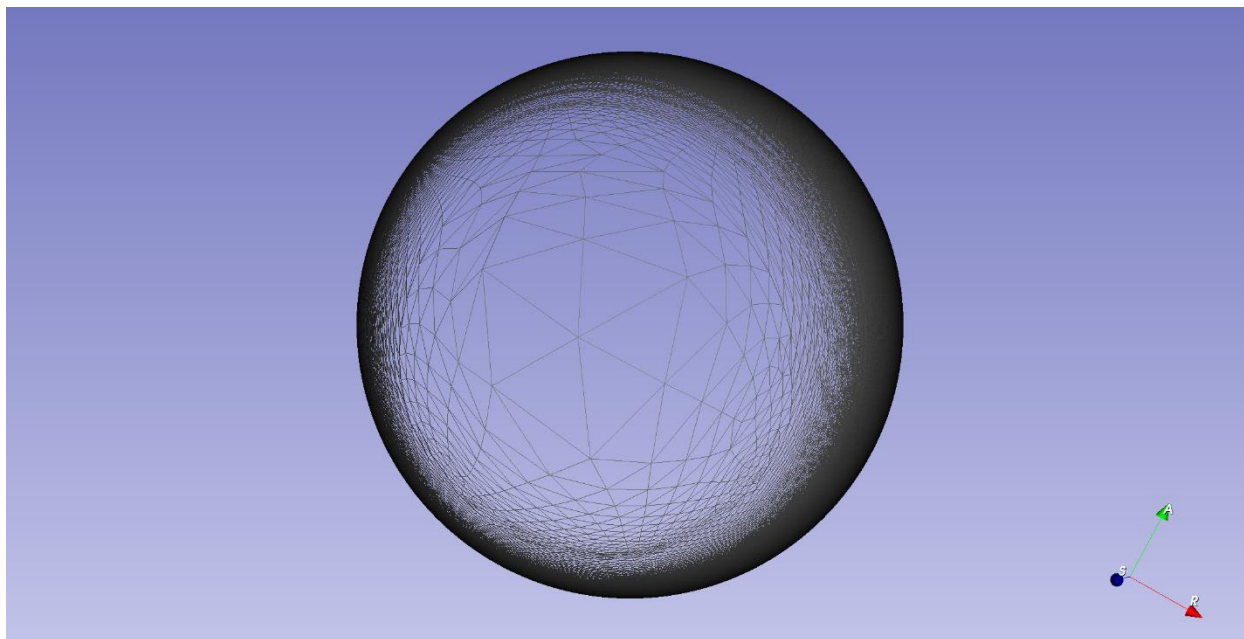


Figure 20: Heat equation mapping as initialization parametrization parametrized sphere of the femur dataset labeled 002 with iteration 0. Because the variation of the triangle size is huge, it has a poor quality. Visualized in 3D Slicer [11] Model Module.

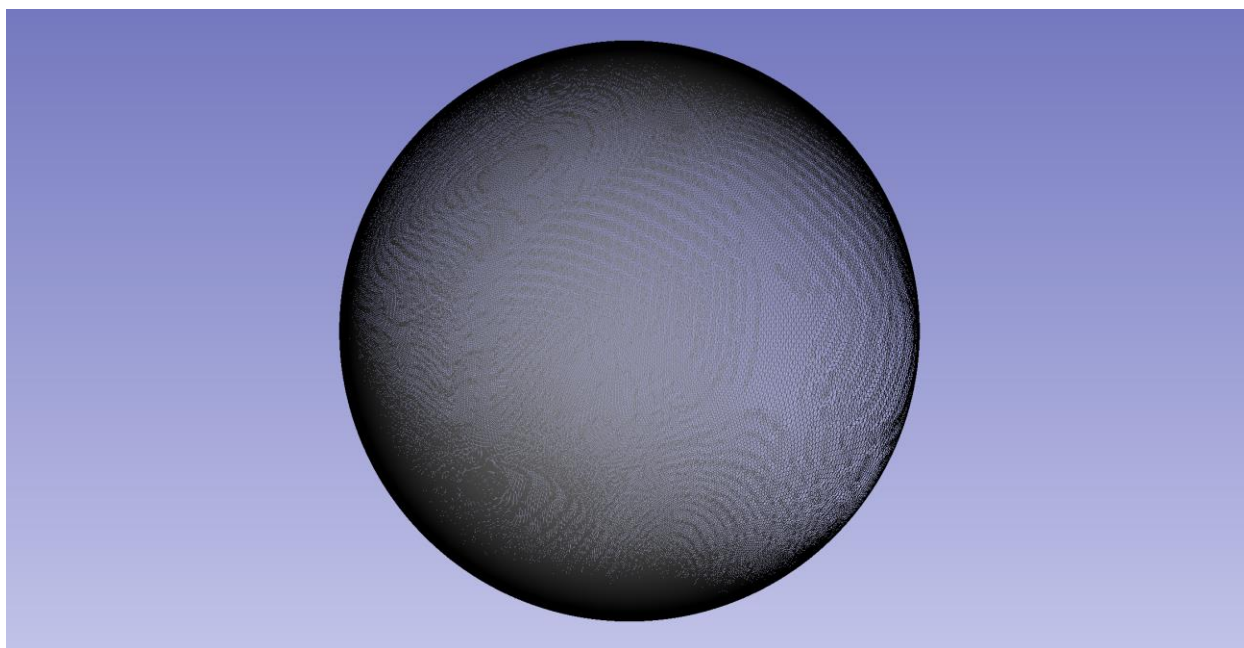


Figure 21: Conformal mapping as initialization parametrization parametrized sphere of the femur dataset labeled 002 with iteration 0. It is a parametrized sphere with small variation in size of triangles and has near uniform density. It can be improved further with more iterations because it has a lot of tilted lines and ripples. Visualized in 3D Slicer [11] Model Module.

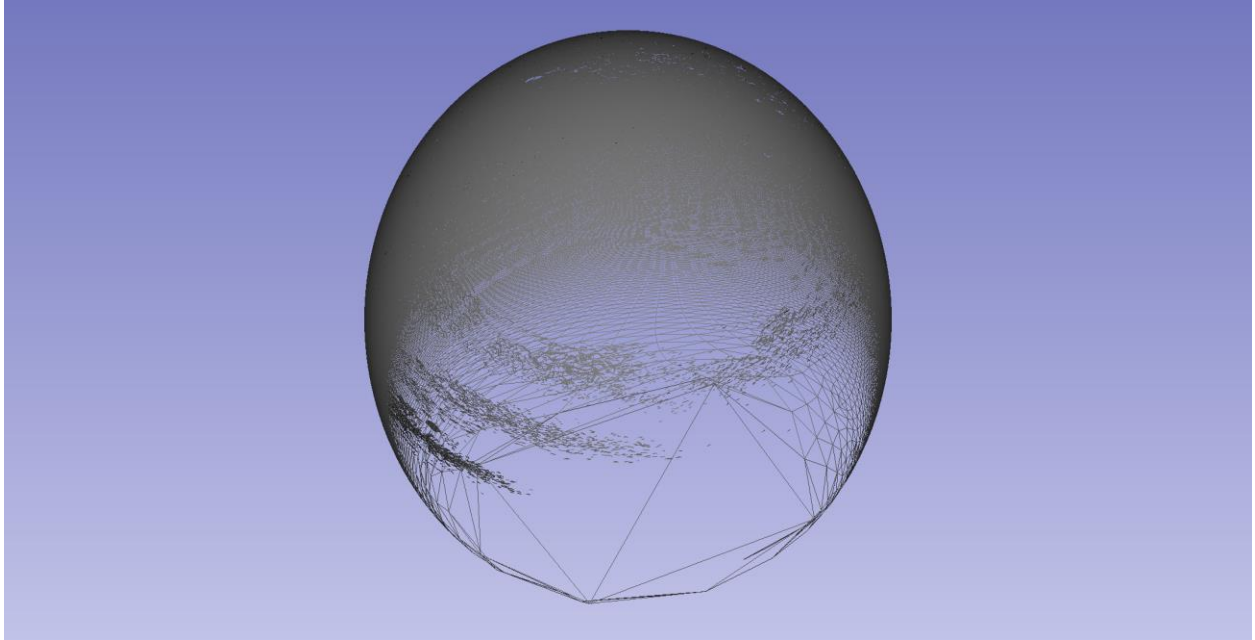


Figure 22: Heat equation mapping as initialization parametrization parametrized sphere of the femur dataset labeled 002 with iteration 50. Since the size of large triangles becomes larger than those in 0 iteration, the quality also becomes poorer. Visualized in 3D Slicer [11] Model Module.

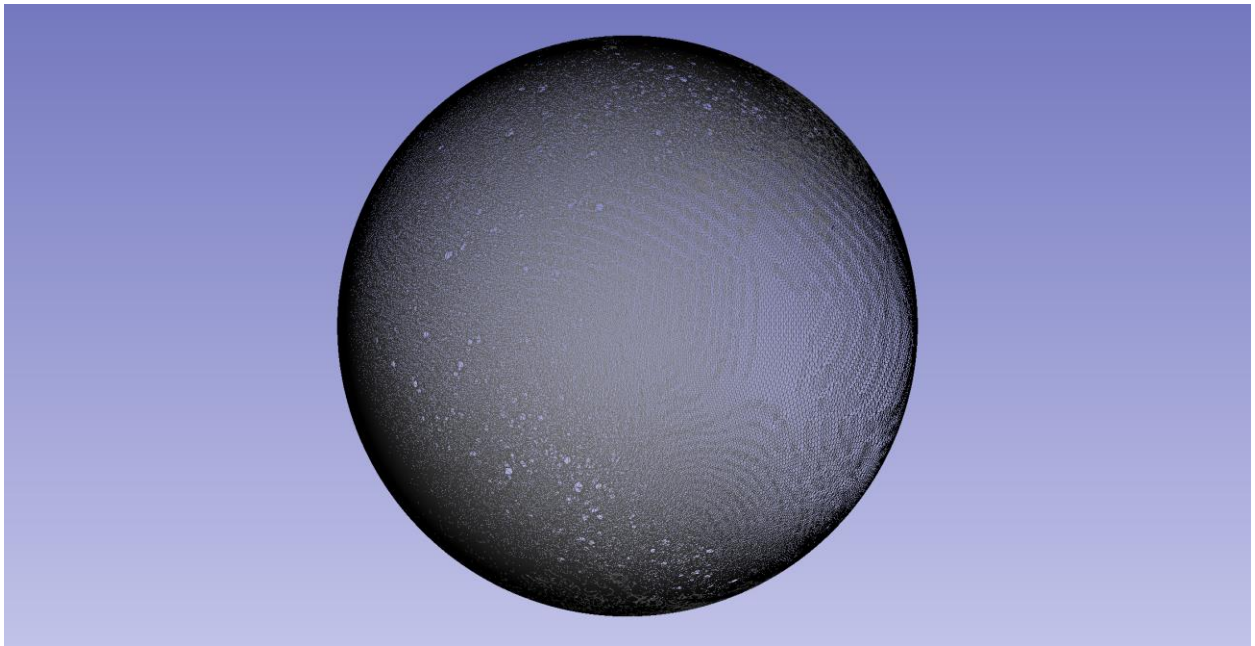


Figure 23: Conformal mapping as initialization parametrization parametrized sphere of the femur dataset labeled 002 with iteration 50. Since there is reduced number of tilted lines and ripples, the quality has also increased from the one with 0 iteration. Visualized in 3D Slicer [11] Model Module.

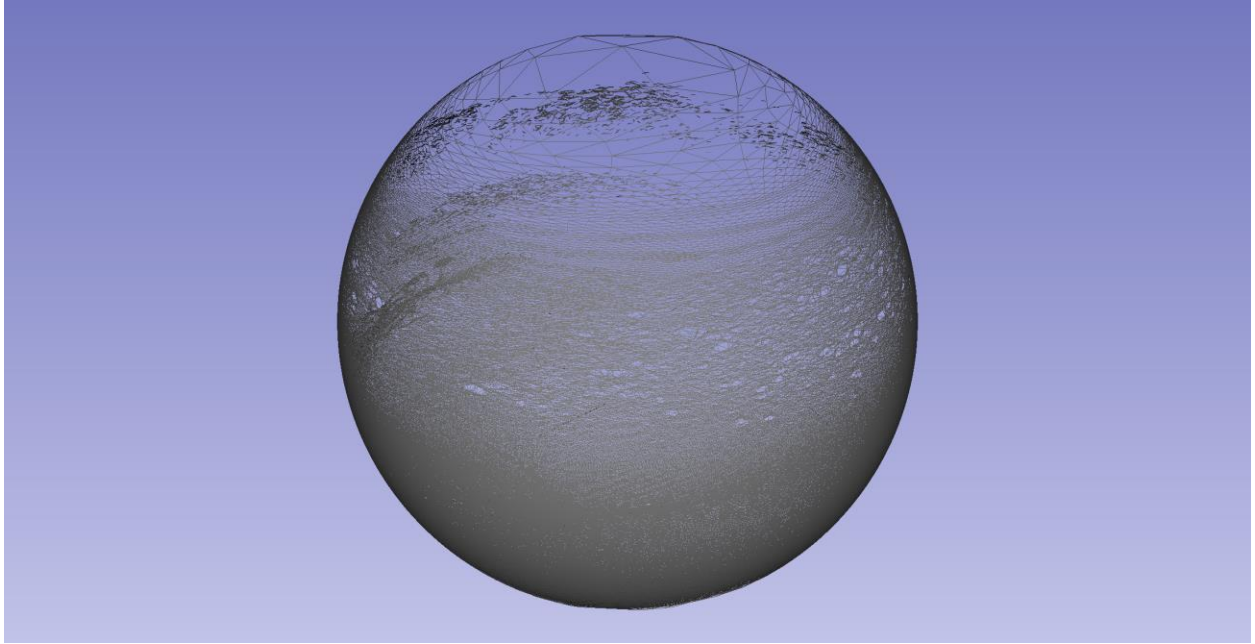


Figure 24: Heat equation mapping as initialization parametrization parametrized sphere of the femur dataset labeled 002 with iteration 100. Since the uniformity of triangle size has increased, it has improved in quality from the one with iteration 50 (even though still not great). Visualized in 3D Slicer [11] Model Module.

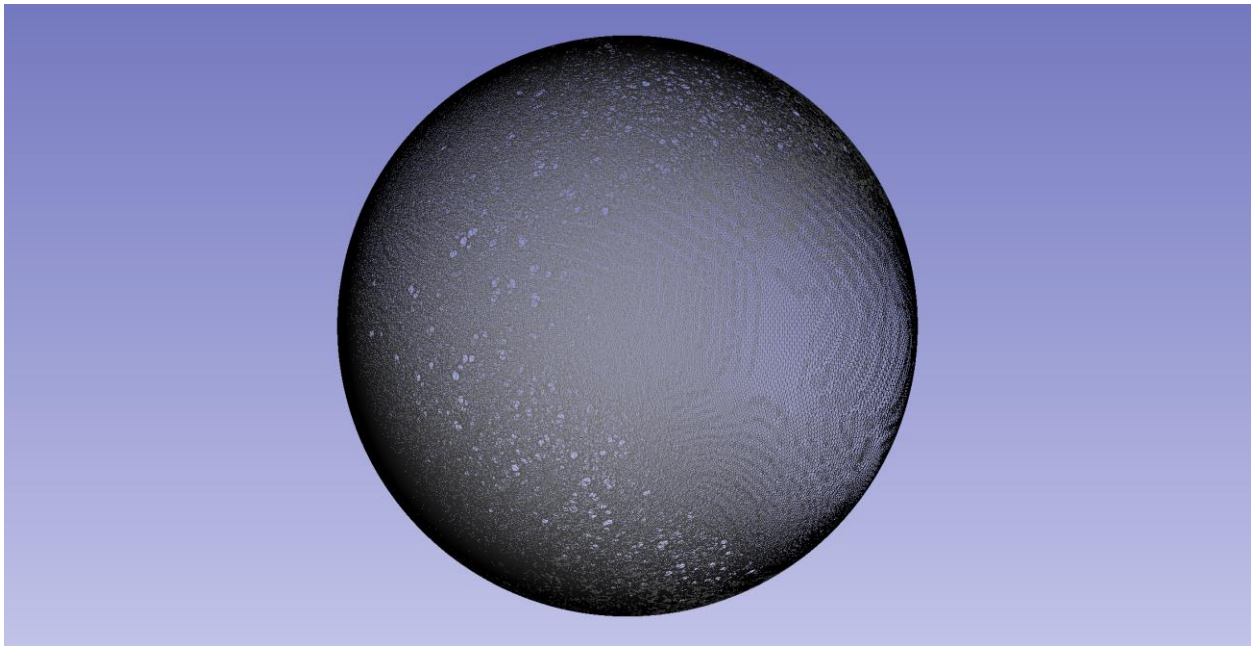


Figure 25: Conformal mapping as initialization parametrization parametrized sphere of the femur dataset labeled 002 with iteration 100. It has nearly the same quality as the one with iteration 50. Visualized in 3D Slicer [11] Model Module.

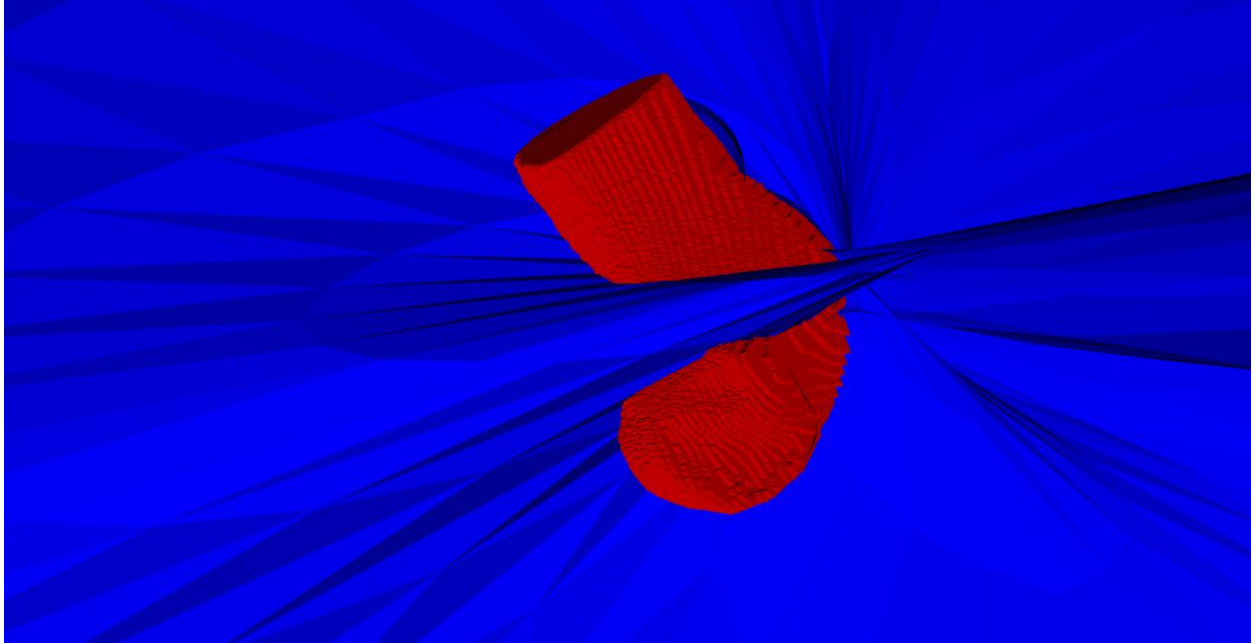


Figure 26: The overlay of the original surface mesh (red) of the femur dataset labeled 002 and the SPHARM surface mesh of it with heat equation mapping initialization parametrization with iteration 500 (blue). Since the SPHARM surface (blue) does not even look like the femur structure, it is clear that the SPHARM surface with heat equation mapping initialization parametrization failed to provide a good representation of the original surface mesh. Visualized in 3D Slicer [11] Model Module.

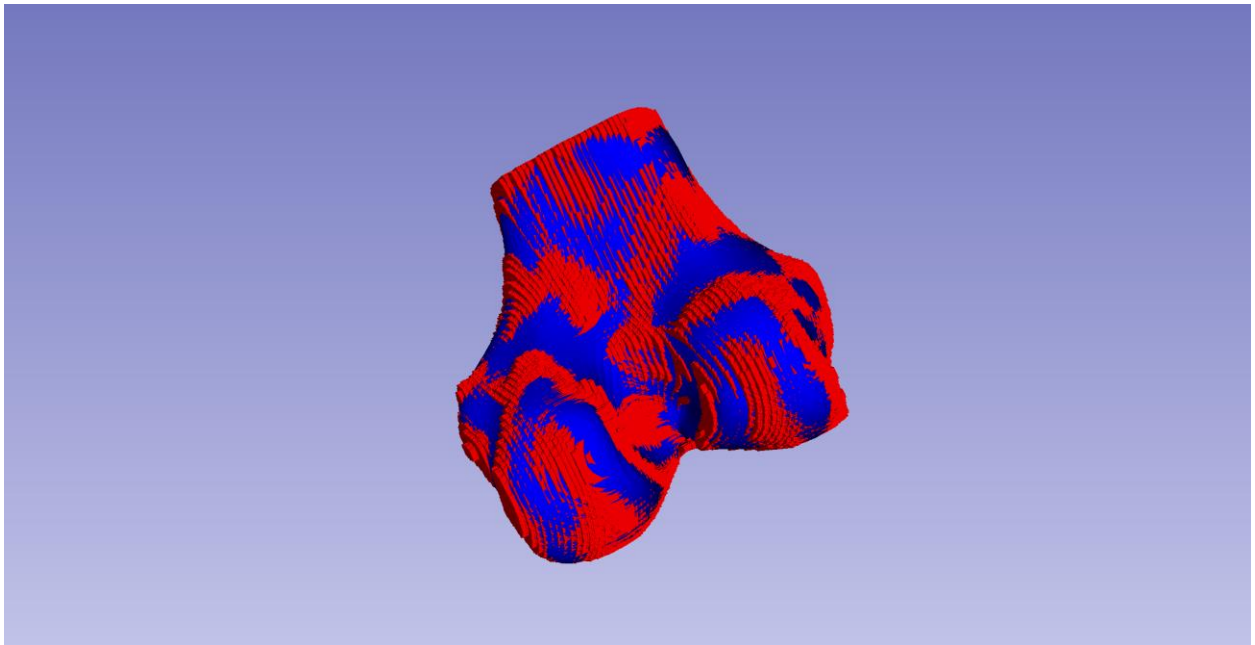


Figure 27: The overlay of the original surface mesh (red) of the femur dataset labeled 002 and the SPHARM surface mesh of it with conformal mapping initialization parametrization with iteration 500 (blue). Since the SPHARM surface with conformal mapping initialization parametrization looks like the femur structure and has a lot of overlapping regions, the SPHARM surface mesh with conformal mapping initialization parametrization is a clear winner over that with heat equation mapping initialization parametrization with 500 iterations. Visualized in 3D Slicer [11] Model Module.

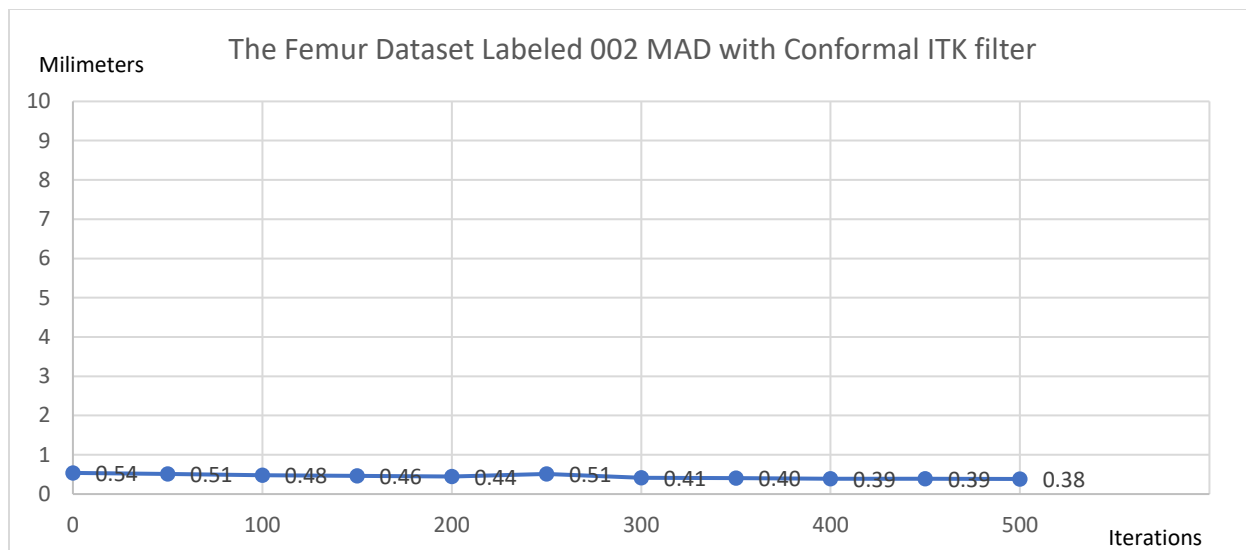


Figure 28: The femur dataset labeled 002 Mean Absolute Distance (MAD). MeshValMet Software failed to make measurement between the SPHARM surface mesh with heat equation mapping initialization parametrization and the original surface, so unfortunately, I am unable to compare the mean absolute distance in this dataset. However, it is certain that the conformal mapping initialization parametrization performs well.

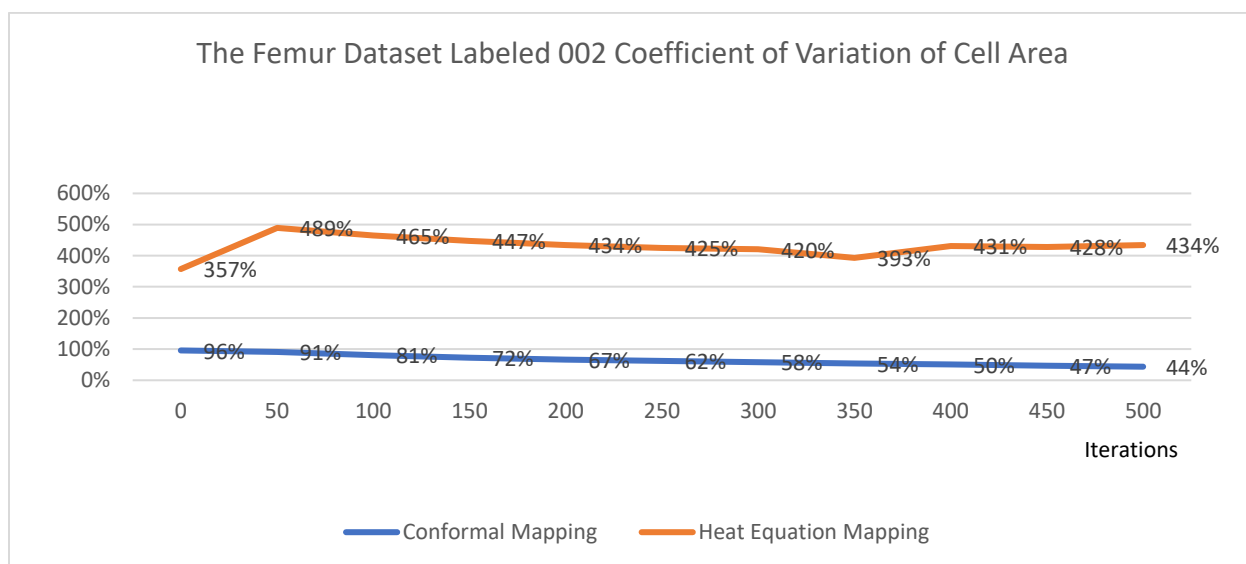


Figure 29: The femur dataset labeled 002 Coefficient of Variation of Cell Area. It is clear that conformal mapping initialization parametrization is better than heat equation mapping initialization parametrization for the femur dataset labeled 002. In general, the heat equation mapping initialization parametrization does 4-5 times worse than the conformal mapping initialization parametrization and nearly 10 times worse when iteration increases to 500

Since we are only able to acquire the MAD of SPHARM surface mesh with conformal mapping initialization parametrization because of the MeshValMat software's limitation, we can only argue that conformal mapping initialization parametrization performs well on the femur dataset labeled 002. With the Coefficient of Variation of Cell Area chart, we can clearly see that the quality of the SPHARM surface meshes with conformal mapping initialization parametrization is significantly better than those with heat equation mapping initialization parametrization for the femur datasets.

The molar datasets:

All of the sixteen Molar datasets can be reconstructed as SPHARM surface using either conformal mapping initialization parametrization or heat equation mapping initialization parametrization. I measured three of the sixteen datasets to compare the quality of reconstructed SPHARM surface with two initialization parametrization.

The molar dataset labeled a10:

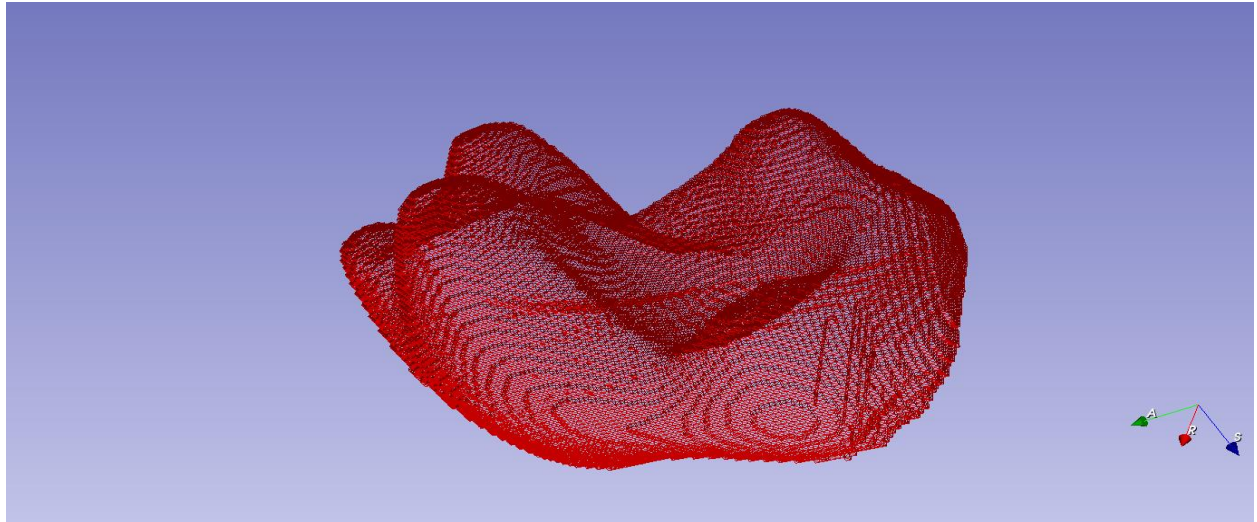


Figure 30: Surface mesh of the molar Dataset labeled a10, which is the output of GenParaMesh and will then be mapped onto parametrized spheres with different iterations. Visualized in 3D Slicer[11] Model Module.

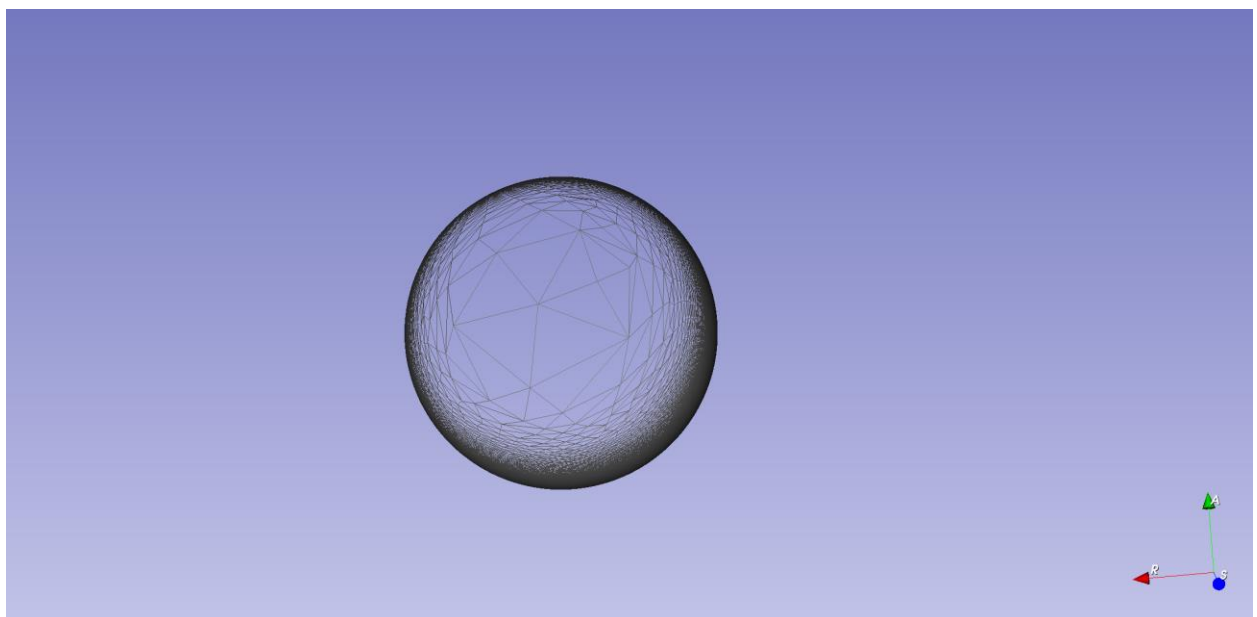


Figure 11: Heat equation mapping as initialization parametrization parametrized sphere of the molar dataset labeled a10 with iteration 0, it is not a good parametrization because it has a large variation in triangle size. Visualized in 3D Slicer [11] Model Module

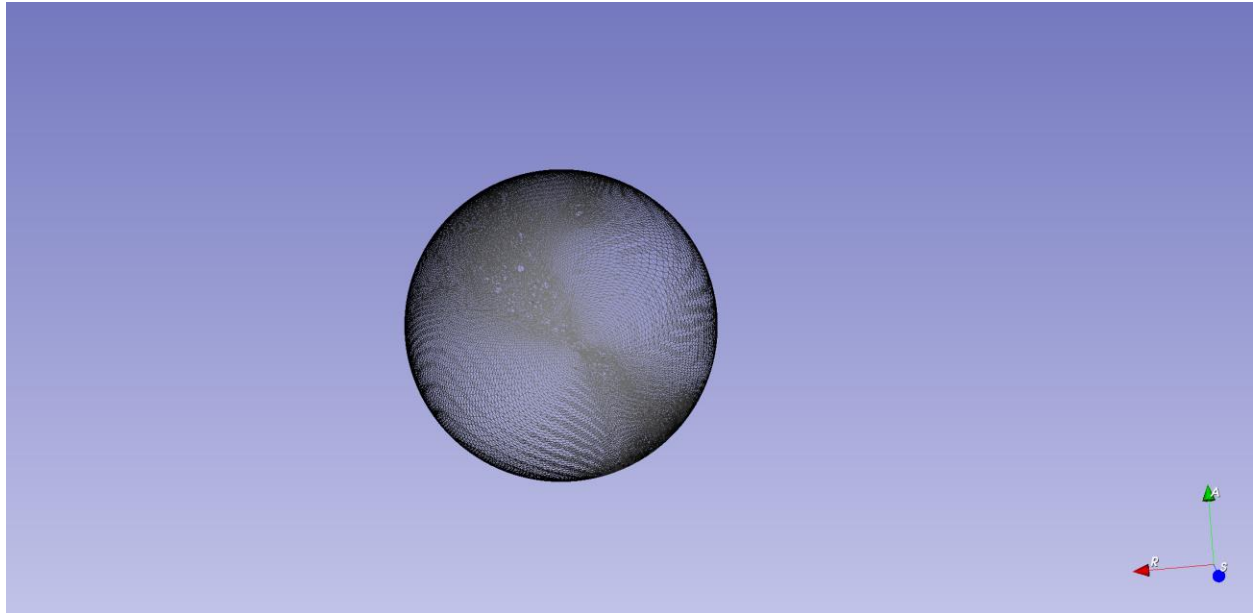


Figure 32: Conformal mapping as initialization parametrization parametrized sphere of the molar dataset labeled a10 with iteration 0. It is a parametrized sphere with small variation in size of triangles and has near uniform density. Visualized in 3D Slicer [11] Model Module.

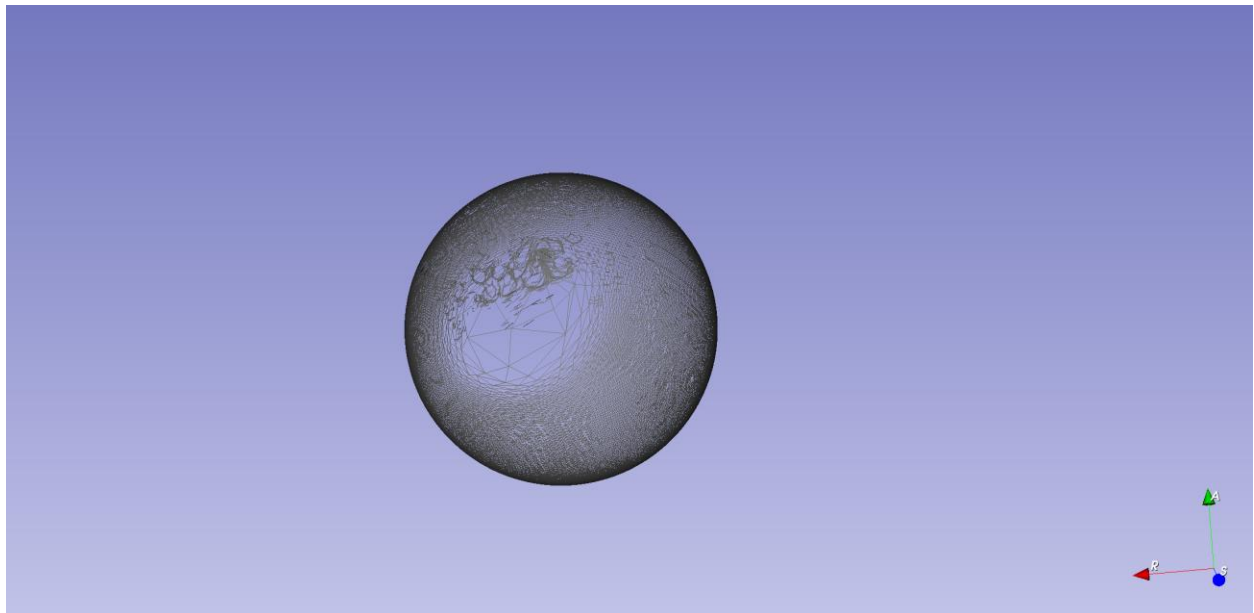


Figure 33: Heat equation mapping as initialization parametrization parametrized sphere of the molar dataset labeled a10 with iteration 50, it is still not a good parametrization because it has a large variation in the size of triangles (even though increasing in uniformity of the triangle size than the one with 0 iteration). Visualized in 3D Slicer [11] Model Module

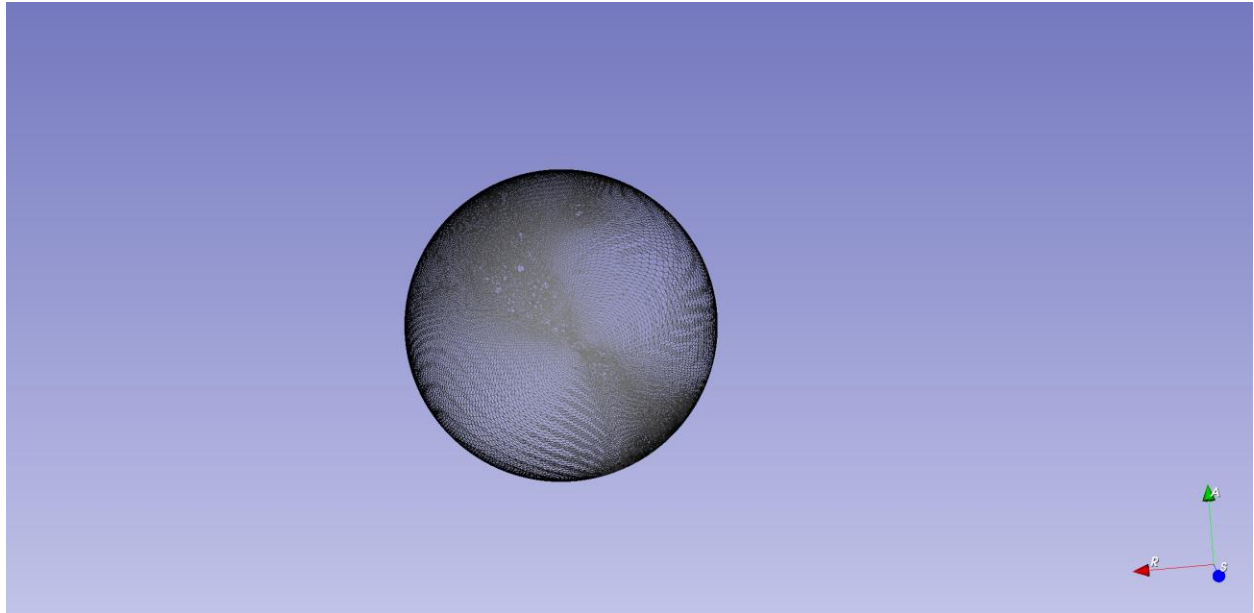


Figure 34: Conformal mapping as initialization parametrization parametrized sphere of the molar dataset labeled a10 with iteration 50. It is a parametrized sphere with small variation in size of triangles and has near uniform density. However, it does not improve much from iteration 0. Visualized in 3D Slicer [11] Model Module.

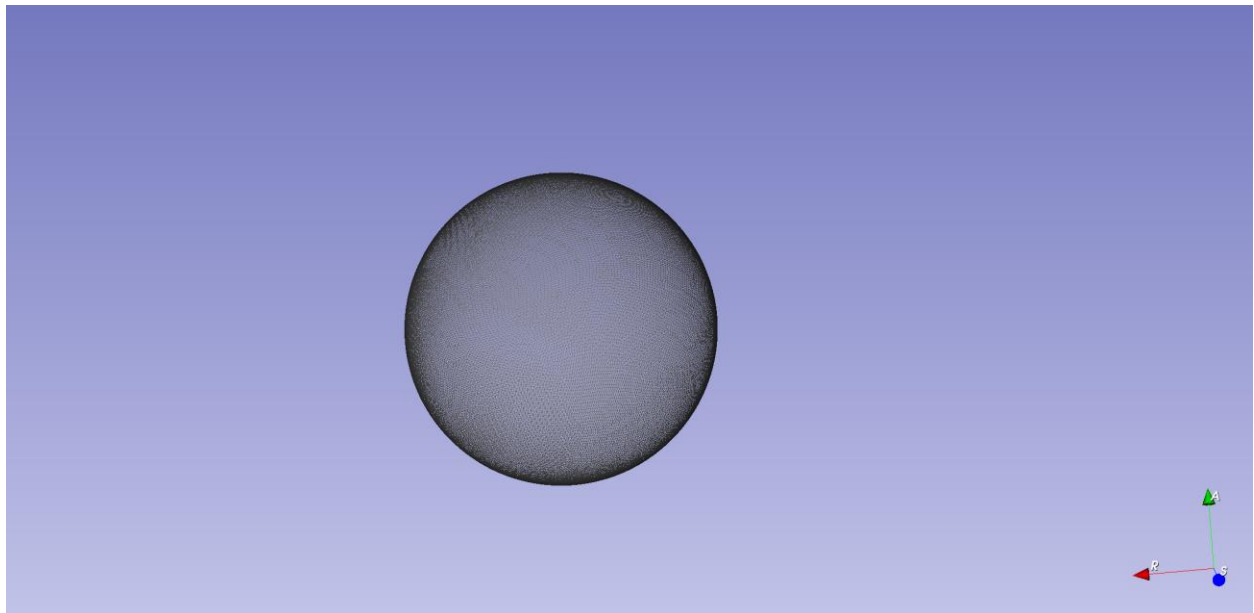


Figure 35: Heat equation mapping as initialization parametrization parametrized sphere of the molar dataset labeled a10 with iteration 100, it is an extremely good parametrization since it has excellent uniformity in triangle size and even looks slightly better compared with conformal mapping initialization parametrization parametrized sphere with same number of iterations. Visualized in 3D Slicer [11] Model Module

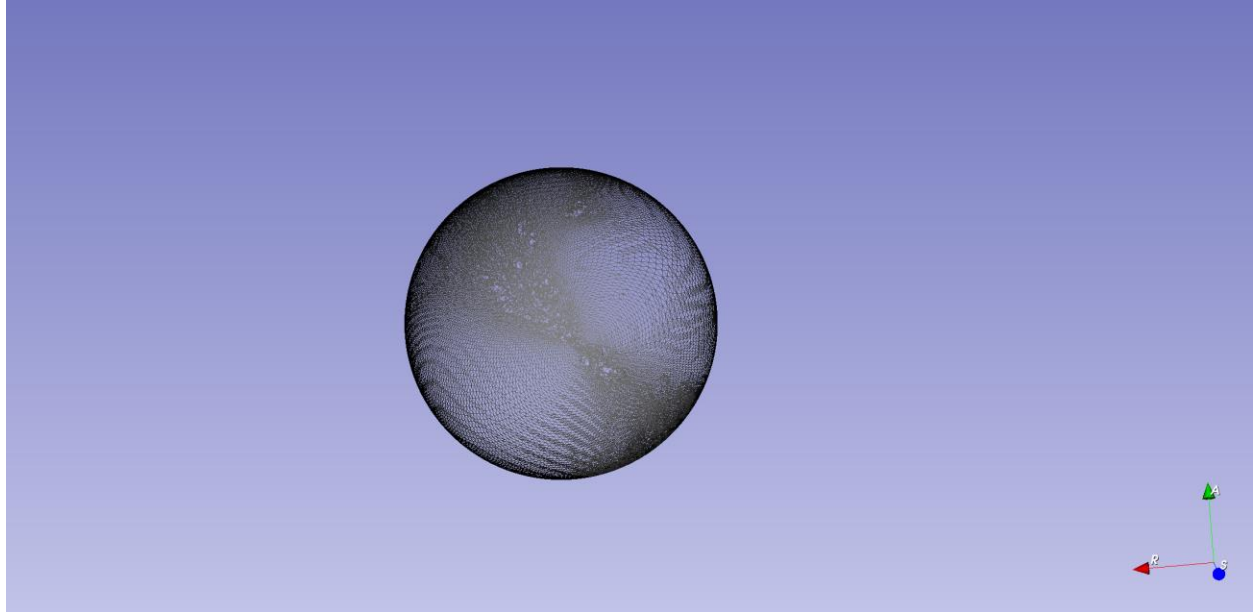


Figure 36: Conformal mapping as initialization parametrization parametrized sphere of the molar dataset labeled a10 with iteration 100. It is a parametrized sphere with small variation in size of triangles and has near uniform density and is consistent in quality as the one with iteration 0 and 50. Visualized in 3D Slicer [11] Model Module.

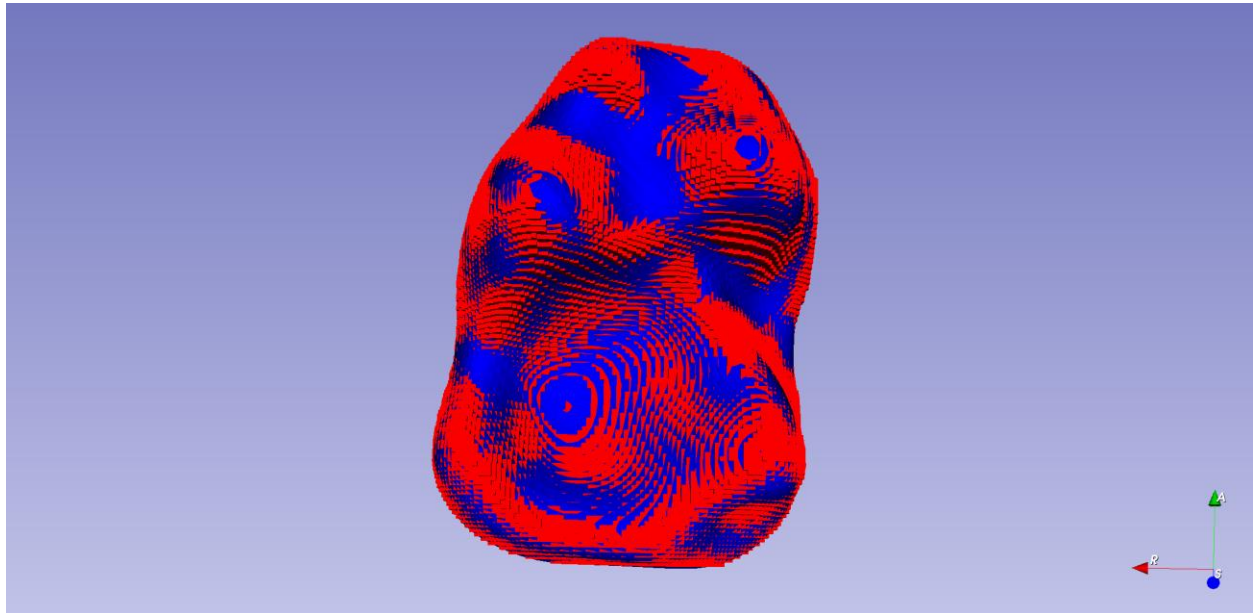


Figure 37: The overlay of the original surface mesh (red) of the molar dataset labeled a10 and the SPHARM surface mesh of it with heat equation mapping initialization parametrization with iteration 500 (blue). It has extremely high level of overlay since the blue and the red one intervened with each other; both have the correct and similar shape. Visualized in 3D Slicer [11] Model Module.

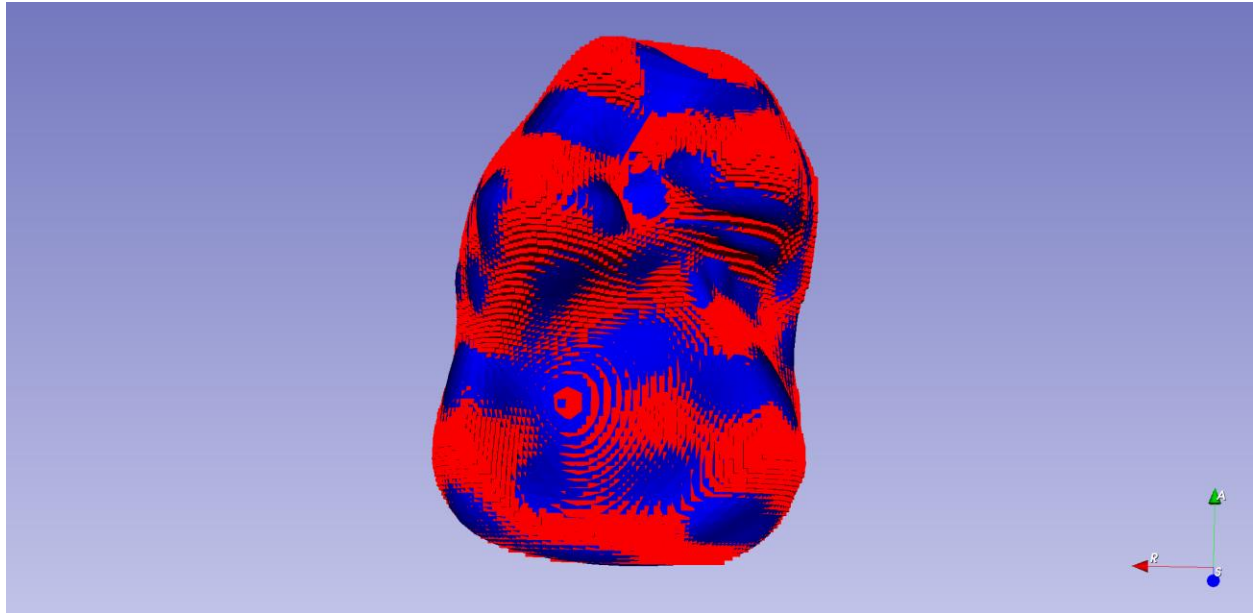


Figure 38: The surface mesh overlay of the femur dataset labeled 002 of the original surface mesh (red) and the SPHARM surface mesh with conformal mapping initialization with iteration 500 (blue). It is hard to tell whether conformal mapping initialization parametrization or heat equation initialization parametrization is better because both have similar level of overlapping with the original surface and slimier shape as the original surface. Visualized in 3D Slicer [11] Model Module.

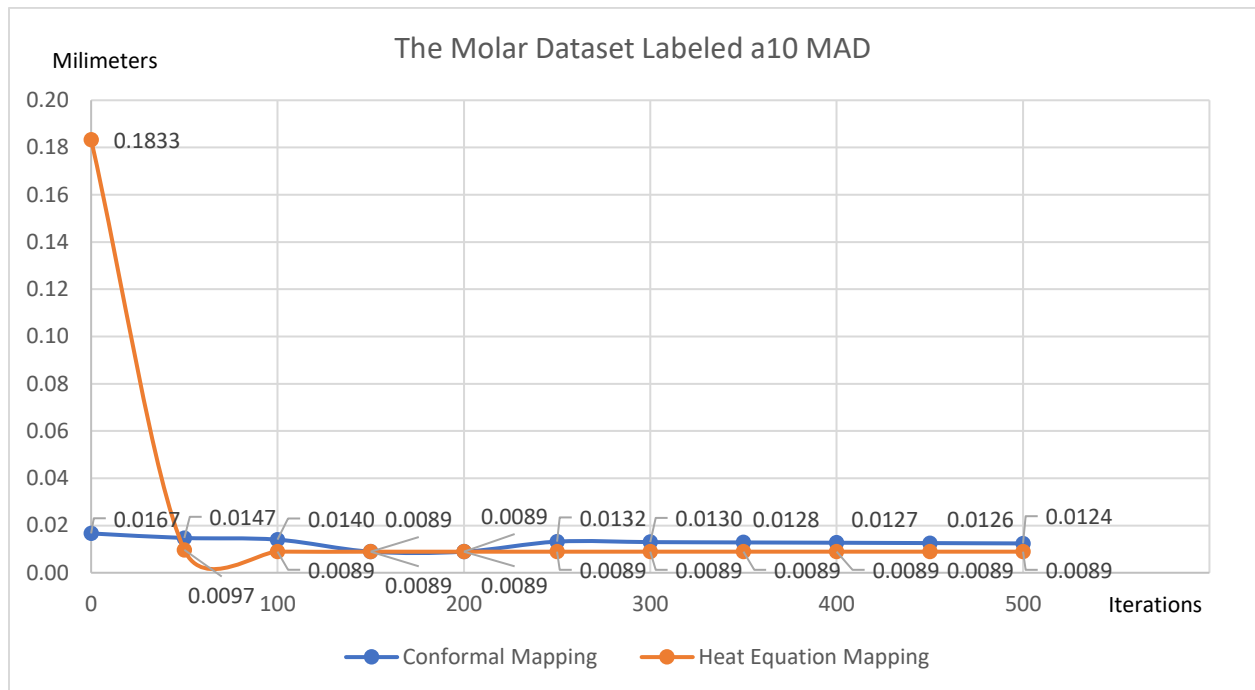


Figure 39: Molar Dataset Labeled a10 Mean Absolute Distance (MAD). Clearly, the heat equation mapping initialization parametrization does poorly with 0 iteration but the improvement by the following optimization procedure is huge. On the contrary, the conformal mapping initialization parametrization does extremely well with 0 iterations and performs very consistently with more iterations. Surprisingly, the heat equation mapping initialization parametrization, after being corrected by its following optimization procedure, does slightly better than conformal mapping initialization parametrization

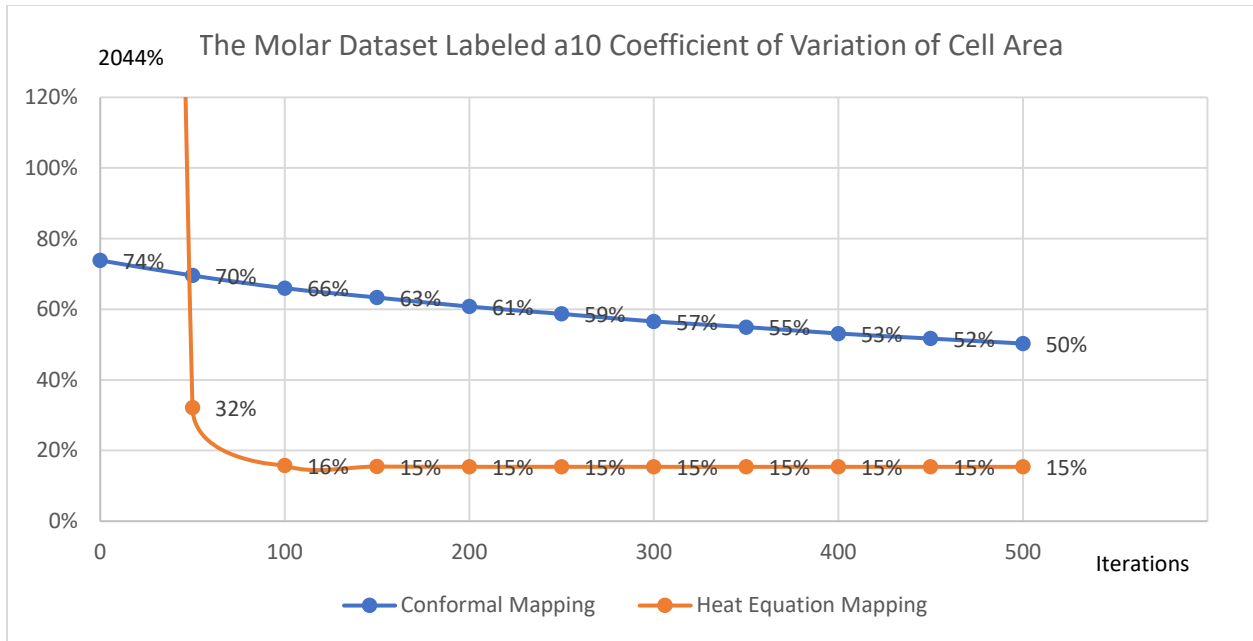


Figure 40: Molar Dataset Labeled a10 Coefficient of Variation of Cell Area. At iterations 0, heat equation mapping initialization parametrization performs extremely bad but when iteration number becomes larger, it quickly converges to a level of extremely good quality. Comparatively, conformal mapping initialization parametrization does well on 0 iteration but the optimization procedure does not improve its quality too much. With iterations at or above 50 (at most), the heat equation mapping initialization parametrization outperforms the conformal mapping initialization parametrization.

The molar dataset labeled a13:

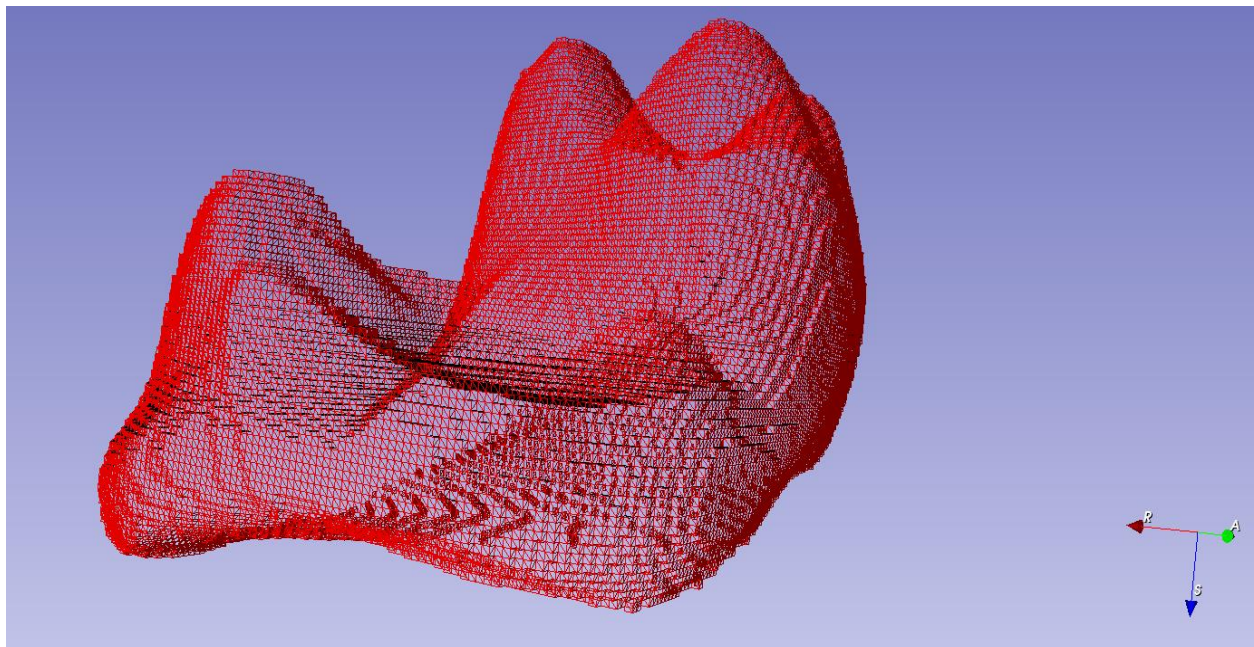


Figure 41: Surface mesh of the molar Dataset labeled a13, which is the output of GenParaMesh and will then be mapped onto parametrized spheres with different iterations. Visualized in 3D Slicer [11] Model Module.

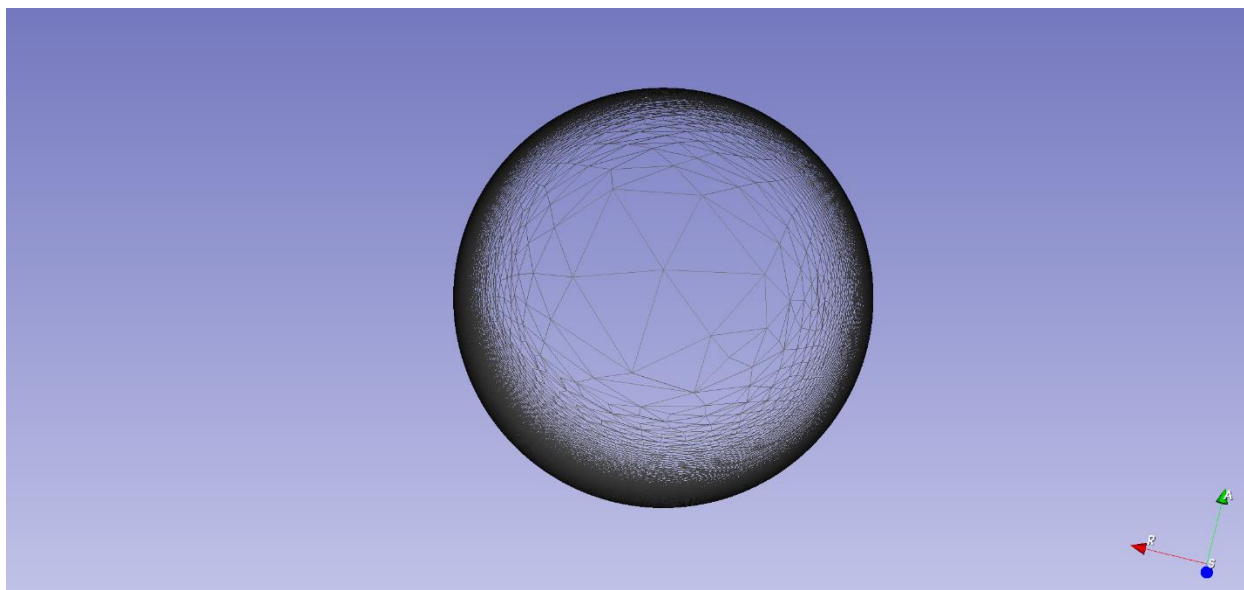


Figure 42: Heat equation mapping as initialization parametrization parametrized sphere of the molar dataset labeled a13 with iteration 0, it is not a good parametrization because the variation of triangle size is huge. Visualized in 3D Slicer [11] Model Module

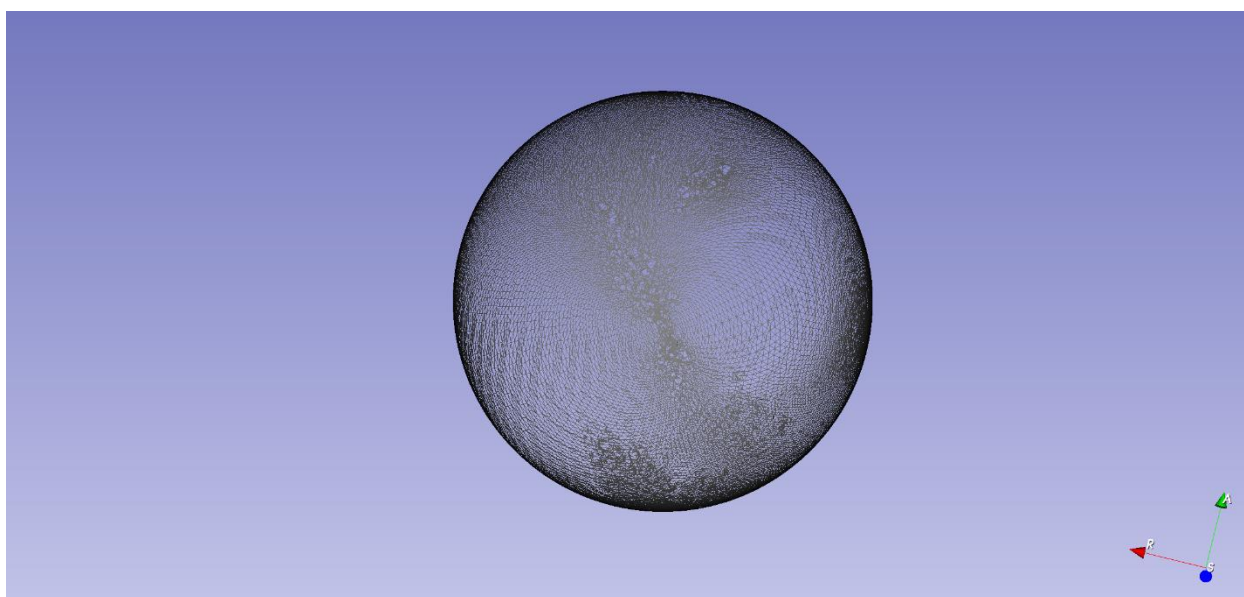


Figure 43: Conformal mapping as initialization parametrization parametrized sphere of the molar dataset labeled a13 with iteration 0. It is a parametrized sphere with small variation in size of triangles and has near uniform density. Visualized in 3D Slicer [11] Model Module.

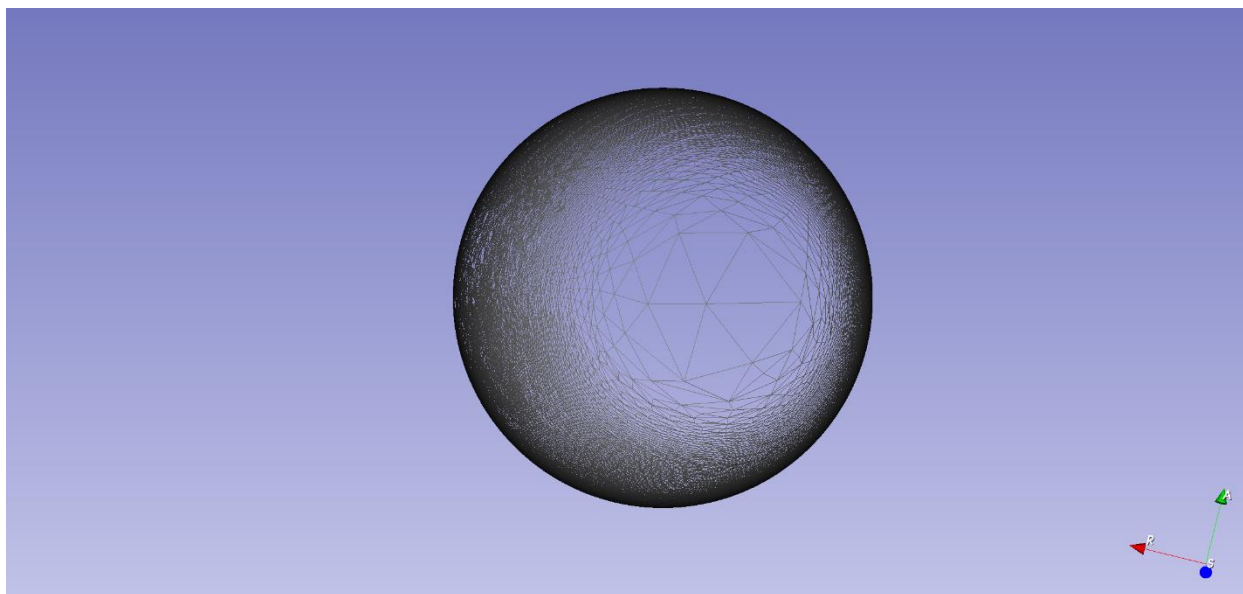


Figure 44: Heat equation mapping as initialization parametrization parametrized sphere of the molar dataset labeled a13 with iteration 50, it is not a good parametrization because it has a large variation in triangle size but it is better (increase in uniformity of triangle size) than iteration 0. Visualized in 3D Slicer [11] Model Module

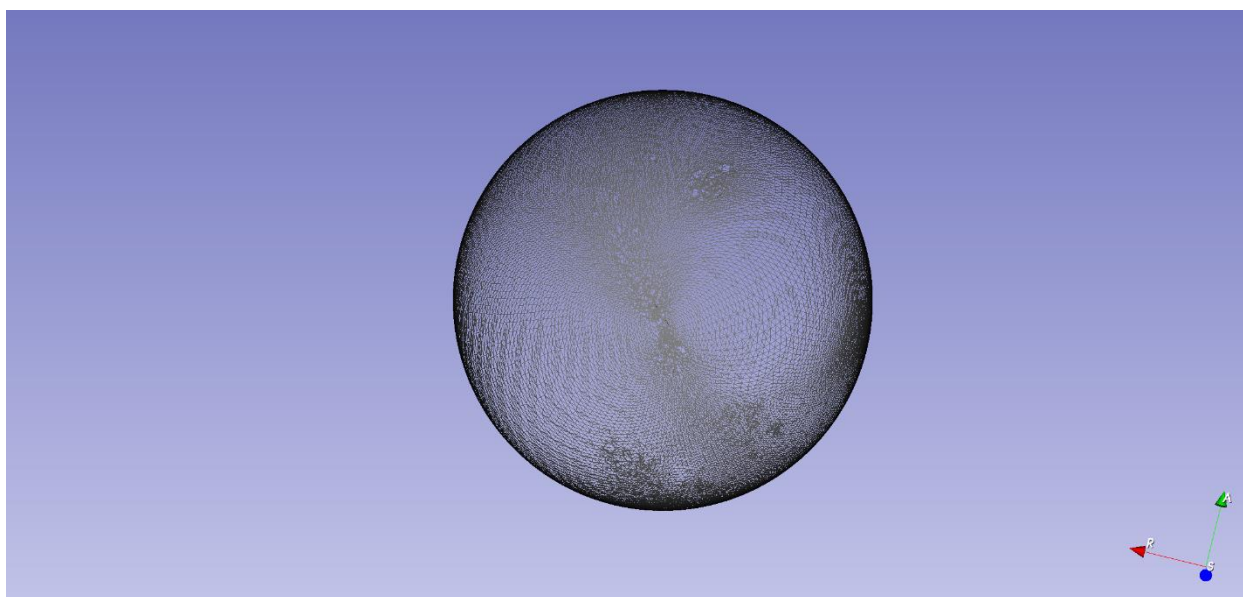


Figure 45: Conformal mapping as initialization parametrization parametrized sphere of the molar dataset labeled a13 with iteration 50. It is a parametrized sphere with small variation in size of triangles and has near uniform density, consistent in quality with the one with iteration 0. Visualized in 3D Slicer [11] Model Module.

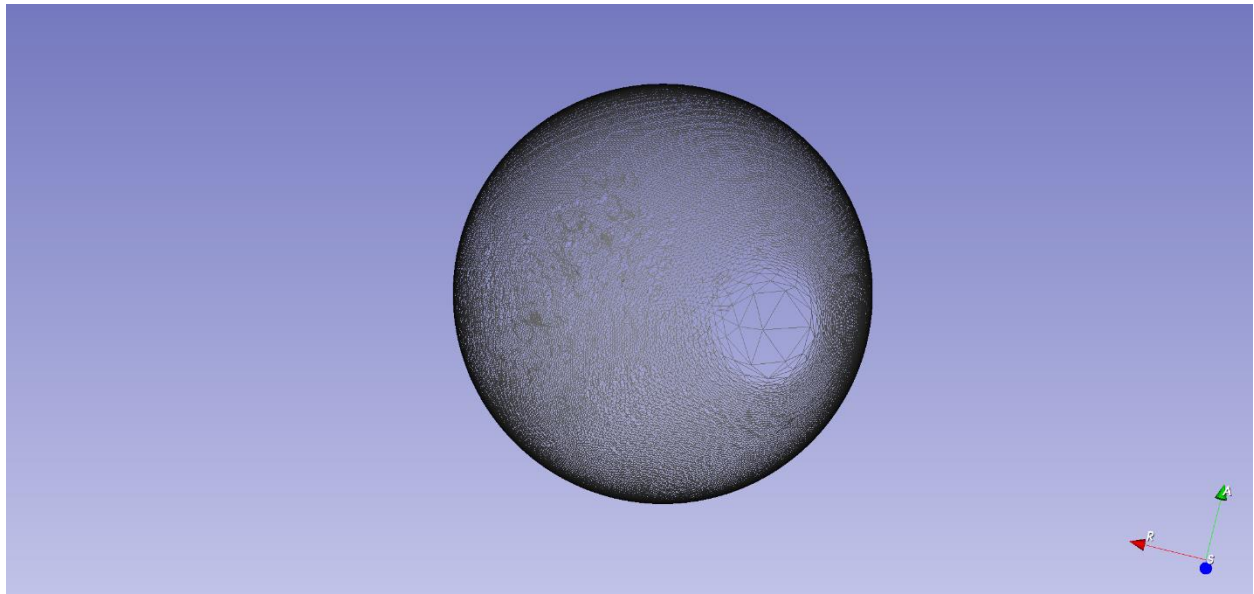


Figure 46: Heat equation mapping as initialization parametrization parametrized sphere of the molar dataset labeled a13 with iteration 100, it is not a good parametrization because it has a large variation of triangle size, but it is better (increase in uniformity of triangle size) than iteration 50. Visualized in 3D Slicer [11] Model Module

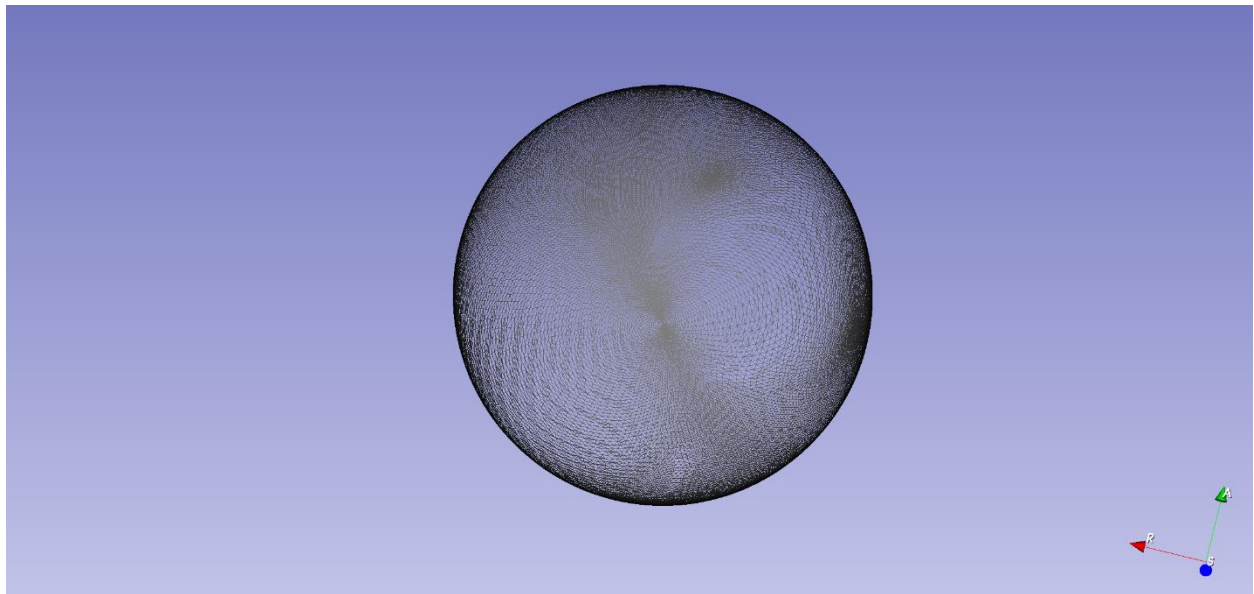


Figure 47: Conformal mapping as initialization parametrization parametrized sphere of the molar dataset labeled a13 with iteration 100. It is parametrized sphere with small variation in size of triangles and has near uniform density, consistent with the one with iteration 0 and 50. Visualized in 3D Slicer [11] Model Module.

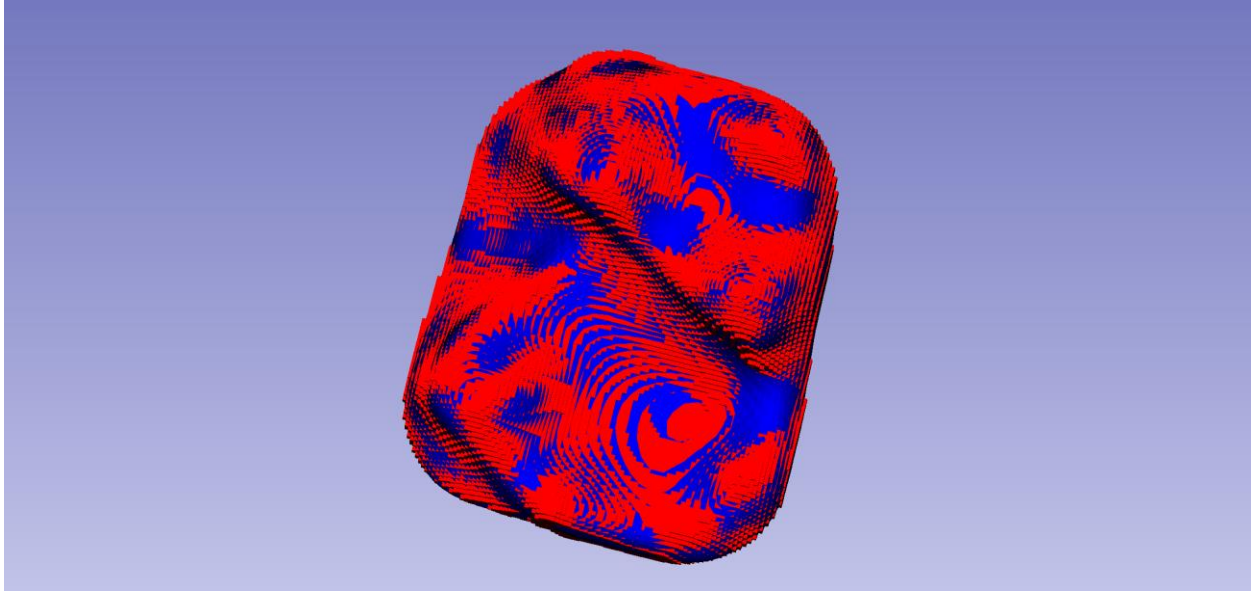


Figure 48: The surface mesh overlay of the molar dataset labeled a13 of the original surface mesh (red) and the SPHARM surface mesh with heat equation mapping initialization parametrization with iteration 500 (blue). The rate of overlapping and the level of similarity between the two surfaces is high, so the reconstruction quality is fairly good. Visualized in 3D Slicer [11] Model Module.

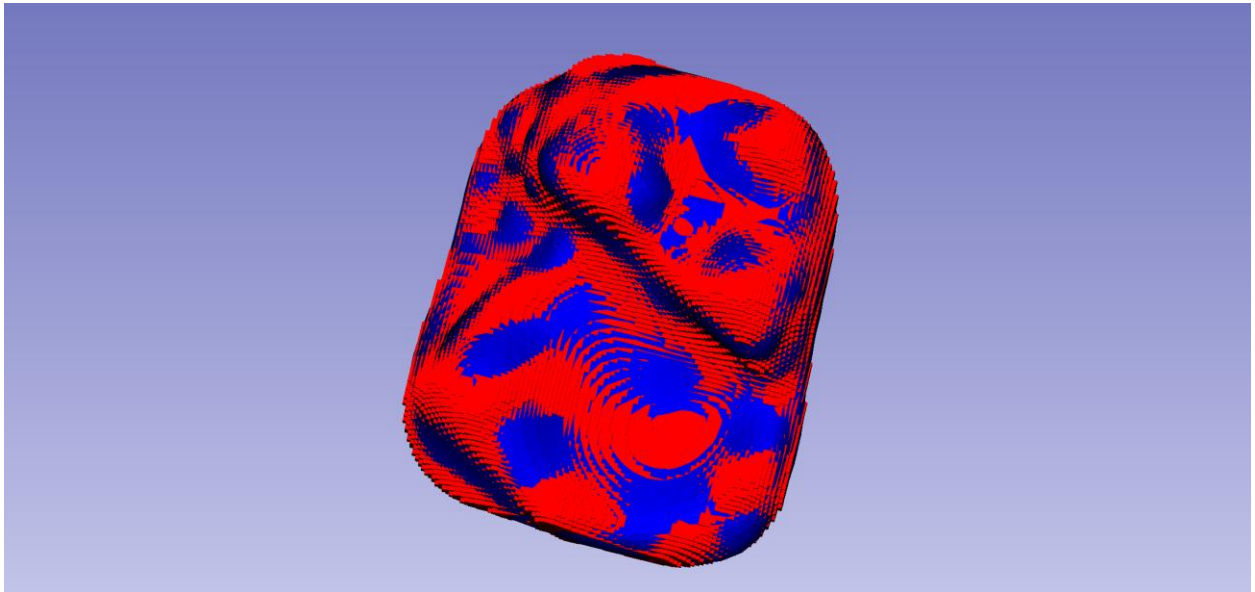


Figure 49: The surface mesh overlay of the molar dataset labeled a13 of the original surface mesh (red) and the SPHARM surface mesh with conformal mapping initialization parametrization with iteration 500 (blue). The quality of reconstruction is also good. It is hard to tell whether the SPHARM surface mesh with conformal mapping initialization parametrization or heat equation initialization parametrization is better through visualization. Visualized in 3D Slicer [11] Model Module.

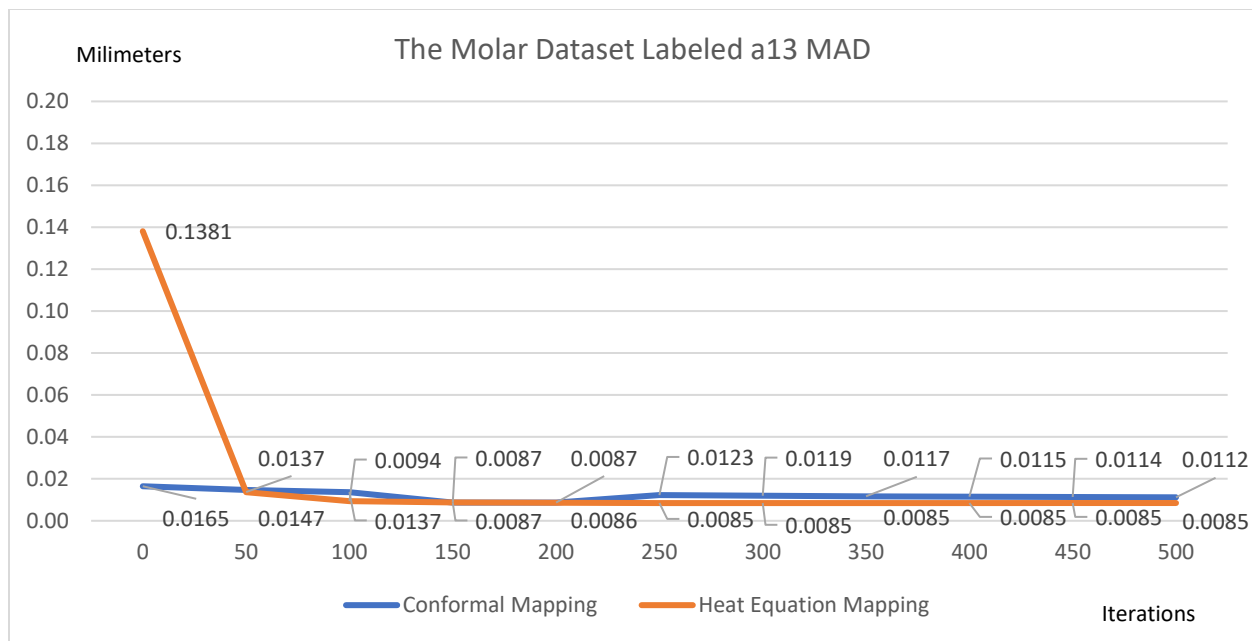


Figure 50: Molar Dataset Labeled a13 Mean Absolute Distance (MAD). The pattern is similar to that of the molar dataset labeled a10.

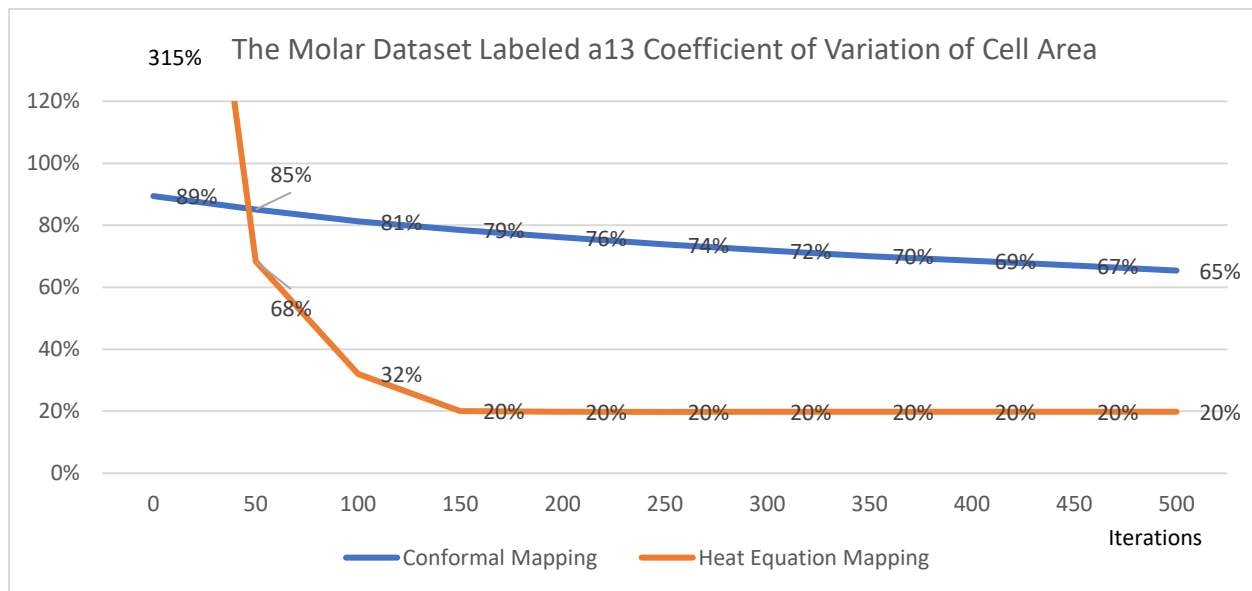


Figure 51: Molar Dataset Labeled a13 Coefficient of Variation of Cell Area. The pattern of Coefficient of variation of Cell Area is similar to that of the molar dataset labeled a10.

The molar dataset labeled b01:

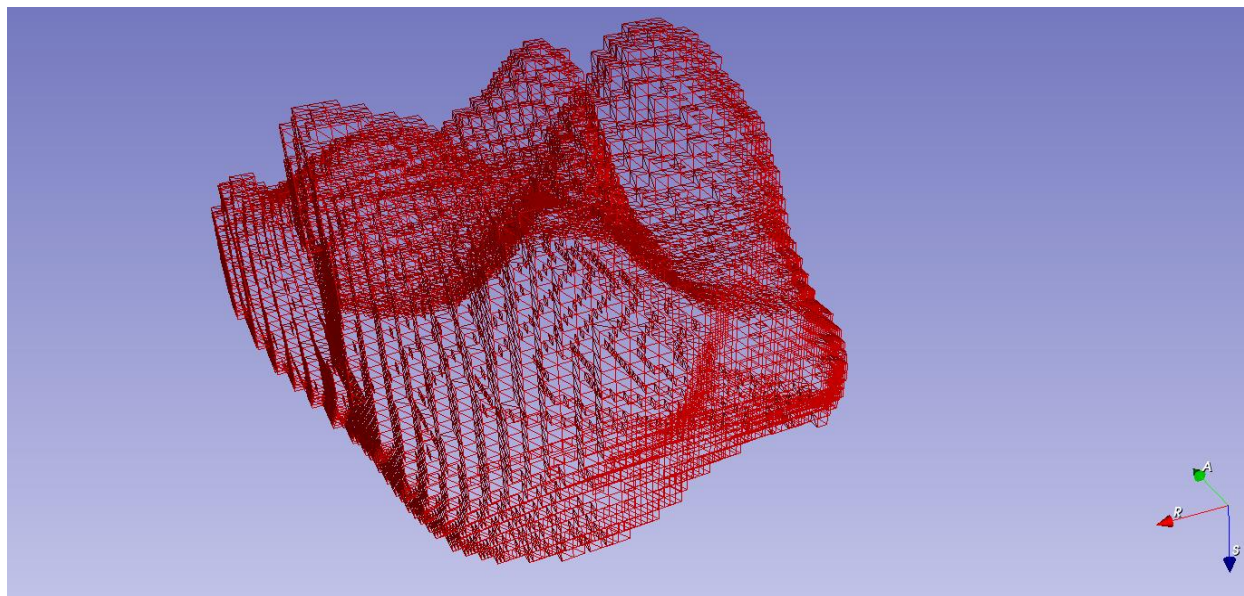


Figure 52: Surface mesh of the molar Dataset labeled b01, which is the output of GenParaMesh and will then be mapped onto parametrized spheres with different iterations. Visualized in 3D Slicer [11] Model Module.

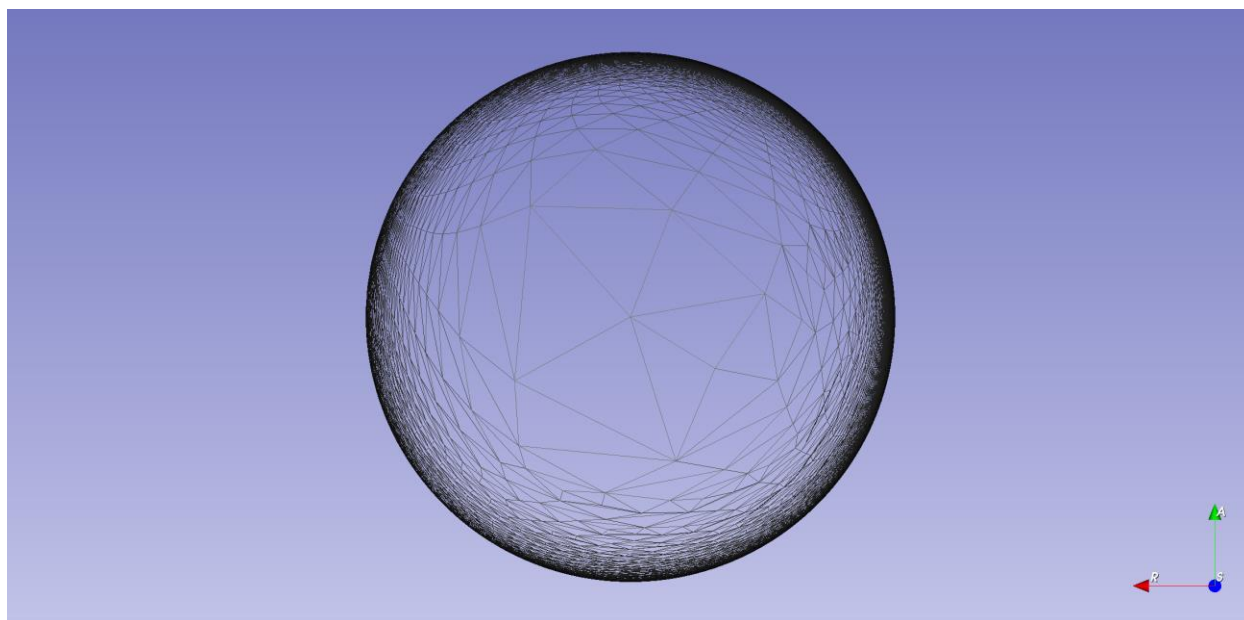


Figure 53: Heat equation mapping as initialization parametrization parametrized sphere of the molar dataset labeled b01 with iteration 0, it is not a good parametrization because it has a large variation in size of triangles. Visualized in 3D Slicer [11] Model Module

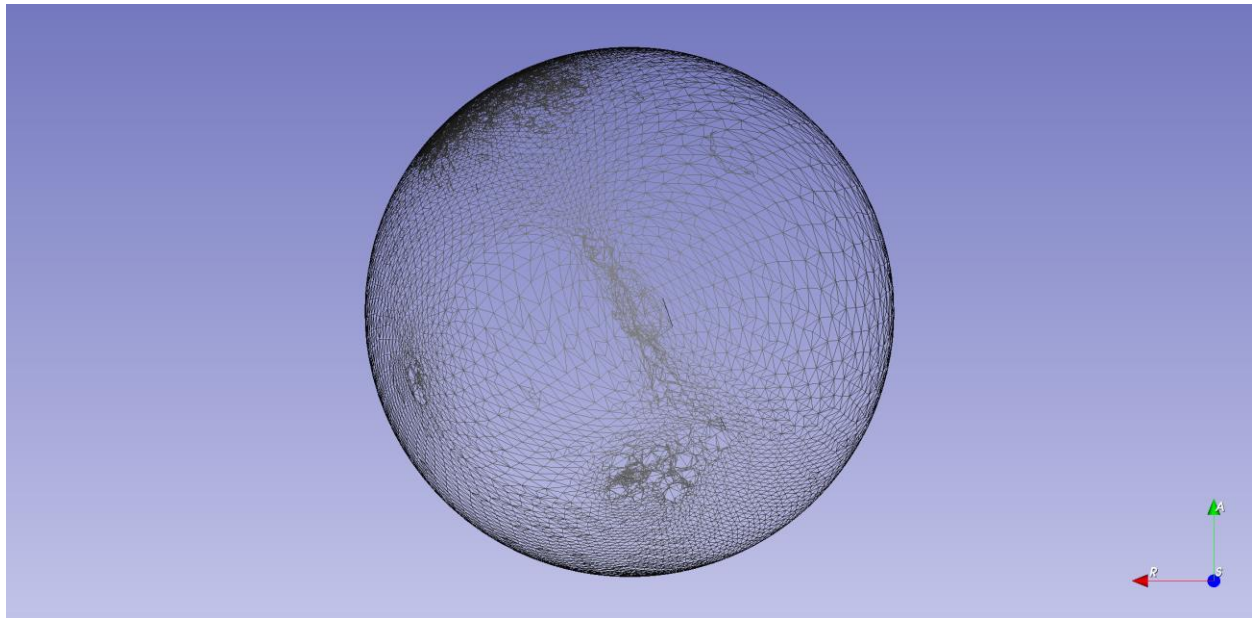


Figure 54: Conformal mapping as initialization parametrization parametrized sphere of the molar dataset labeled b01 with iteration 0. It is parametrized sphere with small variation in size of triangles and has near uniform density. Visualized in 3D Slicer [11] Model Module.

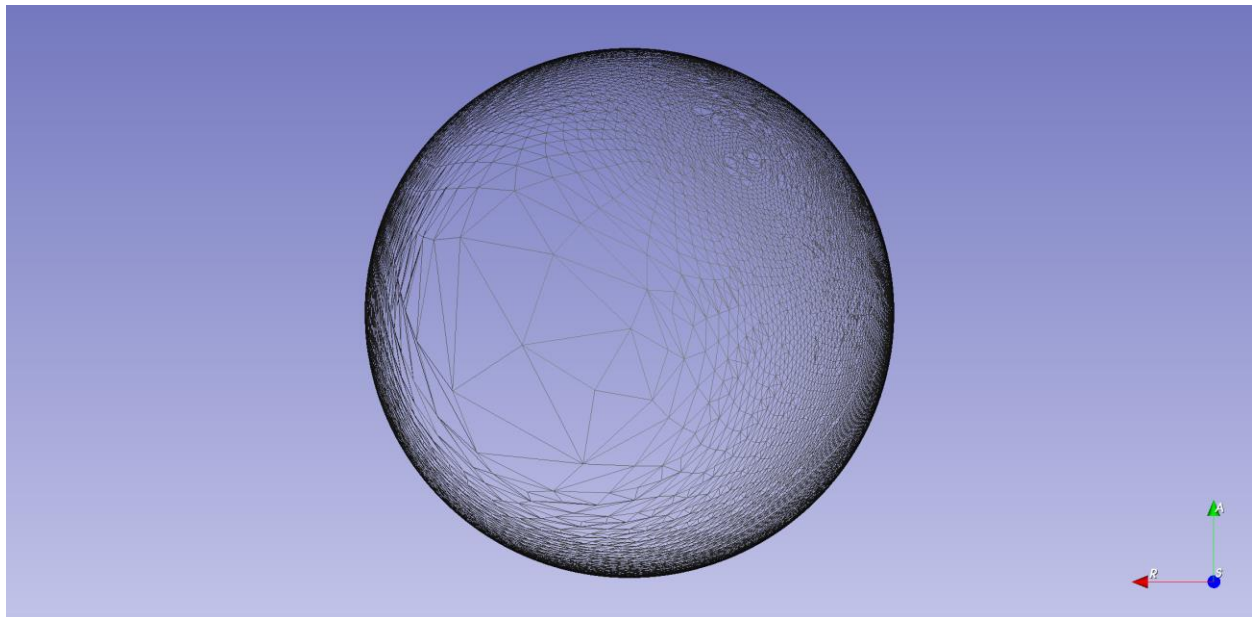


Figure 55: Heat equation mapping as initialization parametrization parametrized sphere of the molar dataset labeled b01 with iteration 50, it is not a good parametrization because it has a large variation in size of triangles, but it is better (increase in uniformity of triangle size) than iteration 0. Visualized in 3D Slicer [11] Model Module

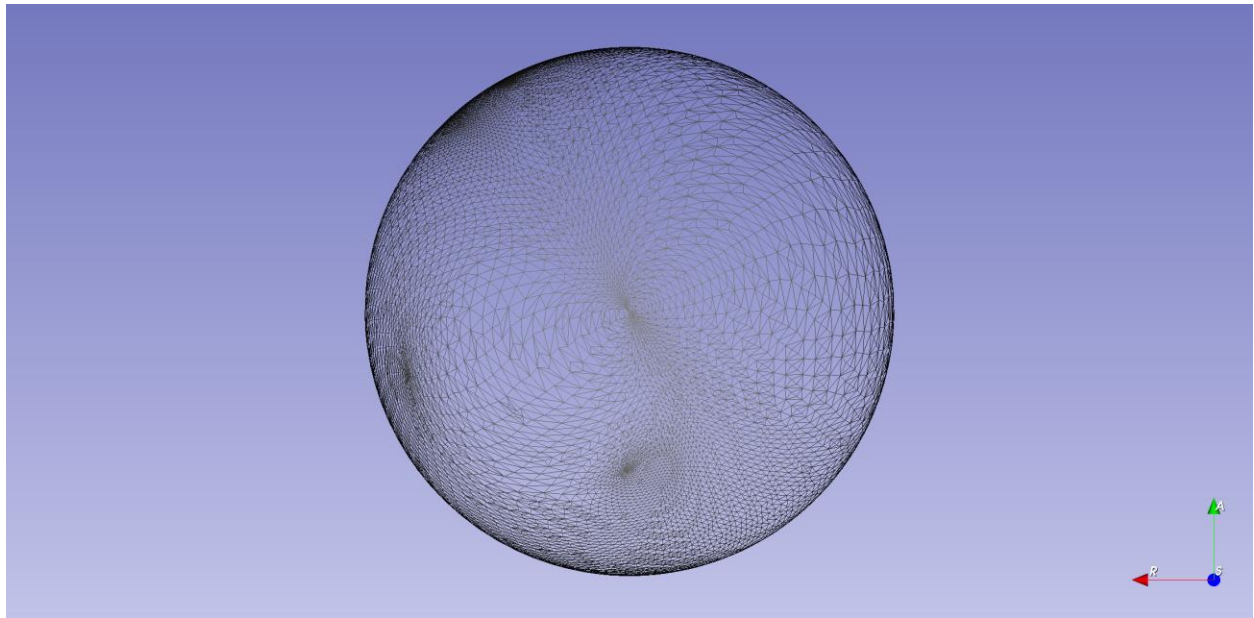


Figure 56: Conformal mapping as initialization parametrization parametrized sphere of the molar dataset labeled b01 with iteration 50. It is a parametrized sphere with small variation in size of triangles and has near uniform density, consistent with the one with iteration 0. Visualized in 3D Slicer [11] Model Module.

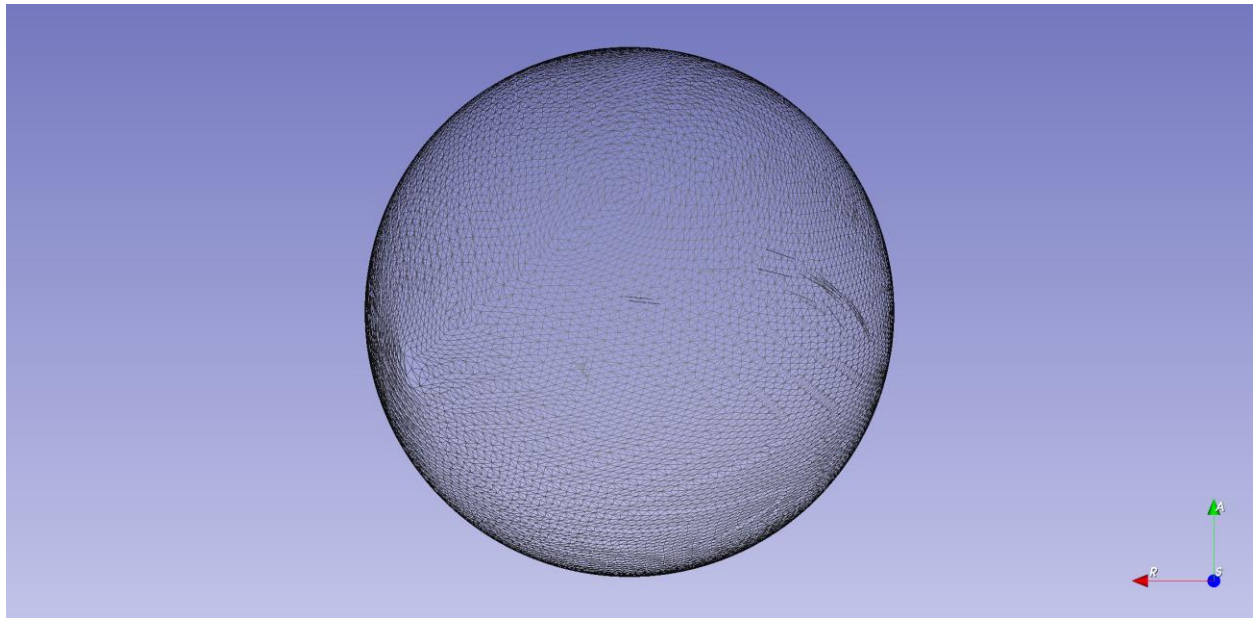


Figure 57: Heat equation mapping as initialization parametrization parametrized sphere of the molar dataset labeled b01 with iteration 100, it is not a good parametrization because it has a uniform distributed size of triangles, but it is better (increase in uniformity) than iteration 0. Visualized in 3D Slicer [11] Model Module

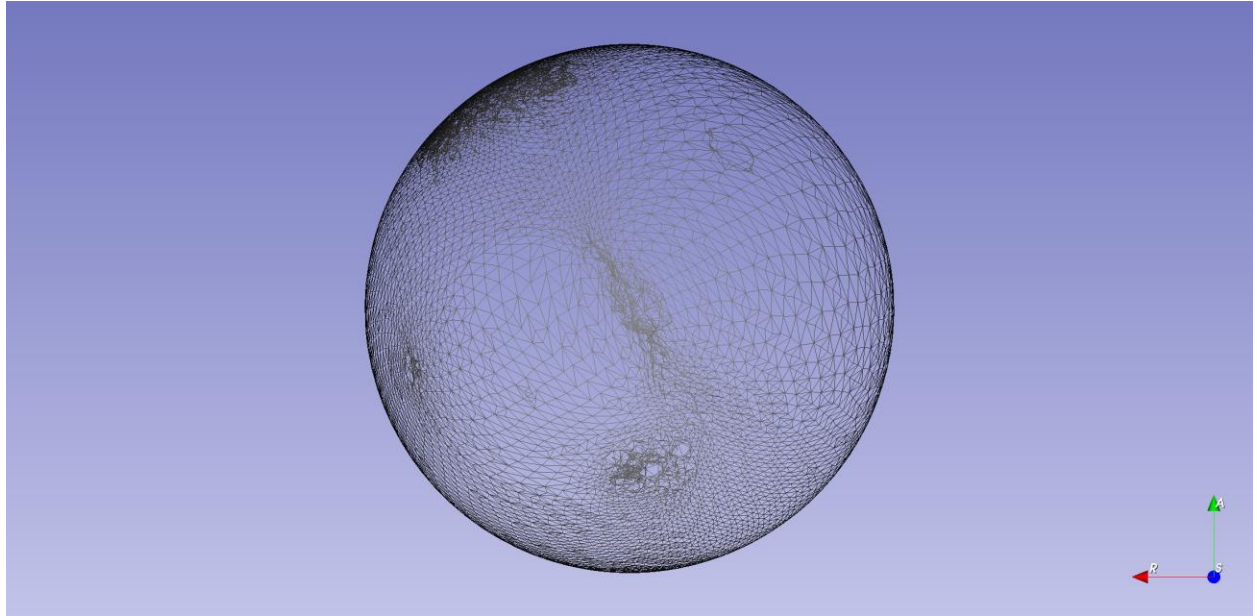


Figure 58: Conformal mapping as initialization parametrization parametrized sphere of the molar dataset labeled b01 with iteration 100. It is a parametrized sphere with small variation in size of triangles and has near uniform density and is consistent in quality with iteration 0 and 50. Visualized in 3D Slicer [11] Model Module.

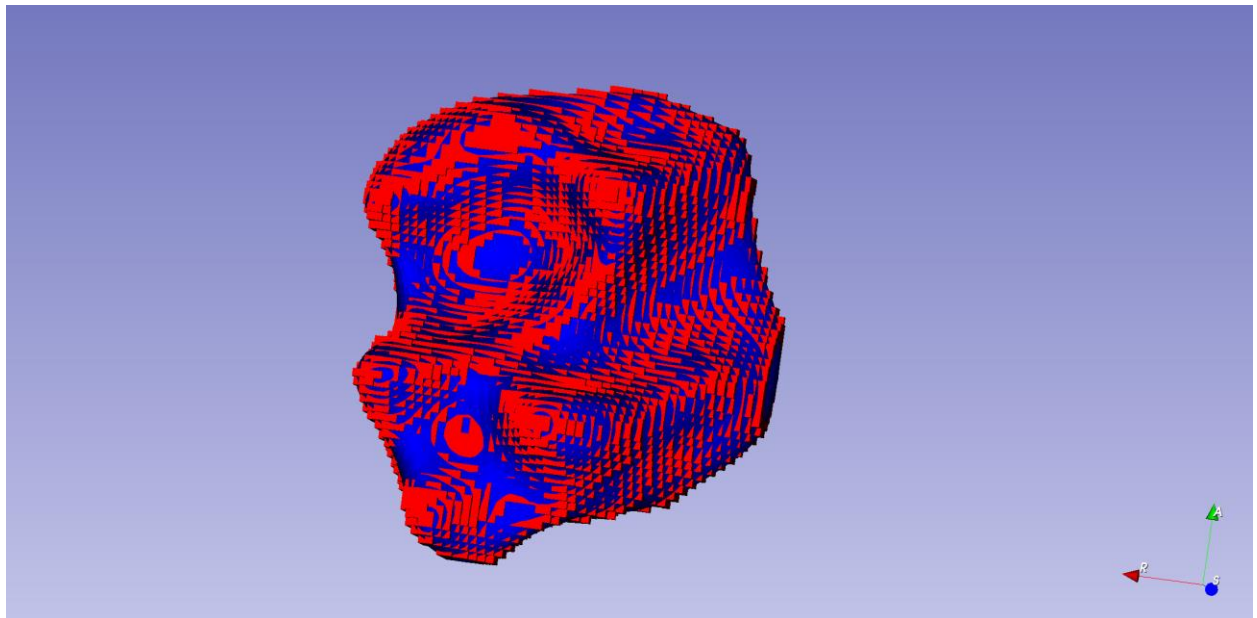


Figure 59: The surface mesh overlay of the molar dataset labeled b01 of the original surface mesh (red) and the SPHARM surface mesh with heat equation mapping initialization with iteration 500 (blue). The level of overlapping and the rate of similarity is huge between the red and blue surface. Thus, it has a great reconstruction quality. Visualized in 3D Slicer [11] Model Module

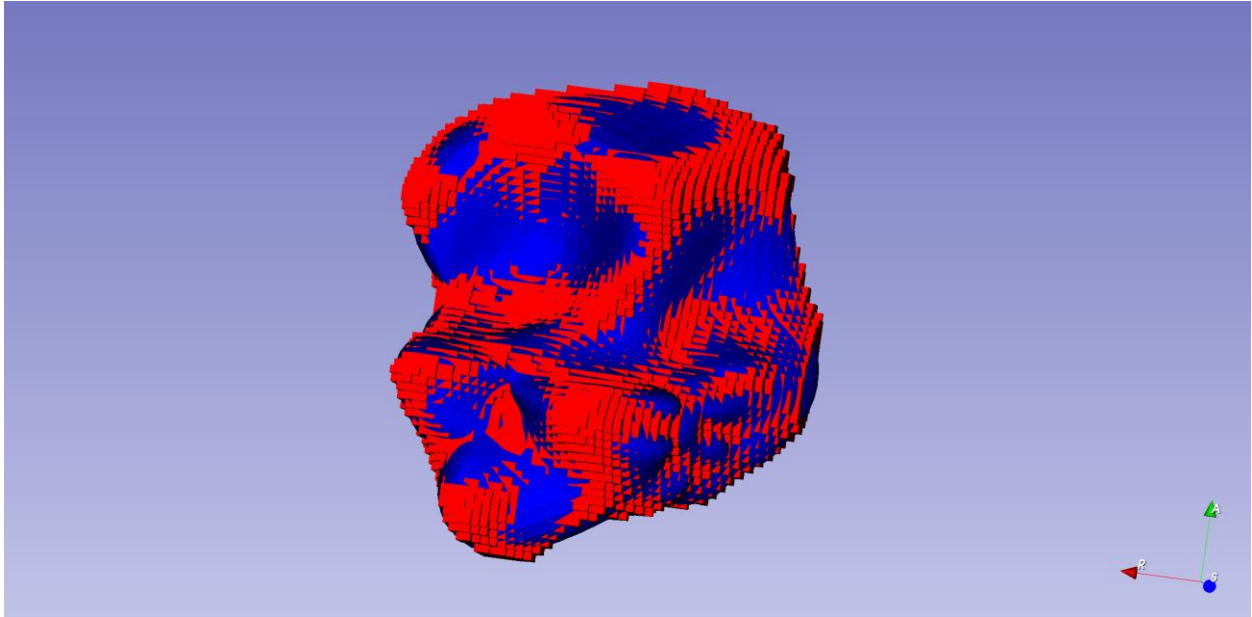


Figure 60: The surface mesh overlay of the molar dataset labeled b01 of the original surface mesh (red) and the SPHARM surface mesh with conformal mapping initialization with iteration 500 (blue). It also has a great reconstruction quality. But It is hard to tell whether conformal mapping initialization parametrization or heat equation initialization parametrization is better through visualization. Visualized in 3D Slicer [11] Model Module.

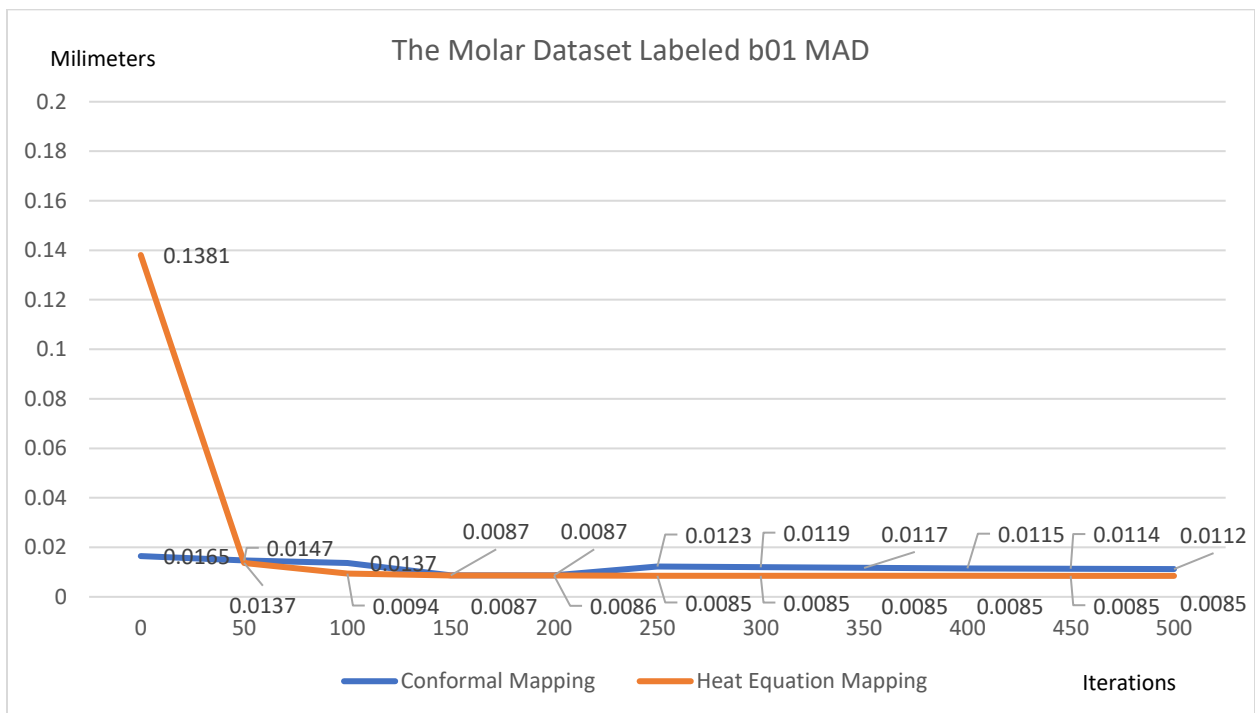


Figure 61: Molar Dataset Labeled b01 Mean Absolute Distance (MAD). The pattern is similar to that of the molar dataset labeled a10 and a13.

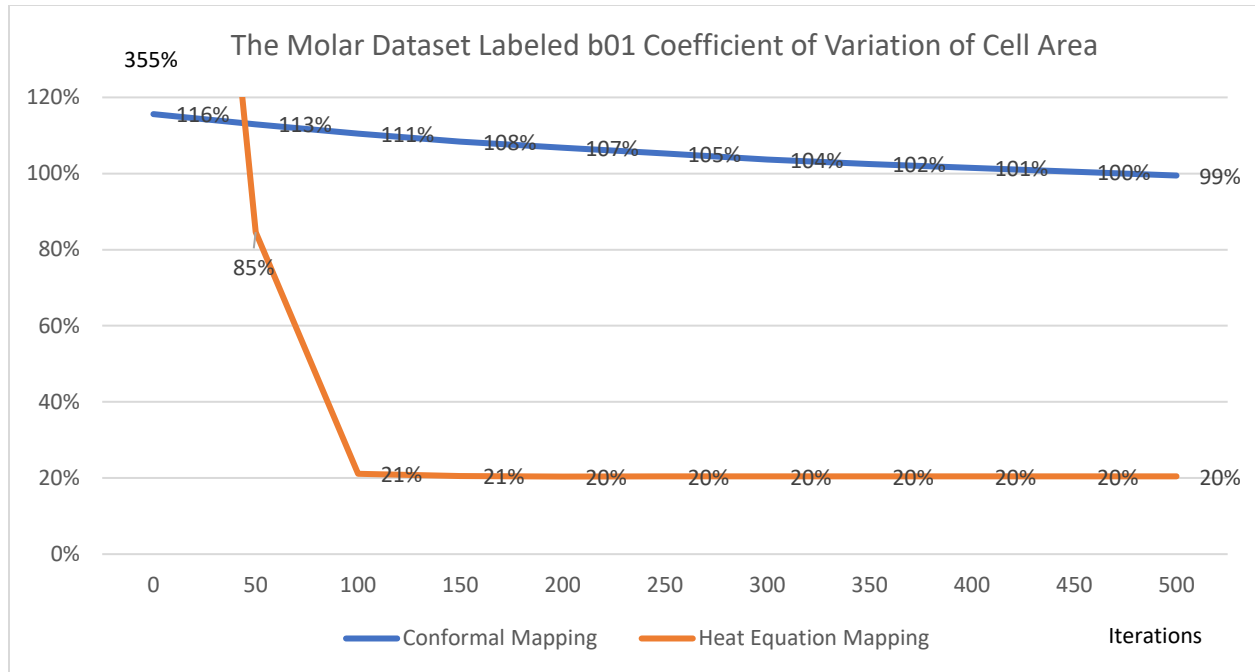


Figure 62: Molar Dataset Labeled a_{13} Coefficient of Variation of Cell Area. The pattern of Coefficient of variation of Cell Area is similar to that of that of the molar dataset labeled a_{10} and a_{13} .

For molar data, we can clearly see that conformal mapping initialization parametrization performs much better than heat equation mapping initialization parametrization with few iterations and it converges faster than the heat equation mapping initialization parametrization. However, with larger iteration number, conformal mapping initialization parametrization performs slightly worse than the heat equation mapping initialization parametrization.

The mandible dataset:

From the four Mandible datasets acquired, I successfully reconstructed one of them following the SPHARM-PDM pipeline with both conformal mapping method and heat equation mapping method.

The mandible dataset labeled 002:

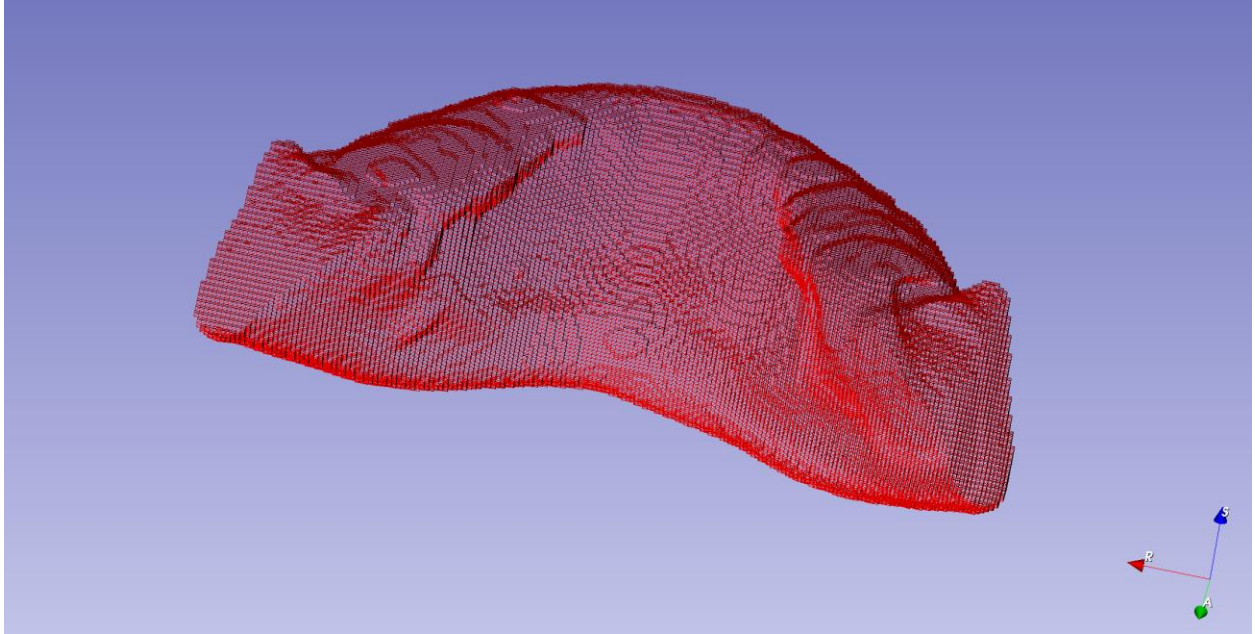


Figure 63: Surface mesh of the mandible dataset labeled 002, which is the output of GenParaMesh and will then be mapped onto parametrized spheres with different iterations. Visualized in 3D Slicer [11] Model Module.

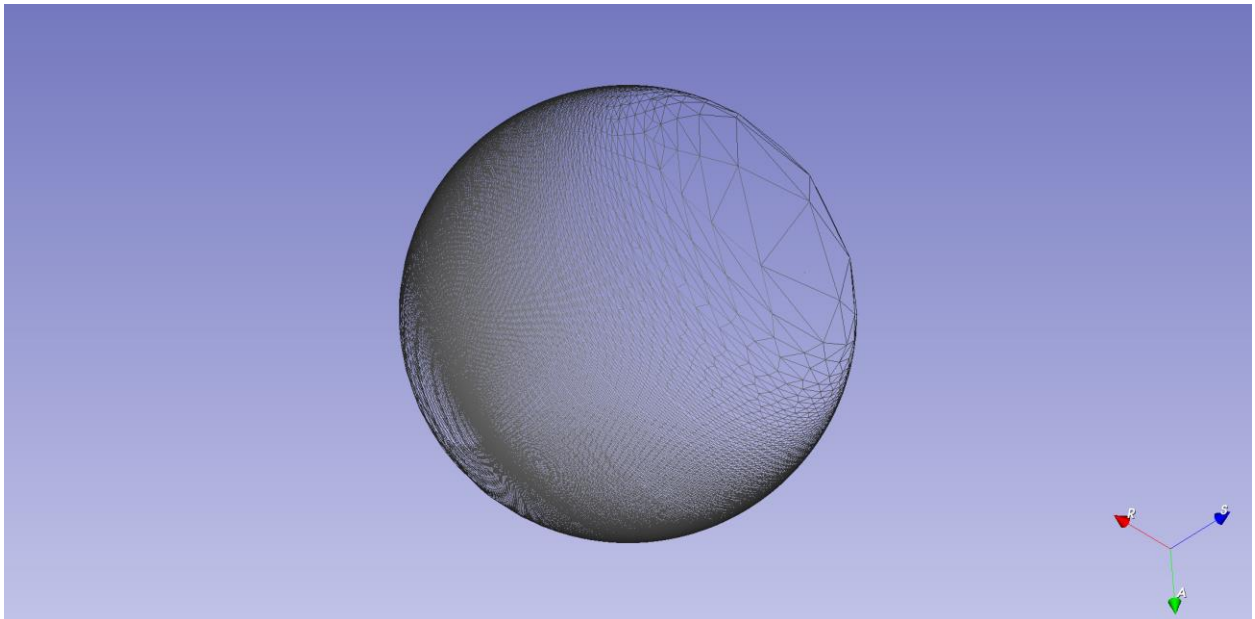


Figure 64: Heat equation mapping as initialization parametrization parametrized sphere of the mandible dataset labeled 002 with iteration 0, it is not a good parametrization because it has a huge variation in triangle size. Visualized in 3D Slicer [11] Model Module

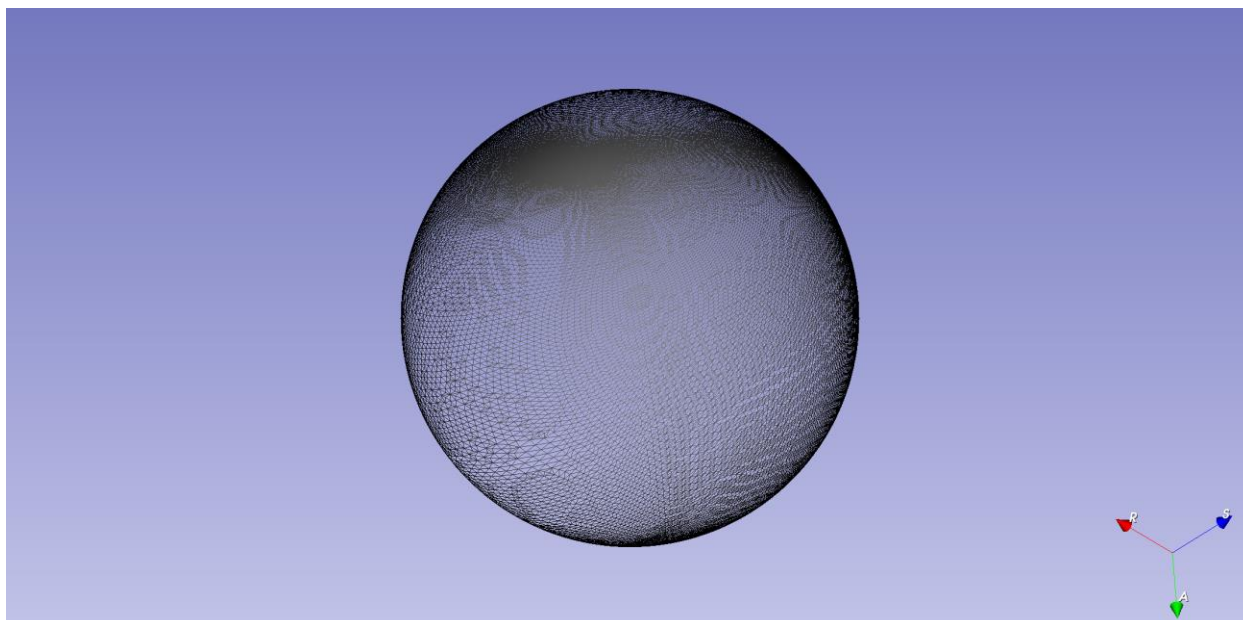


Figure 65: Conformal mapping as initialization parametrization parametrized sphere of the mandible dataset labeled 002 with iteration 0. It is a parametrized sphere with small variation in size of triangles and has near uniform density. Visualized in 3D Slicer [11] Model Module.

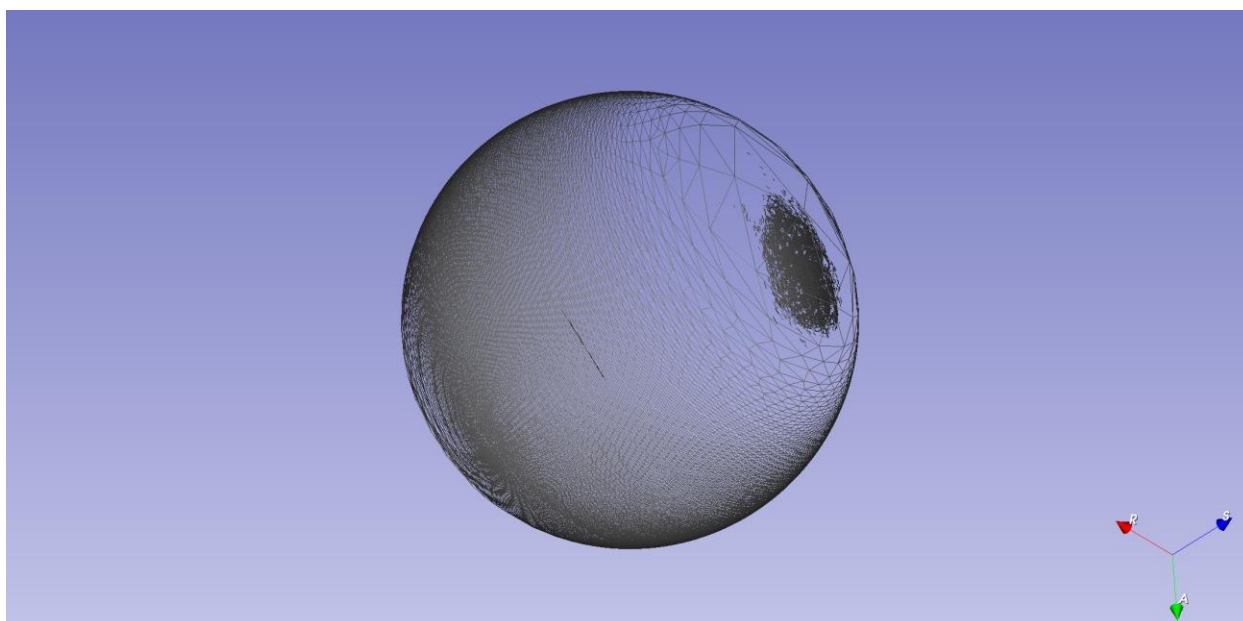


Figure 66: Heat equation mapping as initialization parametrization parametrized sphere of the mandible dataset labeled 002 with iteration 50, it is much better in triangle uniformity than iteration 0. Visualized in 3D Slicer [11] Model Module

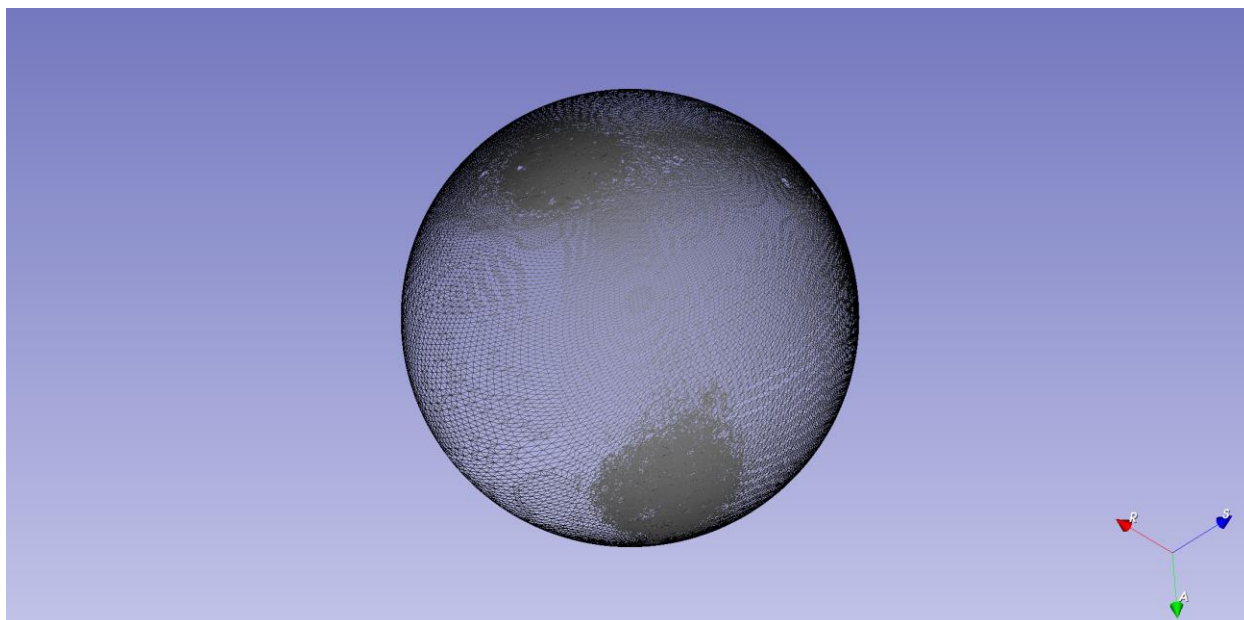


Figure 67: Conformal mapping as initialization parametrization parametrized sphere of the mandible dataset labeled 002 with iteration 50. It is a parametrized sphere with small variation in size of triangles and has near uniform density. Visualized in 3D Slicer [11] Model Module.

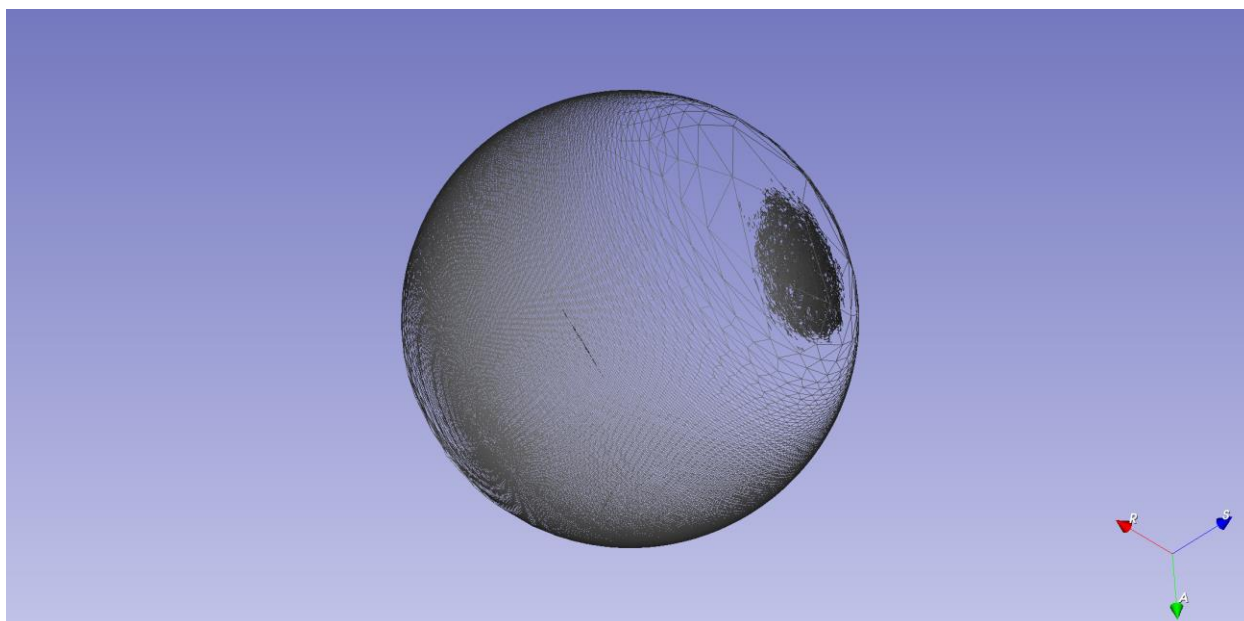


Figure 68: Heat equation mapping as initialization parametrization parametrized sphere of the mandible dataset labeled 002 with iteration 100, it is slightly improved in triangle uniformity from 50 iterations. Visualized in 3D Slicer [11] Model Module

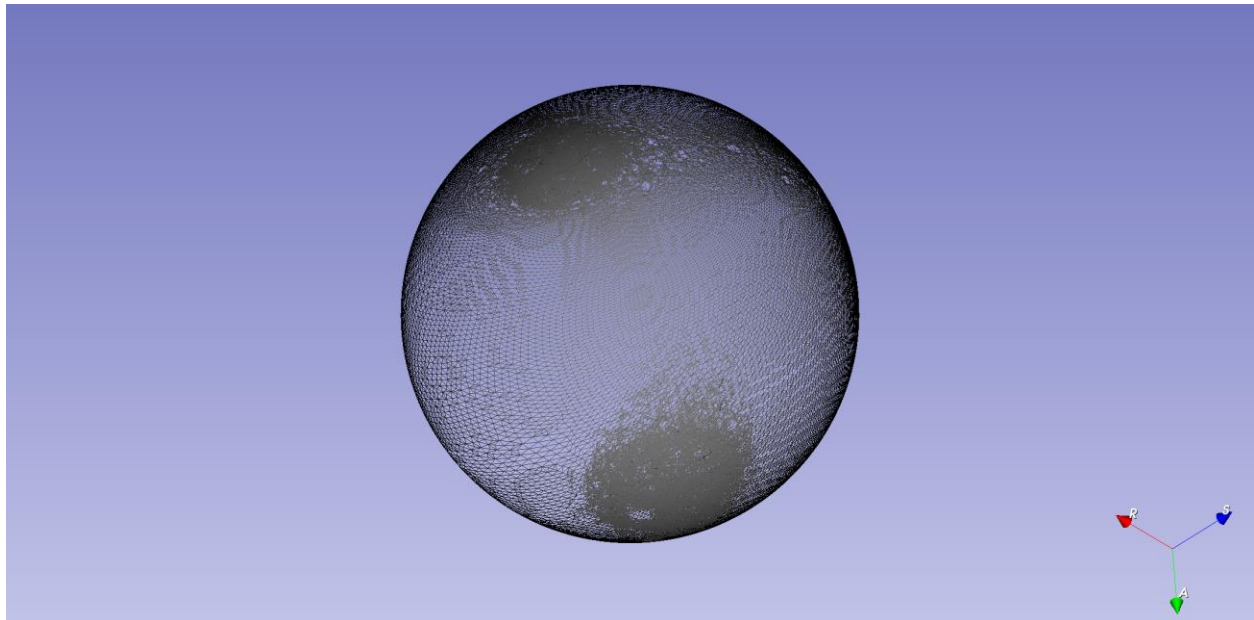


Figure 69: Conformal mapping as initialization parametrization parametrized sphere of the mandible dataset labeled 002 with iteration 100. It is parametrized sphere with small variation in size of triangles and has near uniform density. Visualized in 3D Slicer [11] Model Module.

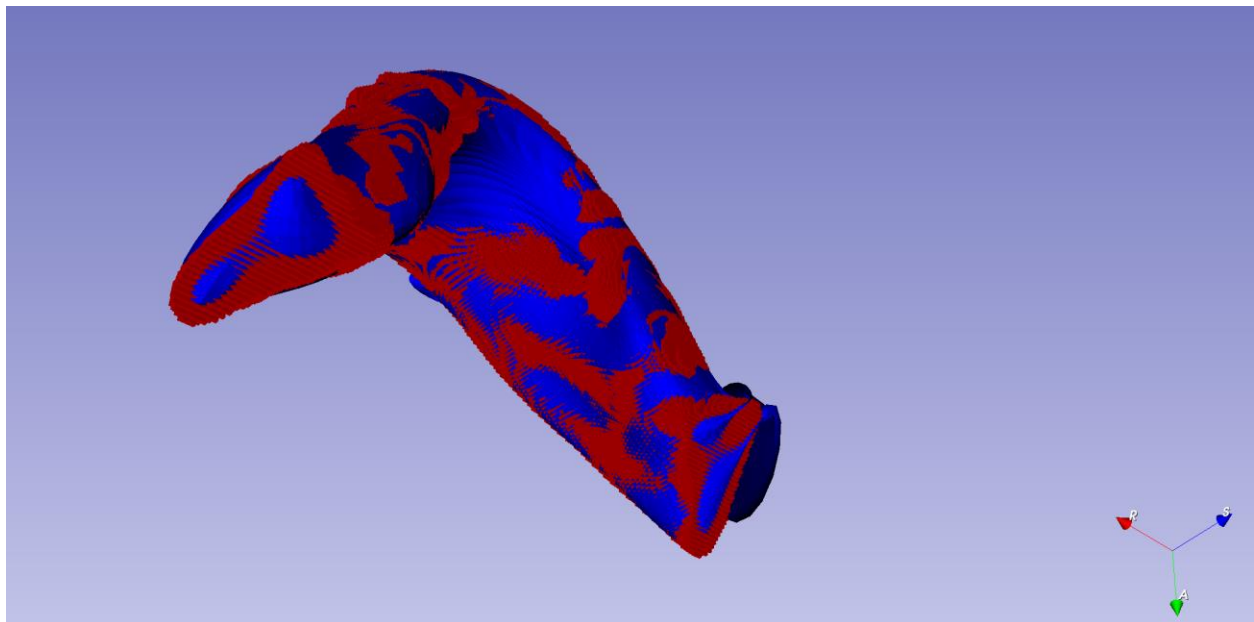


Figure 70: The surface mesh overlay of the mandible dataset labeled 002 of the original surface mesh (red) and the SPHARM surface mesh with heat equation mapping initialization parametrization with iteration 500 (blue). The level of overlapping and the rate of similarity is top-notch, so the quality of reconstruction is fairly good. Visualized in 3D Slicer [11] Model Module

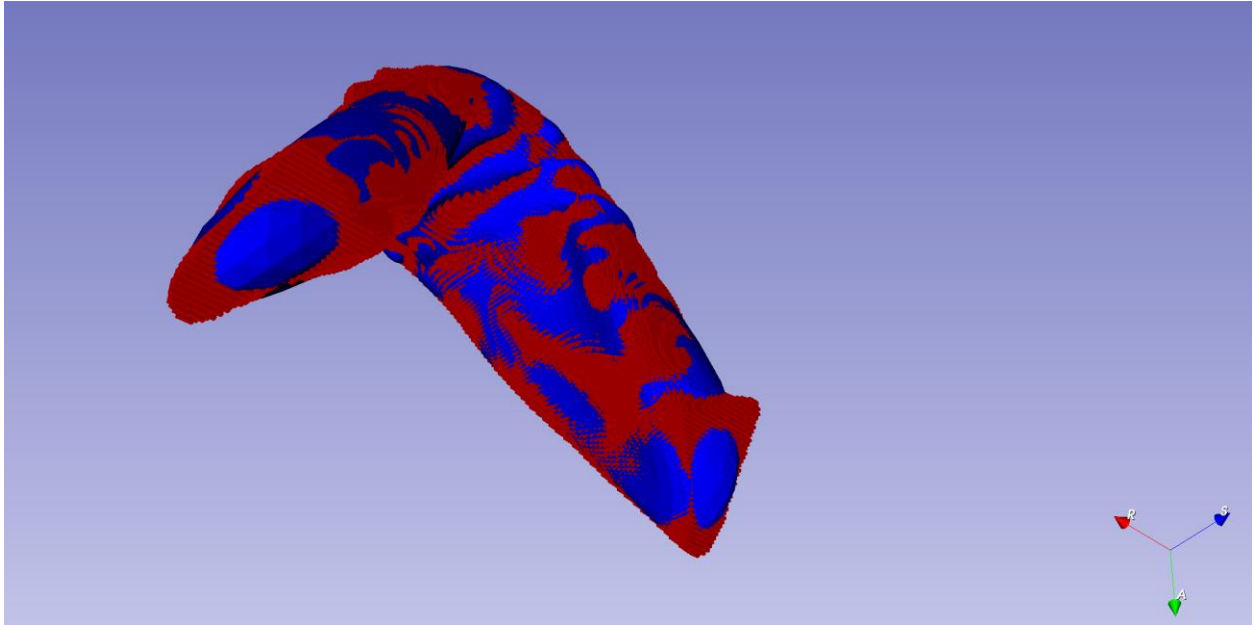


Figure 71: The surface mesh overlay of the mandible dataset labeled 002 of the original surface mesh (red) and the SPHARM surface mesh with conformal mapping initialization with iteration 500 (blue). It also has a good quality. But it is hard to tell whether conformal mapping initialization parametrization or heat equation initialization parametrization is better through visualization. Visualized in 3D Slicer [11] Model Module.

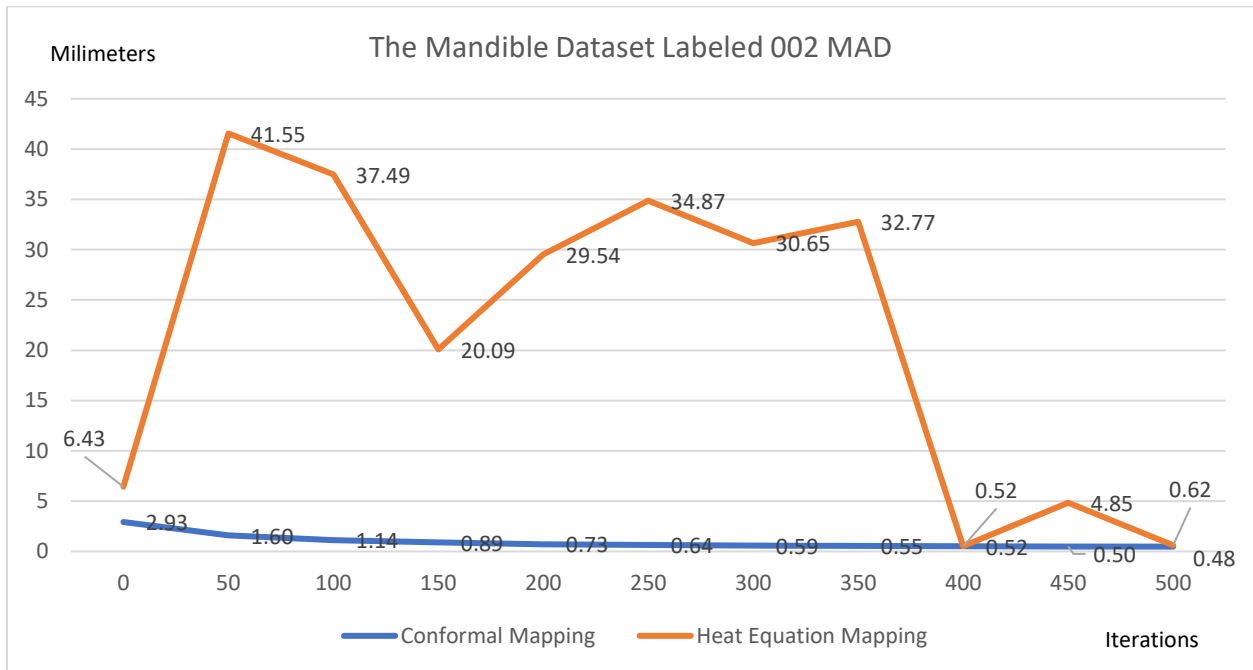


Figure 72: Mandible dataset Labeled 002 Mean Absolute Distance (MAD). It is clear that the heat equation mapping initialization parametrization both performs worse and is less stable than conformal mapping initialization parametrization. The irregularity of the quality of heat equation mapping initialization parametrization suggests the mandible structure is unstable with the optimization procedure of the GenParaMesh.

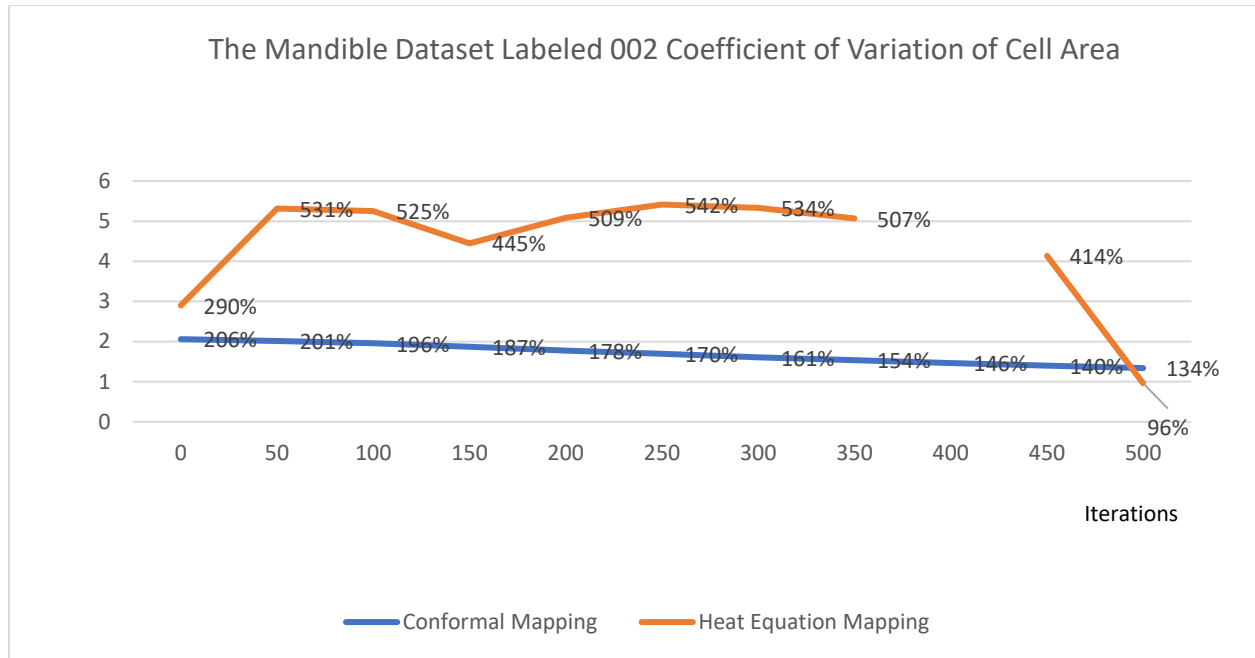


Figure 73: Mandible dataset Labeled 002 Coefficient of Variation of Cell Area. The pattern of Coefficient of variation of Cell Area is similar to that of Mean Absolute Distance (MAD). Mesh Quality software failed to analyze the data at 400 iterations, so there is a blank at 400 iterations.

From the mandible dataset, we can see a very clear comparison of MAD and coefficient of variation value between two initialization parametrization. As it turns out, the conformal mapping initialization parametrization yields a significantly better result of MAD and coefficient of variation of cell area than the heat equation mapping initialization parametrization.

The condyle dataset:

All Condyle data can be analyzed through both the old and the newly proposed SPHARM-PDM pipeline. I picked one of the nine Condyle datasets to investigate the quality of 3D reconstruction with different initialization parametrization.

The condyle dataset labeled AC10_Left:

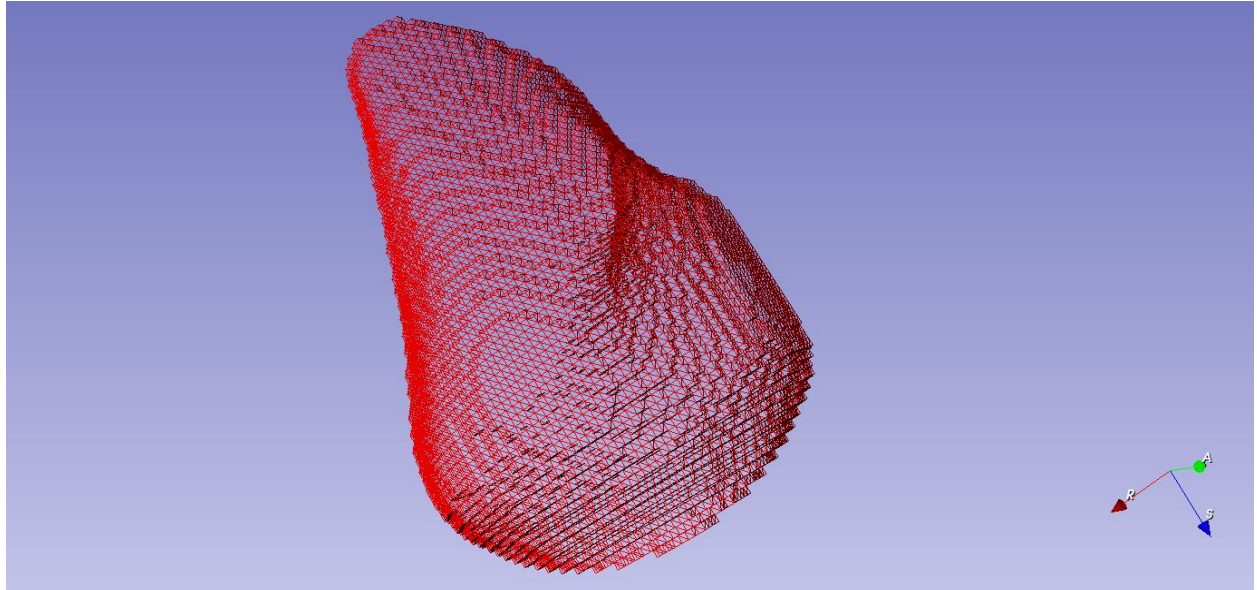


Figure 74: Surface mesh of the condyle Dataset labeled AC10_Left, which is the output of GenParaMesh and will then be mapped onto parametrized spheres with different iterations. Visualized in 3D Slicer [11] Model Module.

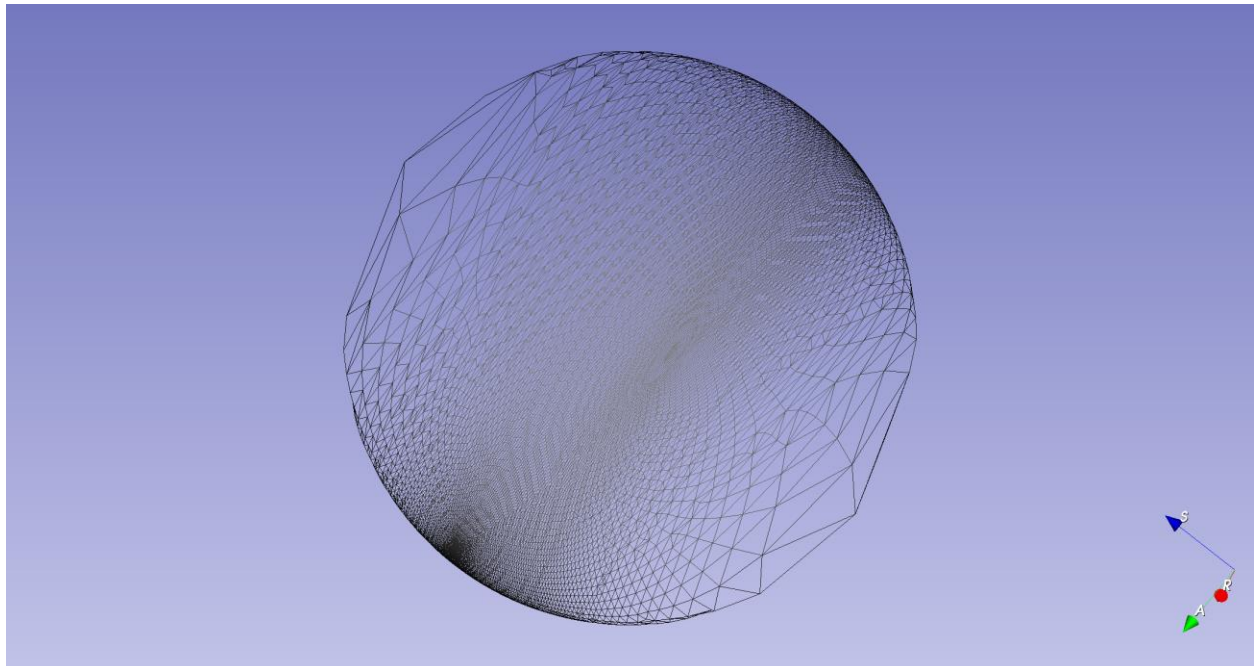


Figure 75: Heat equation mapping as initialization parametrization parametrized sphere of the condyle Dataset labeled AC10_Left with iteration 0, it is not a good parametrization because it has an extremely large variation in triangle size. Visualized in 3D Slicer [11] Model Module

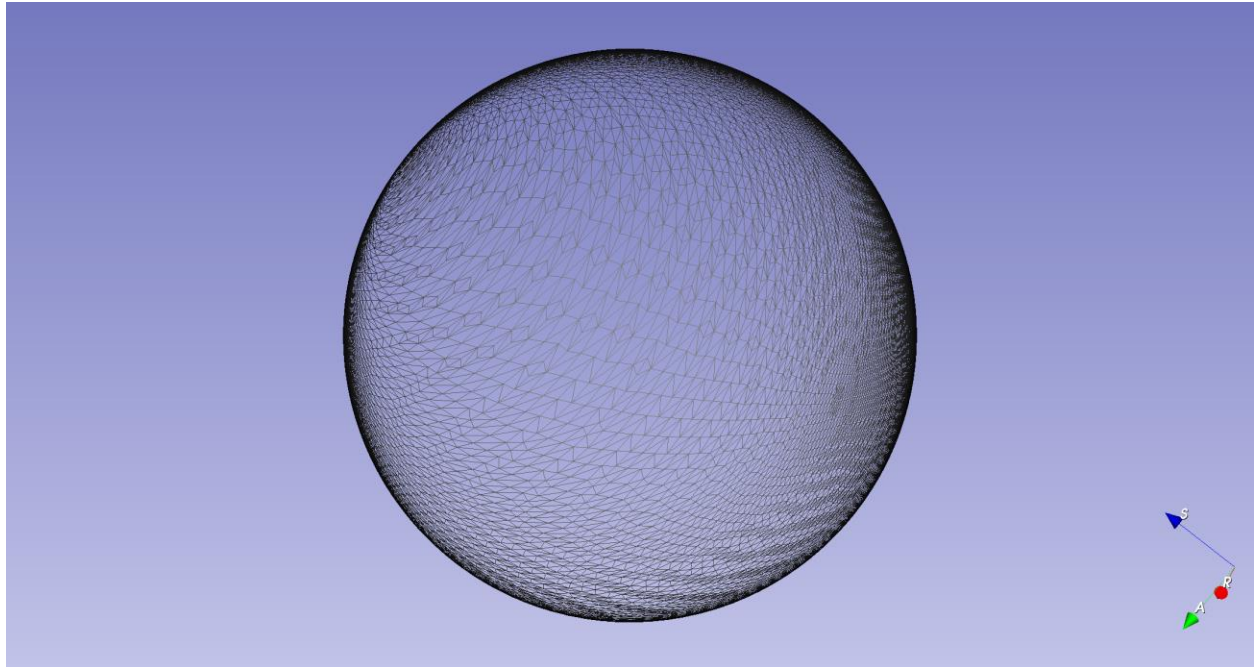


Figure 76: Conformal mapping as initialization parametrization parametrized sphere of the condyle Dataset labeled AC10_Left with iteration 0. It is a parametrized sphere with small variation in size of triangles and has near uniform density. Visualized in 3D Slicer [11] Model Module.

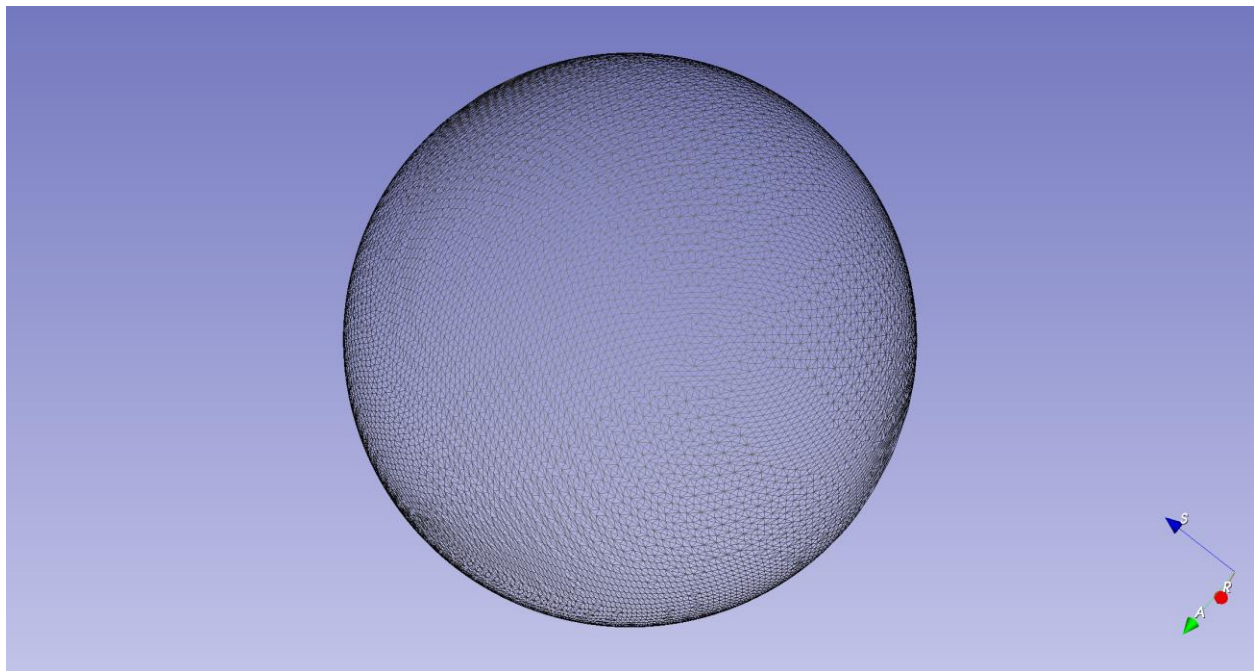


Figure 77: Heat equation mapping as initialization parametrization parametrized sphere of the condyle Dataset labeled AC10_Left with iteration 50, it is a parametrized sphere with small variation in size of triangles and has a near uniform density distribution. Visualized in 3D Slicer [11] Model Module

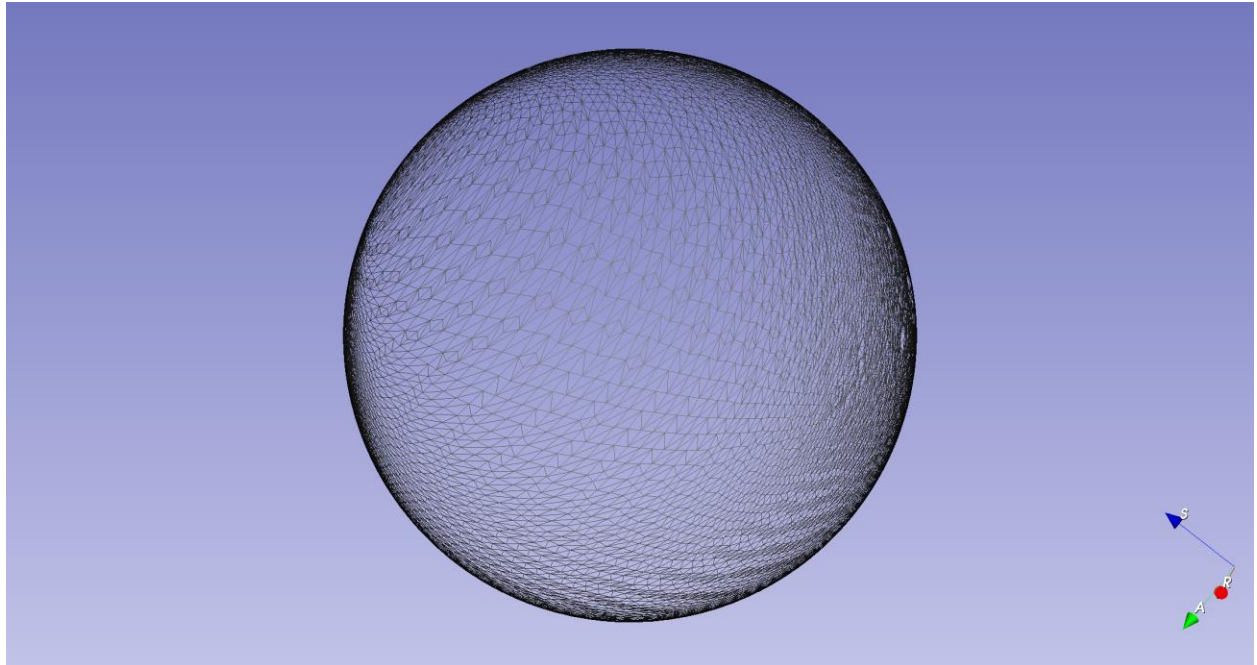


Figure 78: Conformal mapping as initialization parametrization parametrized sphere of the condyle Dataset labeled AC10_Left with iteration 50. It is a parametrized sphere with small variation in size of triangles and has near uniform density. Visualized in 3D Slicer [11] Model Module.

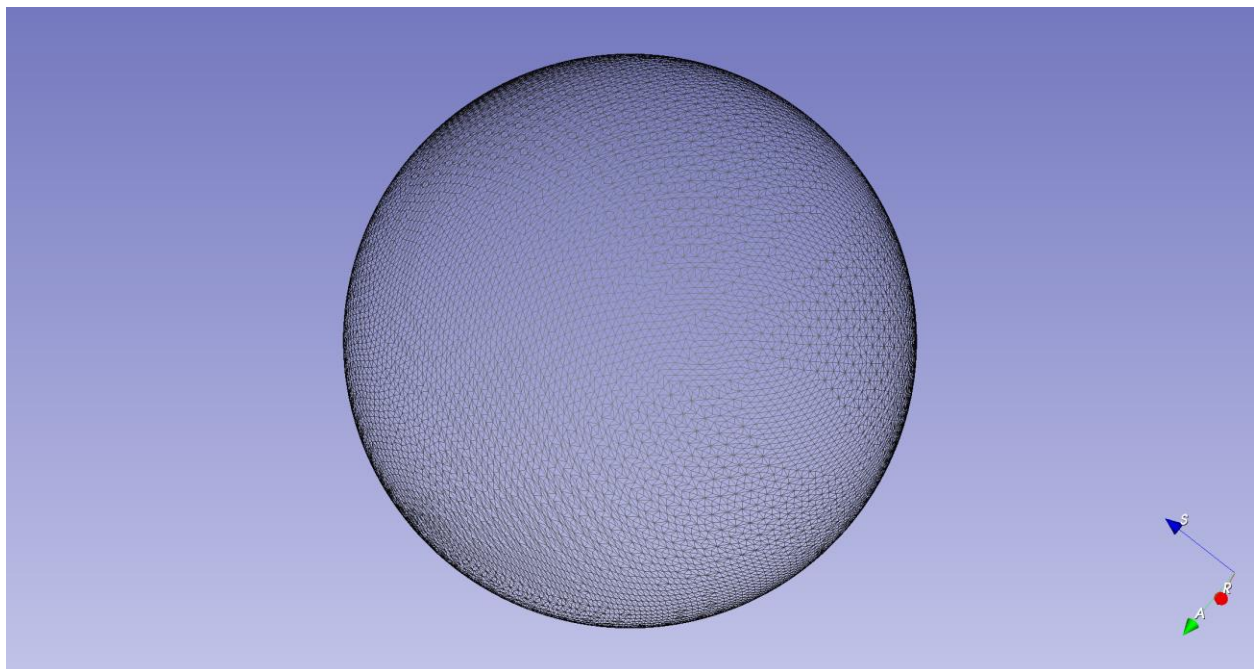


Figure 79: Heat equation mapping as initialization parametrization parametrized sphere of the condyle Dataset labeled AC10_Left with iteration 100, it is parametrized sphere with small variation in size of triangles and has near uniform density. Visualized in 3D Slicer [11] Model Module

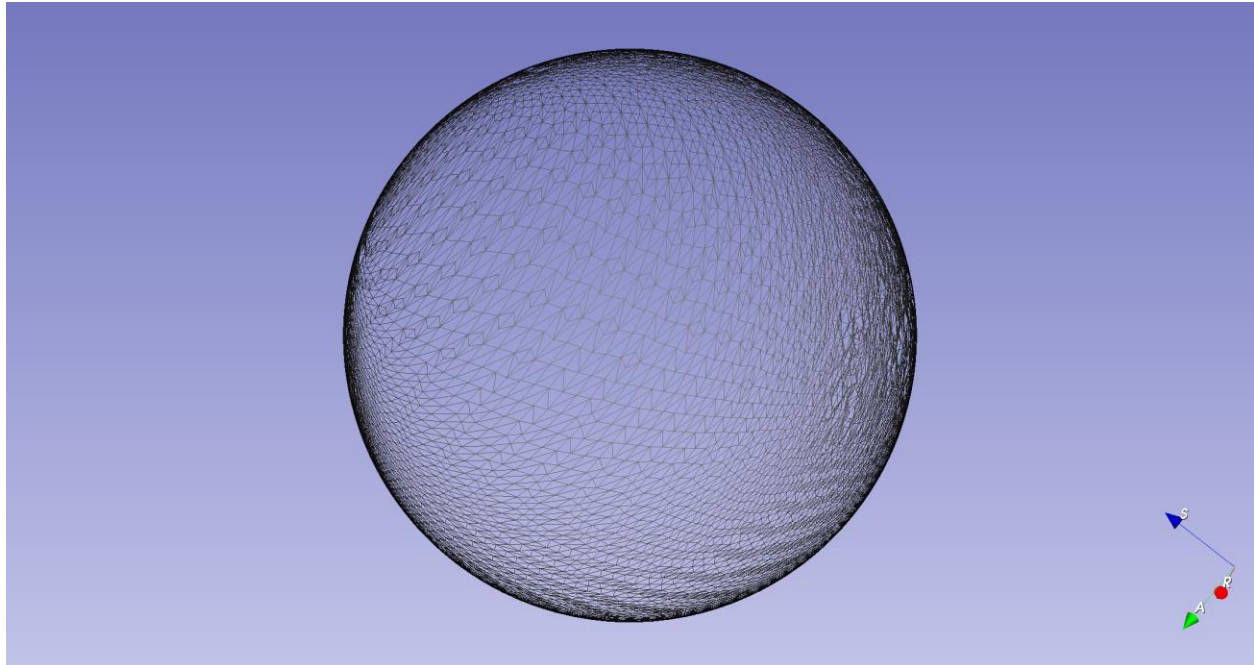


Figure 78: Conformal mapping as initialization parametrization parametrized sphere of the condyle Dataset labeled AC10_Left with iteration 100. It is a parametrized sphere with small variation in size of triangles and has near uniform density. Visualized in 3D Slicer [11] Model Module.

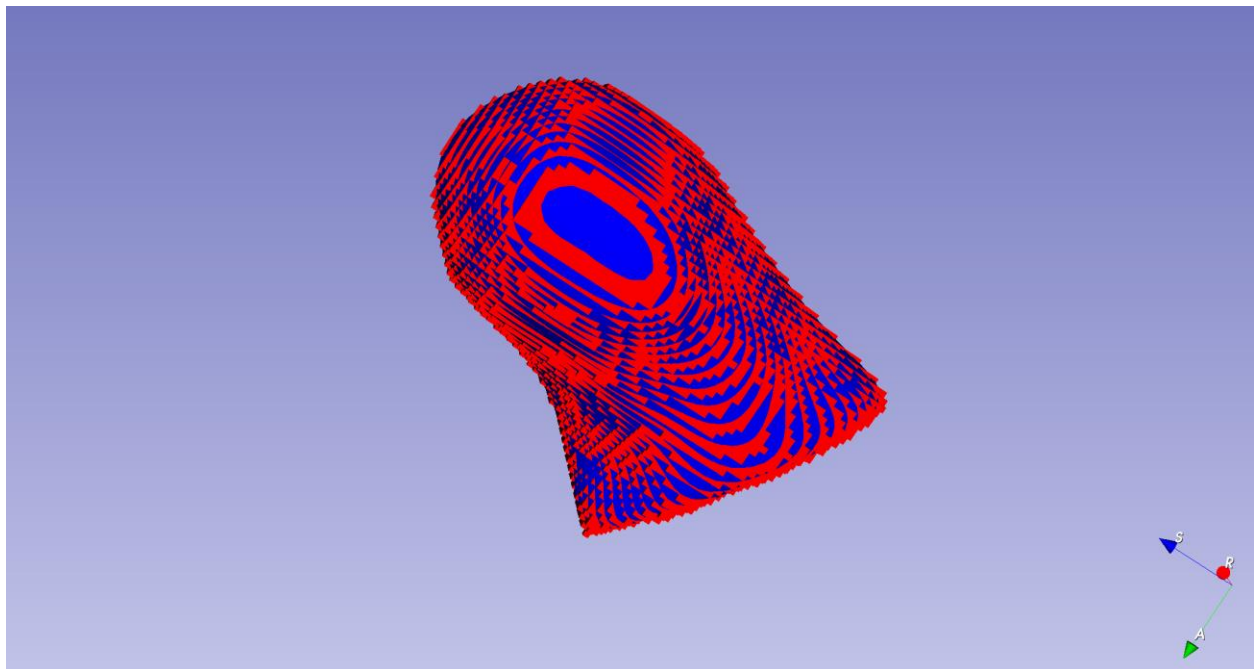


Figure 79: The surface mesh overlay of the condyle Dataset labeled AC10_Left of the original surface mesh (red) and the SPHARM surface mesh with heat equation mapping initialization with iteration 500 (blue). The level of similarity and the rate of overlapping between two surfaces is high, so the quality of reconstruction is pretty good. Visualized in 3D Slicer [11] Model Module

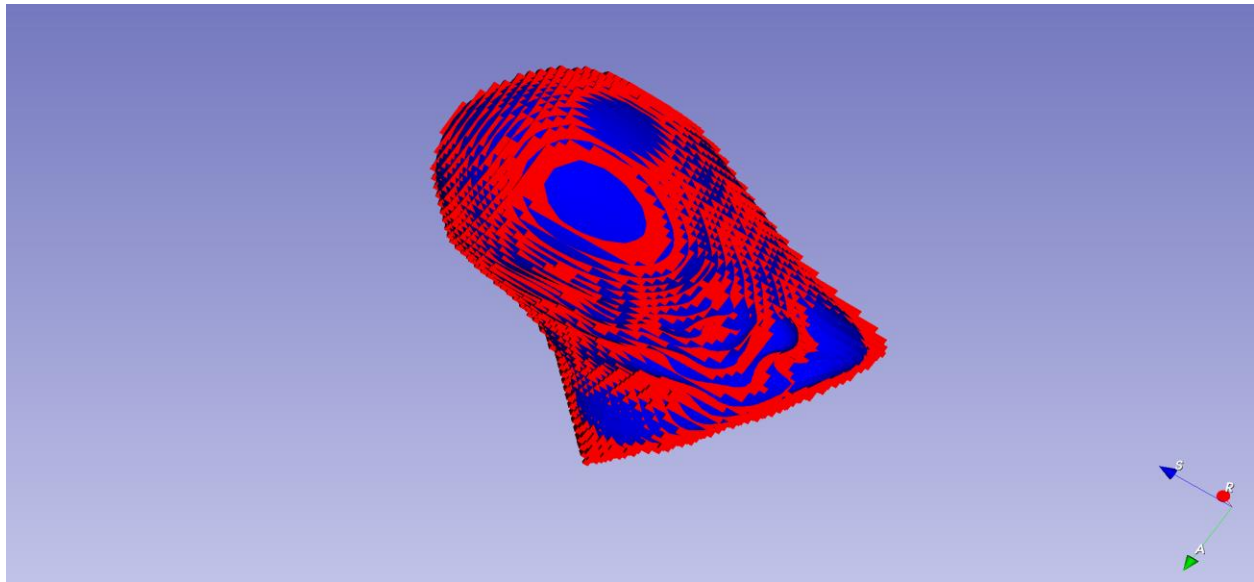


Figure 80: The surface mesh overlay of the condyle Dataset labeled AC10_Left of the original surface mesh (red) and the SPHARM surface mesh with conformal mapping initialization with iteration 500 (blue). It also has a great reconstruction quality. But it is hard to tell whether conformal mapping initialization parametrization or heat equation initialization parametrization is better through visualization. Visualized in 3D Slicer [11] Model Module.

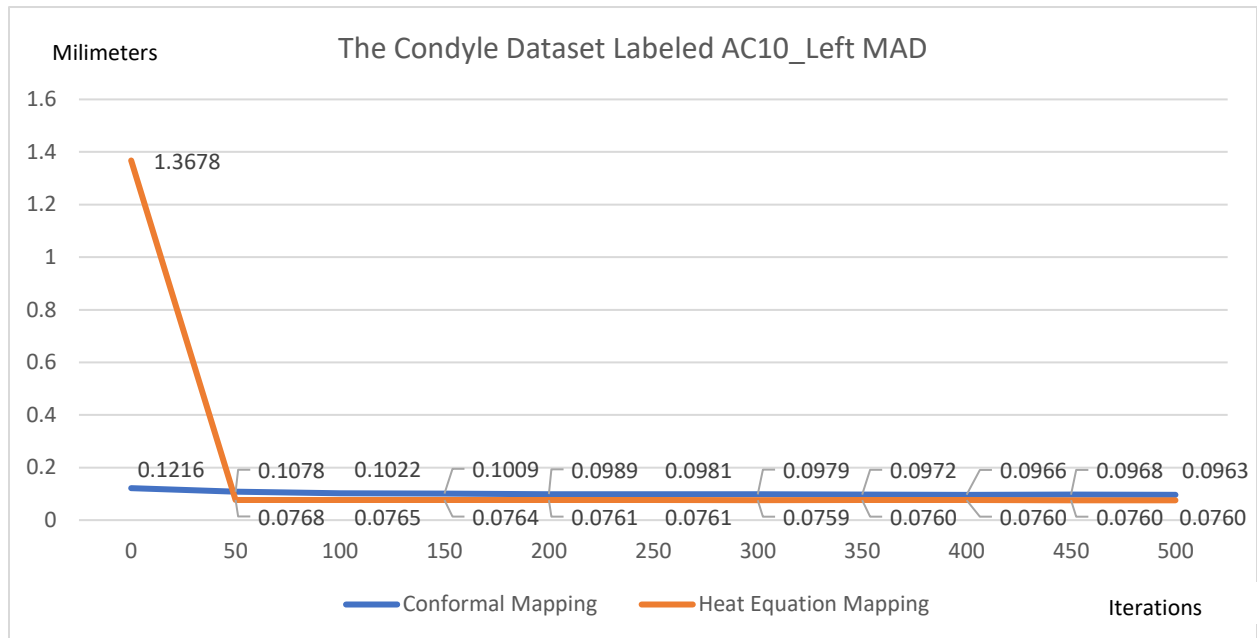


Figure 81: Condyle Dataset labeled AC10_Left Mean Absolute Distance (MAD). Clearly, the heat equation mapping initialization parametrization does poorly with 0 iterations but the improvement by the following optimization procedure is huge. On the contrary, the conformal mapping initialization parametrization does extremely well with 0 iteration and performs very consistently. Surprisingly, the heat equation mapping initialization parametrization, after being corrected by its following optimization procedure, does slightly better than conformal mapping initialization parametrization. The pattern is similar to that of all the molar datasets evaluated.

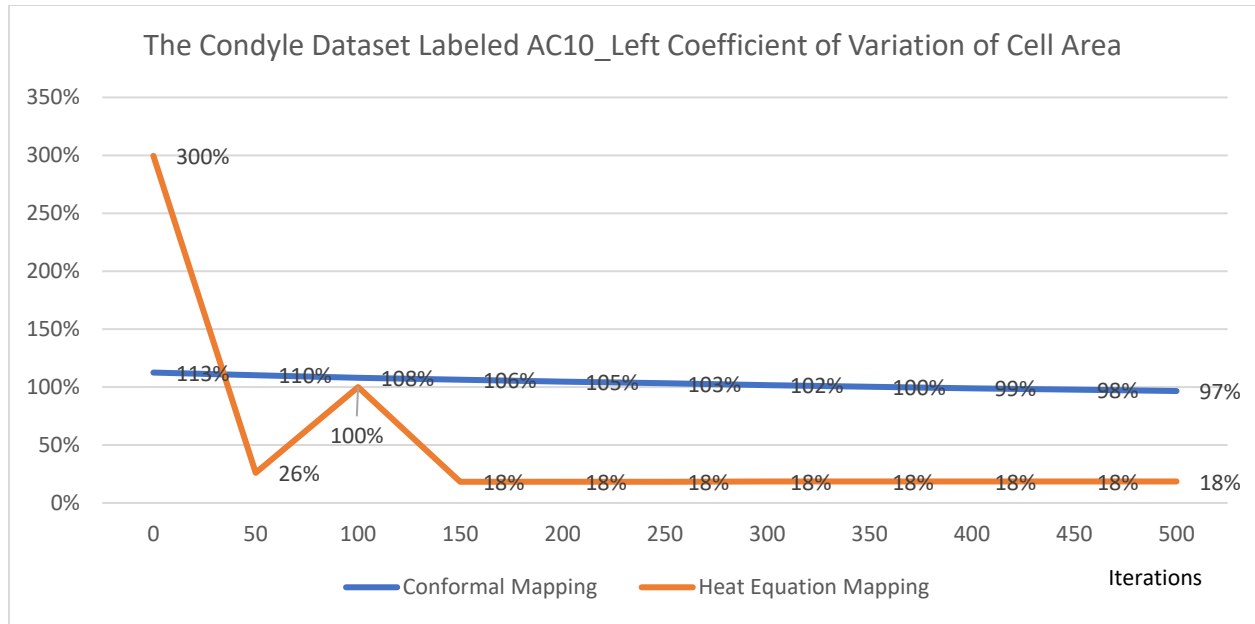


Figure 28: Condyle Dataset labeled AC10_Left Coefficient of Variation of Cell Area. Measurements were taken on the reconstructed SPHARM surface mesh with different iterations (0, 50, 100, ..., 500) and with different initialization parametrization (conformal mapping or heat equation mapping initialization parametrization). The pattern of Coefficient of variation of Cell Area is similar to that of Mean Absolute Distance (MAD).

The pattern of the condyle dataset result, as we can observe easily, is very similar to that of the molar. The quality of the 3D surface reconstruction also converges faster with conformal mapping initialization parametrization and with larger iteration number, the heat equation mapping initialization parametrization performs slightly better than the conformal mapping initialization parametrization.

The ventricle dataset:

While we can use the original SPHARM-PDM pipeline to analyze all four Ventricle datasets, the use of conformal mapping method failed on all four Ventricle datasets. I will discuss the reason of failing in the DISCUSSION AND CONCLUSION section.

4. DISCUSSION AND CONCLUSION

In summary, this thesis discussed a shape analysis framework called SPHARM-PDM and I proposed the use of conformal flattening ITK filter in the parametrization step of the framework. An important contribution of this thesis is a command line tool based on the Slicer Execution Model that will be used in Slicer SALT Shape Analysis Toolbox in the future. With the current implementation, the user of SPHARM-PDM pipeline can choose to use conformal mapping spherical parametrization instead of the default heat equation mapping spherical parametrization by setting the “—conf” flag on. I tested the old and newly proposed framework on five different groups of complex surfaces and discussed the results in the RESULTS section.

As I have shown in the RESULTS section, the experiments are not exhaustive. For future work, one of the femur datasets, twelve of the molar datasets and eight of the condyle datasets can still be analyzed via MeshValMet and MeshQuality command line tool.

Another direction of future work is to troubleshoot two of the mandible datasets and all four of the ventricle datasets that failed to be analyzed. For the two mandible datasets, both the original SPHARM-PDM pipeline and the newly proposed one works with 0 iterations of optimization only. With more than 0 iterations, the GenParaMesh command line tool will be caught in an infinite

loop. It is likely to be a bug in the GenParaMesh command line tool; we were hoping to solve it in the future. As for all the ventricle datasets, the original SPHARM-PDM shape analysis pipeline can be used and we can also apply the conformal flattening ITK filter on all of the surface meshes of the segmentations. However, the GenParaMesh command line tool will encounter “Segmentation Fault” problem when we set the conformal mapping spherical parametrization result as the initial parametrization. I used the debugger gdb to backtrace the command line tool while running and the problem appears in the algorithm part of the GenParaMesh command line tool. We are devoting time to understanding the logic for running the ventricle dataset and are hoping to solve the problem in the future. In summary, from all the result of working datasets, we can see that the newly proposed SPHARM-PDM pipeline performs well on complex surfaces including the femur, the condyle, the molar and the mandible. For the condyle and the molar, conformal mapping initialization parametrization converges in fewer iterations than the heat equation mapping initialization parametrization despite the fact that with larger iteration numbers, the conformal mapping initialization parametrization performs slightly worse than the heat equation mapping initialization parametrization. For the femur and the mandible, the proposed conformal mapping initialization parametrization leads to faster convergence and better performance than the heat equation mapping initialization parametrization.

REFERENCES

- [1] M. Styner, I. Oguz, S. Xu, C. Brechbühler, D. Pantazis, J. J. Levitt, M. E. Shenton, and G. Gerig, “Framework for the Statistical Shape Analysis of Brain Structures using SPHARM-PDM,” *The insight journal*, no. 1071, p. 242, 2006.
- [2] S. Angenent, S. Haker, A. Tannenbaum, and R. Kikinis, “On the Laplace-Beltrami Operator and Brain Surface Flattening.,” *IEEE Trans. Med. Imaging*, vol. 18, no. 8, pp. 700–711, 1999.
- [3] Y. Gao, J. Melonakos, and A. R. Tannenbaum, “Conformal Flattening ITK Filter,” Oct. 2006.
- [4] C. Brechbühler, G. Gerig, and O. Kübler, “Parametrization of Closed Surfaces for 3-D Shape Description.,” *Computer Vision and Image Understanding*, vol. 61, no. 2, pp. 154–170, 1995.
- [5] N. Aspert, D. S. Cruz, and T. Ebrahimi, “MESH - measuring errors between surfaces using the Hausdorff distance.,” *ICME*, pp. 705–708, 2002.
- [6] L. H. S. Cevdanes, L. R. Gomes, B. T. Jung, M. R. Gomes, A. C. O. Ruellas, J. R. Goncalves, J. Schilling, M. Styner, T. Nguyen, S. Kapila, and B. Paniagua, “3D superimposition and understanding temporomandibular joint arthritis,” *Orthodontics & Craniofacial Research*, vol. 18, pp. 18–28, Apr. 2015.
- [7] D. M. Boyer, Y. Lipman, E. S. Clair, J. Puente, T. A. Funkhouser, B. Patel, J. Jernvall, and I. Daubechies, “Algorithms to automatically quantify the geometric similarity of anatomical surfaces,” *arXiv*, vol. math.NA, no. 45, pp. 18221–18226, 2011.

- [8] I. Lyu, J. Perdomo, G. S. Yapuncich, B. Paniagua, D. M. Boyer, and M. A. Styner, “Group-wise shape correspondence of variable and complex objects.,” *Medical Imaging - Image Processing*, p. 98, 2018.
- [9] D. M. Boyer, “Relief index of second mandibular molars is a correlate of diet among prosimian primates and other euarchontan mammals,” *Journal of Human Evolution*, vol. 55, no. 6, pp. 1118–1137, Dec. 2008.
- [10] M. Styner, J. A. Lieberman, R. K. McClure, D. R. Weinberger, D. W. Jones, and G. Gerig, “Morphometric analysis of lateral ventricles in schizophrenia and healthy controls regarding genetic and disease-specific factors,” *Proceedings of the National Academy of Sciences*, vol. 102, no. 13, pp. 4872–4877, Mar. 2005.
- [11] A. Fedorov, R. Beichel, J. Kalpathy-Cramer, J. Finet, J.-C. Fillion-Robin, S. Pujol, C. Bauer, D. Jennings, F. Fennessy, M. Sonka, J. Buatti, S. Aylward, J. V. Miller, S. Pieper, and R. Kikinis, “3D Slicer as an image computing platform for the Quantitative Imaging Network,” *Magnetic Resonance Imaging*, vol. 30, no. 9, pp. 1323–1341, Nov. 2012.
- [12] Lars F. (2010). PolyDataToImageData: a tool to convert poly data into image data.
Available online at:
<https://www.vtk.org/Wiki/VTK/Examples/Cxx/PolyData/PolyDataToImageData>